

Issue 4

2015 | Volume 11

The Journal on Advanced Studies in Theoretical and Experimental Physics,
including Related Themes from Mathematics

PROGRESS IN PHYSICS



“All scientists shall have the right to present their scientific research results, in whole or in part, at relevant scientific conferences, and to publish the same in printed scientific journals, electronic archives, and any other media.” — Declaration of Academic Freedom, Article 8

ISSN 1555-5534

PROGRESS IN PHYSICS

A quarterly issue scientific journal, registered with the Library of Congress (DC, USA). This journal is peer reviewed and included in the abstracting and indexing coverage of: Mathematical Reviews and MathSciNet (AMS, USA), DOAJ of Lund University (Sweden), Zentralblatt MATH (Germany), Scientific Commons of the University of St. Gallen (Switzerland), Open-J-Gate (India), Referativnyi Zhurnal VINITI (Russia), etc.

Electronic version of this journal:
<http://www.ptep-online.com>

Advisory Board

Dmitri Rabounski,
Editor-in-Chief, Founder
Florentin Smarandache,
Associate Editor, Founder
Larissa Borissova,
Associate Editor, Founder

Editorial Board

Pierre Millette
millette@ptep-online.com
Andreas Ries
ries@ptep-online.com
Gunn Quznetsov
quznetsov@ptep-online.com
Felix Scholkmann
scholkmann@ptep-online.com
Ebenezer Chifu
chifu@ptep-online.com

Postal Address

Department of Mathematics and Science,
University of New Mexico,
705 Gurley Ave., Gallup, NM 87301, USA

Copyright © *Progress in Physics*, 2015

All rights reserved. The authors of the articles do hereby grant *Progress in Physics* non-exclusive, worldwide, royalty-free license to publish and distribute the articles in accordance with the Budapest Open Initiative: this means that electronic copying, distribution and printing of both full-size version of the journal and the individual papers published therein for non-commercial, academic or individual use can be made by any user without permission or charge. The authors of the articles published in *Progress in Physics* retain their rights to use this journal as a whole or any part of it in any other publications and in any way they see fit. Any part of *Progress in Physics* howsoever used in other publications must include an appropriate citation of this journal.

This journal is powered by \LaTeX

A variety of books can be downloaded free from the Digital Library of Science:
<http://www.gallup.unm.edu/~smarandache>

ISSN: 1555-5534 (print)

ISSN: 1555-5615 (online)

Standard Address Number: 297-5092

Printed in the United States of America

October 2015

Vol. 11, Issue 4

CONTENTS

Millette P. A. Dislocations in the Spacetime Continuum: Framework for Quantum Physics	287
Daywitt W. C. A Planck Vacuum Pilot Model for Inelastic Electron-Proton Scattering ..	308
Daywitt W. C. Antiparticles and Charge Conjugation in the Planck Vacuum Theory	311
Millette P. A. The Burgers Spacetime Dislocation Constant b_0 and the Derivation of Planck's Constant	313
Cahill R. T. Quantum Gravity Experiments	317
Spivey R. J. Dispelling Black Hole Pathologies Through Theory and Observation	321
Vrba A. L. Reservations on Cahill's Quantum Gravity Experiment (<i>Letters to Progress in Physics</i>)	330
Piñol M. A Model of Dust-like Spherically Symmetric Gravitational Collapse without Event Horizon Formation	331
Rossler O. E. The c -global Revival in Physics	340

Information for Authors and Subscribers

Progress in Physics has been created for publications on advanced studies in theoretical and experimental physics, including related themes from mathematics and astronomy. All submitted papers should be professional, in good English, containing a brief review of a problem and obtained results.

All submissions should be designed in \LaTeX format using *Progress in Physics* template. This template can be downloaded from *Progress in Physics* home page <http://www.ptep-online.com>. Abstract and the necessary information about author(s) should be included into the papers. To submit a paper, mail the file(s) to the Editor-in-Chief.

All submitted papers should be as brief as possible. Short articles are preferable. Large papers can also be considered in exceptional cases. Letters related to the publications in the journal or to the events among the science community can be applied to the section *Letters to Progress in Physics*.

All that has been accepted for the online issue of *Progress in Physics* is printed in the paper version of the journal. To order printed issues, contact the Editors.

This journal is non-commercial, academic edition. It is printed from private donations. (Look for the current author fee in the online version of the journal.)

Dislocations in the Spacetime Continuum: Framework for Quantum Physics

Pierre A. Millette

PierreAMillette@alumni.uottawa.ca, Ottawa, Canada

This paper provides a framework for the physical description of physical processes at the quantum level based on dislocations in the spacetime continuum within STCED (Spacetime Continuum Elastodynamics). In this framework, photon and particle self-energies and interactions are mediated by the strain energy density of the dislocations, replacing the role played by virtual particles in QED. We postulate that the spacetime continuum has a granularity characterized by a length b_0 corresponding to the smallest *STC* elementary Burgers dislocation-displacement vector. Screw dislocations corresponding to transverse displacements are identified with photons, and edge dislocations corresponding to longitudinal displacements are identified with particles. Mixed dislocations give rise to wave-particle duality. The strain energy density of the dislocations are calculated and proposed to explain the QED problem of mass renormalization.

1 Introduction

In a previous paper [1], the deformable medium properties of the spacetime continuum (*STC*) led us to expect dislocations, disclinations and other defects to be present in the *STC*. The effects of such defects would be expected to manifest themselves mostly at the microscopic level. In this paper, we present a framework to show that dislocations in the spacetime continuum are the basis of quantum physics. This paper lays the framework to develop a theory of the physical processes that underlie Quantum Electrodynamics (QED). The theory does not result in the same formalism as QED, but rather results in an alternative formulation that provides a physical description of physical processes at the quantum level. This framework allows the theory to be fleshed out in subsequent investigations.

1.1 Elastodynamics of the Spacetime Continuum

As shown in a previous paper [1], General Relativity leads us to consider the spacetime continuum as a deformable continuum, which allows for the application of continuum mechanical methods and results to the analysis of its deformations. The Elastodynamics of the Spacetime Continuum (*STCED*) [1–7] is based on analyzing the spacetime continuum within a continuum mechanical and general relativistic framework.

The combination of all spacetime continuum deformations results in the geometry of the *STC*. The geometry of the spacetime continuum of General Relativity resulting from the energy-momentum stress tensor can thus be seen to be a representation of the deformation of the spacetime continuum resulting from the strains generated by the energy-momentum stress tensor.

As shown in [1], for an isotropic and homogeneous spacetime continuum, the *STC* is characterized by the stress-strain relation

$$2\bar{\mu}_0\epsilon^{\mu\nu} + \bar{\lambda}_0 g^{\mu\nu}\epsilon = T^{\mu\nu} \quad (1)$$

where $T^{\mu\nu}$ is the energy-momentum stress tensor, $\epsilon^{\mu\nu}$ is the resulting strain tensor, and

$$\epsilon = \epsilon^\alpha{}_\alpha \quad (2)$$

is the trace of the strain tensor obtained by contraction. The volume dilatation ϵ is defined as the change in volume per original volume [8, see pp. 149–152] and is an invariant of the strain tensor. $\bar{\lambda}_0$ and $\bar{\mu}_0$ are the Lamé elastic constants of the spacetime continuum: $\bar{\mu}_0$ is the shear modulus and $\bar{\lambda}_0$ is expressed in terms of $\bar{\kappa}_0$, the bulk modulus:

$$\bar{\lambda}_0 = \bar{\kappa}_0 - \bar{\mu}_0/2 \quad (3)$$

in a four-dimensional continuum.

As shown in [1], energy propagates in the spacetime continuum as wave-like deformations which can be decomposed into *dilatations* and *distortions*. *Dilatations* involve an invariant change in volume of the spacetime continuum which is the source of the associated rest-mass energy density of the deformation. On the other hand, *distortions* correspond to a change of shape of the spacetime continuum without a change in volume and are thus massless. Thus deformations propagate in the spacetime continuum by longitudinal (*dilatation*) and transverse (*distortion*) wave displacements.

This provides a natural explanation for wave-particle duality, with the transverse mode corresponding to the wave aspects of the deformation and the longitudinal mode corresponding to the particle aspects of the deformation [7]. The rest-mass energy density of the longitudinal mode is given by [1, see Eq.(32)]

$$\rho c^2 = 4\bar{\kappa}_0\epsilon \quad (4)$$

where ρ is the rest-mass density, c is the speed of light, $\bar{\kappa}_0$ is the bulk modulus of the *STC* (the resistance of the spacetime continuum to *dilatations*), and ϵ is the volume dilatation.

This equation demonstrates that rest-mass energy density arises from the volume dilatation of the spacetime continuum.

The rest-mass energy is equivalent to the energy required to dilate the volume of the spacetime continuum. It is a measure of the energy stored in the spacetime continuum as mass. The volume dilatation is an invariant, as is the rest-mass energy density.

This is an important result as it demonstrates that mass is not independent of the spacetime continuum, but rather mass is part of the spacetime continuum fabric itself. Mass results from the dilatation of the *STC* in the longitudinal propagation of energy-momentum in the spacetime continuum. Matter does not warp spacetime, but rather, matter *is* warped spacetime (i.e. dilated spacetime). The universe consists of the spacetime continuum and energy-momentum that propagates in it by deformation of its (*STC*) structure.

Note that in this paper, we denote the *STCED* spacetime continuum constants $\bar{\kappa}_0, \bar{\lambda}_0, \bar{\mu}_0, \bar{\rho}_0$ with a diacritical mark over the symbols to differentiate them from similar symbols used in other fields of Physics. This allows us to retain existing symbols such as μ_0 for the electromagnetic permeability of free space, compared to the Lamé elastic constant $\bar{\mu}_0$ used to denote the spacetime continuum shear modulus.

1.2 Defects in the Spacetime Continuum

As discussed in [1], given that the spacetime continuum behaves as a deformable medium, there is no reason not to expect dislocations, disclinations and other defects to be present in the *STC*. Dislocations in the spacetime continuum represent the fundamental displacement processes that occur in its structure. These fundamental displacement processes should thus correspond to basic quantum phenomena and provide a framework for the description of quantum physics in *STCED*.

Defect theory has been the subject of investigation since the first half of the XXth century and is a well-developed discipline in continuum mechanics [9–14]. The recent formulation of defects in solids is based on gauge theory [15, 16].

The last quarter of the XXth century has seen the investigation of spacetime defects in the context of string theory, particularly cosmic strings [17, 18], and cosmic expansion [20, 21]. Teleparallel spacetime with defects [18, 22, 23] has resulted in a differential geometry of defects, which can be folded into the Einstein-Cartan Theory (ECT) of gravitation, an extension of Einstein's theory of gravitation that includes torsion [19, 20]. Recently, the phenomenology of spacetime defects has been considered in the context of quantum gravity [24–26].

In this paper, we investigate dislocations in the spacetime continuum in the context of *STCED*. The approach followed till now by investigators has been to use Einstein-Cartan differential geometry, with dislocations (translational deformations) impacting curvature and disclinations (rotational deformations) impacting torsion. The dislocation itself is modelled via the line element ds^2 [17]. In this paper, we investigate spacetime continuum dislocations using the underlying dis-

placements u^ν and the energy-momentum stress tensor. We thus work from the RHS of the general relativistic equation (the stress tensor side) rather than the LHS (the geometric tensor side). It should be noted that the general relativistic equation used can be the standard Einstein equation or a suitably modified version, as in Einstein-Cartan or Teleparallel formulations.

In Section 2 of this paper, we review the basic physical characteristics and dynamics of dislocations in the spacetime continuum. The energy-momentum stress tensor is considered in Section 2.2. This is followed by a detailed review of stationary and moving screw and edge dislocations in Sections 3, 4 and 5, along with their strain energy density as calculated from *STCED*. The framework of quantum physics, based on dislocations in the spacetime continuum is covered in Section 6. Screw dislocations in quantum physics are considered in Section 6.2 and edge dislocations are covered in Section 6.3. Section 7 covers dislocation interactions in quantum physics, and Section 8 provides physical explanations of QED phenomena provided by dislocations in the *STC*. Section 9 summarizes the framework presented in this paper for the development of a physical description of physical processes at the quantum level, based on dislocations in the spacetime continuum within the theory of the Elastodynamics of the Spacetime Continuum (*STCED*).

2 Dislocations in the Spacetime Continuum

A dislocation is characterized by its dislocation-displacement vector, known as the *Burgers vector*, b^μ in a four-dimensional continuum, defined positive in the direction of a vector ξ^μ tangent to the dislocation line in the spacetime continuum [14, see pp.17–24].

A *Burgers circuit* encloses the dislocation. A similar reference circuit can be drawn to enclose a region free of dislocation (see Fig. 1). The Burgers vector is the vector required to make the Burgers circuit equivalent to the reference circuit (see Fig. 2). It is a measure of the displacement between the initial and final points of the circuit due to the dislocation.

It is important to note that there are two conventions used to define the Burgers vector. In this paper, we use the convention used by Hirth [14] referred to as the local Burgers vector. The local Burgers vector is equivalently given by the line integral

$$b^\mu = \oint_C \frac{\partial u^\mu}{\partial s} ds \quad (5)$$

taken in a right-handed sense relative to ξ^μ , where u^μ is the displacement vector.

A dislocation is thus characterized by a line direction ξ^μ and a Burgers vector b^μ . There are two types of dislocations: an *edge dislocation* for which $b^\mu \xi_\mu = 0$ and a *screw dislocation* which can be right-handed for which $b^\mu \xi_\mu = b$, or left-handed for which $b^\mu \xi_\mu = -b$, where b is the magnitude of the Burgers vector. Arbitrary mixed dislocations can be decom-

Fig. 1: A reference circuit in a region free of dislocation, S: start, F: finish

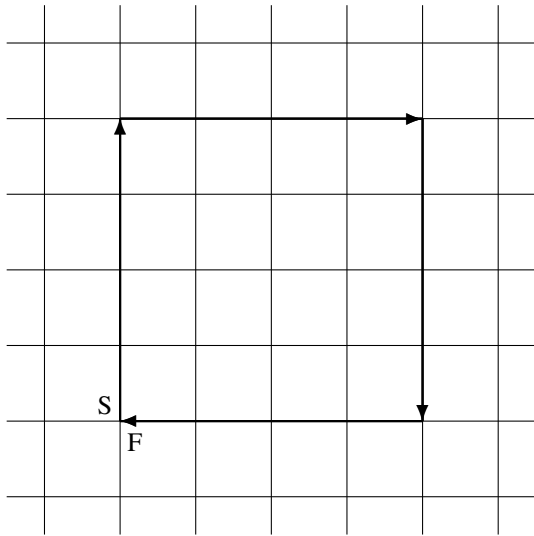
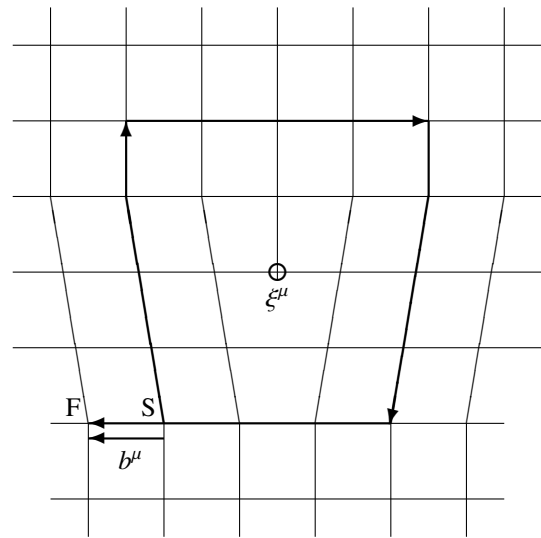


Fig. 2: A dislocation showing the Burgers vector b^μ , direction vector ξ^μ which points into the paper and the Burgers circuit, S: start, F: finish



posed into a screw component, along vector ξ^μ , and an edge component, perpendicular to vector ξ^μ .

The edge dislocation was first proposed by Orowan [27], Polanyi [28] and Taylor [29] in 1934, while the screw dislocation was proposed by Burgers [30] in 1939. In this paper, we extend the concept of dislocations to the elastodynamics of the spacetime continuum. Edge dislocations correspond to *dilatations* (longitudinal displacements) and hence have an associated rest-mass energy, while screw dislocations correspond to *distortions* (transverse displacements) and are massless [1].

2.1 Dislocation dynamics

In three-dimensional space, the dynamic equation is written as [31, see pp. 88–89],

$$T^{ij}_{;j} = -X^i + \bar{\rho}_0 \ddot{u}^i \tag{6}$$

where $\bar{\rho}_0$ is the spacetime continuum density, X^i is the volume (or body) force, the comma (,) represents differentiation and \dot{u} denotes the derivative with respect to time. Substituting for $\varepsilon^{\mu\nu} = \frac{1}{2}(u^{\mu;\nu} + u^{\nu;\mu})$ in (1), using (2) and $u^{\mu}_{;\mu} = \varepsilon^\mu_\mu = \varepsilon$ in this equation, we obtain

$$\bar{\mu}_0 \vec{\nabla}^2 u^i + (\bar{\mu}_0 + \bar{\lambda}_0) \varepsilon^{;i} = -X^i + \bar{\rho}_0 \ddot{u}^i \tag{7}$$

which, upon converting the time derivative to indicial notation and rearranging, is written as

$$\bar{\mu}_0 \vec{\nabla}^2 u^i - \bar{\rho}_0 c^2 u^{i,00} + (\bar{\mu}_0 + \bar{\lambda}_0) \varepsilon^{;i} = -X^i. \tag{8}$$

We use the arrow above the nabla symbol to indicate the 3-dimensional gradient whereas the 4-dimensional gradient is

written with no arrow. Using the relation [1]

$$c = \sqrt{\frac{\bar{\mu}_0}{\bar{\rho}_0}} \tag{9}$$

in the above, (8) becomes

$$\bar{\mu}_0 (\vec{\nabla}^2 u^i - u^{i,00}) + (\bar{\mu}_0 + \bar{\lambda}_0) \varepsilon^{;i} = -X^i \tag{10}$$

and, combining the space and time derivatives, we obtain

$$\bar{\mu}_0 \nabla^2 u^i + (\bar{\mu}_0 + \bar{\lambda}_0) \varepsilon^{;i} = -X^i. \tag{11}$$

This equation is the space portion of the *STCED displacement wave equation* (51) of [1]

$$\bar{\mu}_0 \nabla^2 u^\nu + (\bar{\mu}_0 + \bar{\lambda}_0) \varepsilon^{;\nu} = -X^\nu. \tag{12}$$

Hence the dynamics of the spacetime continuum is described by the dynamic equation (12), which includes the accelerations from the applied forces.

In this analysis, we consider the simpler problem of dislocations moving in an isotropic continuum with no volume force. Then (12) becomes

$$\bar{\mu}_0 \nabla^2 u^\nu + (\bar{\mu}_0 + \bar{\lambda}_0) \varepsilon^{;\nu} = 0, \tag{13}$$

where ∇^2 is the four-dimensional operator and the semi-colon (;) represents covariant differentiation.

Separating u^ν into its longitudinal (irrotational) component u^ν_\parallel and its transverse (solenoidal) component u^ν_\perp using the Helmholtz theorem in four dimensions [32] according to

$$u^\nu = u^\nu_\parallel + u^\nu_\perp, \tag{14}$$

(12) can be separated into a screw dislocation displacement (transverse) equation

$$\bar{\mu}_0 \nabla^2 u_{\perp}^{\nu} = 0 \tag{15}$$

and an edge dislocation displacement (longitudinal) equation

$$\nabla^2 u_{\parallel}^{\nu} = -\frac{\bar{\mu}_0 + \bar{\lambda}_0}{\bar{\mu}_0} \varepsilon^{;\nu}. \tag{16}$$

2.2 The energy-momentum stress tensor

The components of the energy-momentum stress tensor are given by [33]:

$$\begin{aligned} T^{00} &= H \\ T^{0j} &= s^j \\ T^{i0} &= g^i \\ T^{ij} &= \sigma^{ij} \end{aligned} \tag{17}$$

where H is the total energy density, s^j is the energy flux vector, g^i is the momentum density vector, and σ^{ij} is the Cauchy stress tensor which is the i^{th} component of force per unit area at x^j .

From the stress tensor $T^{\mu\nu}$, we can calculate the strain tensor $\varepsilon^{\mu\nu}$ and then calculate the strain energy density of the dislocations. As shown in [3], for a general anisotropic continuum in four dimensions, the spacetime continuum is approximated by a deformable linear elastic medium that obeys Hooke’s law [31, see pp. 50–53]

$$E^{\mu\nu\alpha\beta} \varepsilon_{\alpha\beta} = T^{\mu\nu} \tag{18}$$

where $E^{\mu\nu\alpha\beta}$ is the elastic moduli tensor. For an isotropic and homogeneous medium, the elastic moduli tensor simplifies to [31]:

$$E^{\mu\nu\alpha\beta} = \bar{\lambda}_0 (g^{\mu\nu} g^{\alpha\beta}) + \bar{\mu}_0 (g^{\mu\alpha} g^{\nu\beta} + g^{\mu\beta} g^{\nu\alpha}). \tag{19}$$

For the metric tensor $g_{\mu\nu}$, we use the flat spacetime diagonal metric $\eta_{\mu\nu}$ with signature $(-+++)$ as the *STC* is locally flat at the microscopic level. Substituting for (19) into (18) and expanding, we obtain

$$\begin{aligned} T^{00} &= (\bar{\lambda}_0 + 2\bar{\mu}_0) \varepsilon^{00} - \bar{\lambda}_0 \varepsilon^{11} - \bar{\lambda}_0 \varepsilon^{22} - \bar{\lambda}_0 \varepsilon^{33} \\ T^{11} &= -\bar{\lambda}_0 \varepsilon^{00} + (\bar{\lambda}_0 + 2\bar{\mu}_0) \varepsilon^{11} + \bar{\lambda}_0 \varepsilon^{22} + \bar{\lambda}_0 \varepsilon^{33} \\ T^{22} &= -\bar{\lambda}_0 \varepsilon^{00} + \bar{\lambda}_0 \varepsilon^{11} + (\bar{\lambda}_0 + 2\bar{\mu}_0) \varepsilon^{22} + \bar{\lambda}_0 \varepsilon^{33} \\ T^{33} &= -\bar{\lambda}_0 \varepsilon^{00} + \bar{\lambda}_0 \varepsilon^{11} + \bar{\lambda}_0 \varepsilon^{22} + (\bar{\lambda}_0 + 2\bar{\mu}_0) \varepsilon^{33} \\ T^{\mu\nu} &= 2\bar{\mu}_0 \varepsilon^{\mu\nu}, \quad \mu \neq \nu. \end{aligned} \tag{20}$$

In terms of the stress tensor, the inverse of (20) is given by

$$\begin{aligned} \varepsilon^{00} &= \frac{1}{4\bar{\mu}_0(2\bar{\lambda}_0 + \bar{\mu}_0)} \left[(3\bar{\lambda}_0 + 2\bar{\mu}_0) T^{00} + \bar{\lambda}_0 (T^{11} + T^{22} + T^{33}) \right] \\ \varepsilon^{11} &= \frac{1}{4\bar{\mu}_0(2\bar{\lambda}_0 + \bar{\mu}_0)} \left[(3\bar{\lambda}_0 + 2\bar{\mu}_0) T^{11} + \bar{\lambda}_0 (T^{00} - T^{22} - T^{33}) \right] \\ \varepsilon^{22} &= \frac{1}{4\bar{\mu}_0(2\bar{\lambda}_0 + \bar{\mu}_0)} \left[(3\bar{\lambda}_0 + 2\bar{\mu}_0) T^{22} + \bar{\lambda}_0 (T^{00} - T^{11} - T^{33}) \right] \\ \varepsilon^{33} &= \frac{1}{4\bar{\mu}_0(2\bar{\lambda}_0 + \bar{\mu}_0)} \left[(3\bar{\lambda}_0 + 2\bar{\mu}_0) T^{33} + \bar{\lambda}_0 (T^{00} - T^{11} - T^{22}) \right] \\ \varepsilon^{\mu\nu} &= \frac{1}{2\bar{\mu}_0} T^{\mu\nu}, \quad \mu \neq \nu. \end{aligned} \tag{21}$$

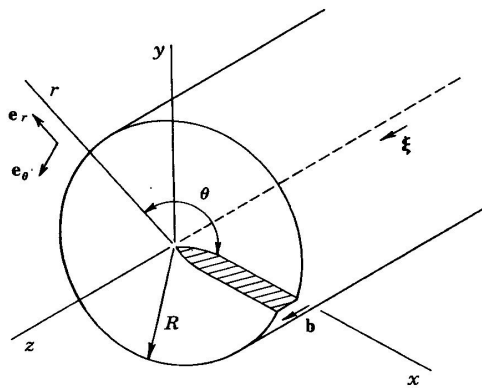
where $T^{ij} = \sigma^{ij}$. We calculate $\varepsilon = \varepsilon^{\alpha}_{\alpha}$ from the values of (21). Using $\eta_{\mu\nu}$, (3) and $T^{\alpha}_{\alpha} = \rho c^2$ from [2], we obtain (4) as required. This confirms the validity of the strain tensor in terms of the energy-momentum stress tensor as given by (21).

Eshelby [34–36] introduced an elastic field energy-momentum tensor for continuous media to deal with cases where defects (such as dislocations) lead to changes in configuration. The displacements u^{ν} are considered to correspond to a field defined at points x^{μ} of the spacetime continuum. This tensor was first derived by Morse and Feshback [37] for an isotropic elastic medium, using dyadics. The energy flux vector s_j and the field momentum density vector g_i are then given by [34, 37]:

$$\begin{aligned} s_j &= -\dot{u}_k \sigma_{kj} \\ g_i &= \bar{\rho}_0 u_{k,i} \dot{u}_k \\ b_{ij} &= L \delta_{ij} - u_{k,i} \sigma_{kj} \end{aligned} \tag{22}$$

where $\bar{\rho}_0$ is the density of the medium, in this case the spacetime continuum, L is the Lagrangian equal to $K - W$ where W is the strain energy density and K is the kinetic energy density ($H = K + W$), and b_{ij} is known as the Eshelby stress tensor [38, see p. 27]. If the energy-momentum stress tensor is symmetric, then $g^i = s^i$. In this paper, we consider the case where there are no changes in configuration, and use the energy-momentum stress tensor given by (17) and (20).

Fig. 3: A stationary screw dislocation in cartesian (x, y, z) and cylindrical polar (r, θ, z) coordinates [14, see p. 60].



3 Screw dislocation

3.1 Stationary screw dislocation

We consider a stationary screw dislocation in the spacetime continuum, with cylindrical polar coordinates (r, θ, z) , with the dislocation line along the z -axis (see Fig. 3). Then the Burgers vector is along the z -axis and is given by $b_r = b_\theta = 0$, $b_z = b$, the magnitude of the Burgers vector. The only non-zero component of the deformations is given by [14, see pp. 60–61] [13, see p. 51]

$$u_z = \frac{b}{2\pi} \theta = \frac{b}{2\pi} \tan^{-1} \frac{y}{x}. \quad (23)$$

This solution satisfies the screw dislocation displacement equation (15).

Similarly, the only non-zero components of the stress and strain tensors are given by

$$\begin{aligned} \sigma_{\theta z} &= \frac{b}{2\pi} \frac{\bar{\mu}_0}{r} \\ \varepsilon_{\theta z} &= \frac{b}{4\pi} \frac{1}{r} \end{aligned} \quad (24)$$

respectively.

3.2 Moving screw dislocation

We now consider the previous screw dislocation, moving along the x -axis, parallel to the dislocation, at a constant speed $v_x = v$. Equation (13) then simplifies to the wave equation for massless transverse shear waves for the displacements u_z along the z -axis, with speed $c_t = c$ given by (9), where c_t is the speed of the transverse waves corresponding to c the speed of light.

If coordinate system (x', y', z', t') is attached to the uniformly moving screw dislocation, then the transformation between the stationary and the moving screw dislocation is given by [14]

$$\begin{aligned} x' &= \frac{x - vt}{(1 - v^2/c^2)^{1/2}} \\ y' &= y \\ z' &= z \\ t' &= \frac{t - vx/c^2}{(1 - v^2/c^2)^{1/2}}. \end{aligned} \quad (25)$$

which is the special relativistic transformation.

The only non-zero component of the deformation in cartesian coordinates is given by [14, see pp. 184–185]

$$u_z = \frac{b}{2\pi} \tan^{-1} \frac{\gamma y}{x - vt}, \quad (26)$$

where

$$\gamma = \sqrt{1 - \frac{v^2}{c^2}}. \quad (27)$$

This solution also satisfies the screw dislocation displacement equation (15). It simplifies to the case of the stationary screw dislocation when the speed $v = 0$.

Similarly, the only non-zero components of the stress tensor in cartesian coordinates are given by [14]

$$\begin{aligned} \sigma_{xz} &= -\frac{b\bar{\mu}_0}{2\pi} \frac{\gamma y}{(x - vt)^2 + \gamma^2 y^2} \\ \sigma_{yz} &= \frac{b\bar{\mu}_0}{2\pi} \frac{\gamma(x - vt)}{(x - vt)^2 + \gamma^2 y^2}. \end{aligned} \quad (28)$$

The only non-zero components of the strain tensor in cartesian coordinates are derived from $\varepsilon^{\mu\nu} = \frac{1}{2}(u^{\mu;\nu} + u^{\nu;\mu})$ [1, see Eq.(41)]:

$$\begin{aligned} \varepsilon_{xz} &= -\frac{b}{4\pi} \frac{\gamma y}{(x - vt)^2 + \gamma^2 y^2} \\ \varepsilon_{yz} &= \frac{b}{4\pi} \frac{\gamma(x - vt)}{(x - vt)^2 + \gamma^2 y^2}, \end{aligned} \quad (29)$$

in an isotropic continuum.

Non-zero components involving time are given by

$$\begin{aligned} \varepsilon_{tz} = \varepsilon_{zt} &= \frac{1}{2} \left(\frac{\partial u_z}{\partial(ct)} + \frac{\partial u_t}{\partial z} \right) \\ \varepsilon_{tz} &= \frac{b}{4\pi} \frac{v}{c} \frac{\gamma y}{(x - vt)^2 + \gamma^2 y^2} \end{aligned} \quad (30)$$

where $u_t = 0$ has been used. This assumes that the screw dislocation is fully formed and moving with velocity v as described. Using (20), the non-zero stress components involving time are given by

$$\sigma_{tz} = \sigma_{zt} = \frac{b\bar{\mu}_0}{2\pi} \frac{v}{c} \frac{\gamma y}{(x - vt)^2 + \gamma^2 y^2}. \quad (31)$$

Screw dislocations are thus found to be Lorentz invariant.

3.3 Screw dislocation strain energy density

We consider the stationary screw dislocation in the spacetime continuum of Section 3.1, with cylindrical polar coordinates (r, θ, z) , with the dislocation line along the z -axis and the Burgers vector along the z -axis $b_z = b$.

Then the strain energy density of the screw dislocation is given by the transverse distortion energy density [1, see Eq. (74)]

$$\mathcal{E}_\perp = \bar{\mu}_0 e^{\alpha\beta} e_{\alpha\beta} \tag{32}$$

where from [1, see Eq. (33)],

$$e^{\alpha\beta} = \varepsilon^{\alpha\beta} - e_s g^{\alpha\beta} \tag{33}$$

where $e_s = \frac{1}{4} \varepsilon^\alpha_\alpha$ is the dilatation which for a screw dislocation is equal to 0. The screw dislocation is thus massless ($\mathcal{E}_\parallel = 0$).

The non-zero components of the strain tensor are as defined in (24). Hence

$$\mathcal{E}_\perp = \bar{\mu}_0 (\varepsilon_{\theta z}^2 + \varepsilon_{z\theta}^2). \tag{34}$$

Substituting from (24),

$$\mathcal{E}_\perp = \frac{\bar{\mu}_0 b^2}{8\pi^2} \frac{1}{r^2} = \mathcal{E}. \tag{35}$$

We now consider the more general case of the moving screw dislocation in the spacetime continuum of Section 3.2, with cartesian coordinates (x, y, z) . The non-zero components of the strain tensor are as defined in (29) and (30). Substituting in (32), the equation becomes [1, see Eqs.(114–115)]

$$\mathcal{E}_\perp = 2\bar{\mu}_0 (-\varepsilon_{tz}^2 + \varepsilon_{xz}^2 + \varepsilon_{yz}^2). \tag{36}$$

Substituting from (29) and (30) into (36), the screw dislocation strain energy density becomes

$$\mathcal{E}_\perp = \frac{\bar{\mu}_0 b^2}{8\pi^2} \frac{\gamma^2}{(x - vt)^2 + \gamma^2 y^2} = \mathcal{E}. \tag{37}$$

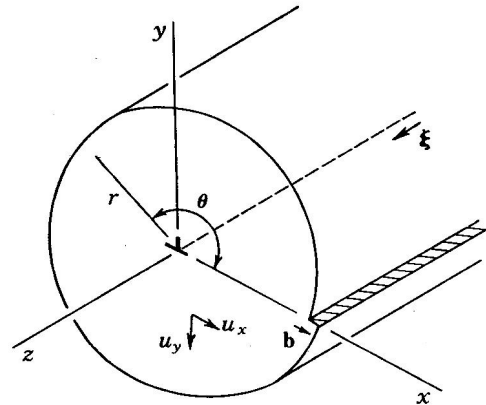
This equation simplifies to (35) in the case where $v = 0$, as expected. In addition, the energy density (which is quadratic in energy as per [1, see Eq.(76)]) is multiplied by the special relativistic γ factor.

4 Edge dislocation

4.1 Stationary edge dislocation

We consider a stationary edge dislocation in the spacetime continuum in cartesian coordinates (x, y, z) , with the dislocation line along the z -axis and the Burgers vector $b_x = b, b_y = b_z = 0$ (see Fig. 4). Then the non-zero components of the deformations are given in cartesian coordinates by [14, see

Fig. 4: A stationary edge dislocation in cartesian (x, y, z) and cylindrical polar (r, θ, z) coordinates [14, see p. 74].



p. 78]

$$\begin{aligned} u_x &= \frac{b}{2\pi} \left(\tan^{-1} \frac{y}{x} + \frac{\bar{\mu}_0 + \bar{\lambda}_0}{2\bar{\mu}_0 + \bar{\lambda}_0} \frac{xy}{x^2 + y^2} \right) \\ u_y &= -\frac{b}{2\pi} \left(\frac{1}{2} \frac{\bar{\mu}_0}{2\bar{\mu}_0 + \bar{\lambda}_0} \log(x^2 + y^2) + \frac{1}{2} \frac{\bar{\mu}_0 + \bar{\lambda}_0}{2\bar{\mu}_0 + \bar{\lambda}_0} \frac{x^2 - y^2}{x^2 + y^2} \right). \end{aligned} \tag{38}$$

This solution results in a non-zero R.H.S. of the edge dislocation displacement equation (16) as required. Equation (16) can be evaluated to give a value of ε in agreement with the results of Section 4.3 as shown in that section.

The cylindrical polar coordinate description of the edge dislocation is more complex than the cartesian coordinate description. We thus use cartesian coordinates in the following sections, transforming to polar coordinate expressions as warranted. The non-zero components of the stress tensor in cartesian coordinates are given by [14, see p. 76]

$$\begin{aligned} \sigma_{xx} &= -\frac{b\bar{\mu}_0}{\pi} \frac{\bar{\mu}_0 + \bar{\lambda}_0}{2\bar{\mu}_0 + \bar{\lambda}_0} \frac{y(3x^2 + y^2)}{(x^2 + y^2)^2} \\ \sigma_{yy} &= \frac{b\bar{\mu}_0}{\pi} \frac{\bar{\mu}_0 + \bar{\lambda}_0}{2\bar{\mu}_0 + \bar{\lambda}_0} \frac{y(x^2 - y^2)}{(x^2 + y^2)^2} \\ \sigma_{zz} &= \frac{1}{2} \frac{\bar{\lambda}_0}{\bar{\mu}_0 + \bar{\lambda}_0} (\sigma_{xx} + \sigma_{yy}) \\ &= -\frac{b\bar{\mu}_0}{\pi} \frac{\bar{\lambda}_0}{2\bar{\mu}_0 + \bar{\lambda}_0} \frac{y}{x^2 + y^2} \\ \sigma_{xy} &= \frac{b\bar{\mu}_0}{\pi} \frac{\bar{\mu}_0 + \bar{\lambda}_0}{2\bar{\mu}_0 + \bar{\lambda}_0} \frac{x(x^2 - y^2)}{(x^2 + y^2)^2}. \end{aligned} \tag{39}$$

The non-zero components of the strain tensor in cartesian coordinates are derived from $\varepsilon^{\mu\nu} = \frac{1}{2}(u^{\mu;\nu} + u^{\nu;\mu})$ [1, see

Eq.(41)]:

$$\begin{aligned} \varepsilon_{xx} &= -\frac{b}{2\pi} \frac{y}{x^2 + y^2} \left(1 + \frac{\bar{\mu}_0 + \bar{\lambda}_0}{2\bar{\mu}_0 + \bar{\lambda}_0} \frac{x^2 - y^2}{x^2 + y^2} \right) \\ &= -\frac{by}{2\pi} \frac{(3\bar{\mu}_0 + 2\bar{\lambda}_0)x^2 + \bar{\mu}_0 y^2}{(2\bar{\mu}_0 + \bar{\lambda}_0)(x^2 + y^2)^2} \\ \varepsilon_{yy} &= -\frac{b}{2\pi} \frac{\bar{\mu}_0}{2\bar{\mu}_0 + \bar{\lambda}_0} \frac{y}{x^2 + y^2} \left(1 - \frac{\bar{\mu}_0 + \bar{\lambda}_0}{\bar{\mu}_0} \frac{2x^2}{x^2 + y^2} \right) \quad (40) \\ &= \frac{by}{2\pi} \frac{(\bar{\mu}_0 + 2\bar{\lambda}_0)x^2 - \bar{\mu}_0 y^2}{(2\bar{\mu}_0 + \bar{\lambda}_0)(x^2 + y^2)^2} \\ \varepsilon_{xy} &= \frac{b}{2\pi} \frac{\bar{\mu}_0 + \bar{\lambda}_0}{2\bar{\mu}_0 + \bar{\lambda}_0} \frac{x(x^2 - y^2)}{(x^2 + y^2)^2} \end{aligned}$$

in an isotropic continuum.

4.2 Moving edge dislocation

We now consider the previous edge dislocation, moving along the x -axis, parallel to the z -axis, along the slip plane $x-z$, at a constant speed $v_x = v$. The solutions of (13) for the moving edge dislocation then include both longitudinal and transverse components. The only non-zero components of the deformations in cartesian coordinates are given by [11, see pp. 39–40] [39, see pp. 218–219]

$$\begin{aligned} u_x &= \frac{bc^2}{\pi v^2} \left(\tan^{-1} \frac{\gamma_l y}{x - vt} - \alpha^2 \tan^{-1} \frac{\gamma y}{x - vt} \right) \\ u_y &= \frac{bc^2}{2\pi v^2} \left(\gamma_l \log \left[(x - vt)^2 + \gamma_l^2 y^2 \right] - \right. \quad (41) \\ &\quad \left. - \frac{\alpha^2}{\gamma} \log \left[(x - vt)^2 + \gamma^2 y^2 \right] \right), \end{aligned}$$

where

$$\alpha = \sqrt{1 - \frac{v^2}{2c^2}}, \quad (42)$$

$$\gamma_l = \sqrt{1 - \frac{v^2}{c_l^2}} \quad (43)$$

and c_l is the speed of longitudinal deformations given by

$$c_l = \sqrt{\frac{2\bar{\mu}_0 + \bar{\lambda}_0}{\bar{\rho}_0}}. \quad (44)$$

This solution again results in a non-zero R.H.S. of the edge dislocation displacement equation (16) as required, and (16) can be evaluated to give a value of ε as in Section 4.3. This solution simplifies to the case of the stationary edge dislocation when the speed $v = 0$.

The non-zero components of the stress tensor in cartesian coordinates are given by [14, see pp. 189–190] [11, see

pp. 39–40]

$$\begin{aligned} \sigma_{xx} &= \frac{bc^2 y}{\pi v^2} \left(\frac{\bar{\lambda}_0 \gamma_l^3 - (2\bar{\mu}_0 + \bar{\lambda}_0) \gamma_l}{(x - vt)^2 + \gamma_l^2 y^2} + \right. \\ &\quad \left. + \frac{2\bar{\mu}_0 \alpha^2 \gamma}{(x - vt)^2 + \gamma^2 y^2} \right) \\ \sigma_{yy} &= \frac{bc^2 y}{\pi v^2} \left(\frac{(2\bar{\mu}_0 + \bar{\lambda}_0) \gamma_l^3 - \bar{\lambda}_0 \gamma_l}{(x - vt)^2 + \gamma_l^2 y^2} - \right. \\ &\quad \left. - \frac{2\bar{\mu}_0 \alpha^2 \gamma}{(x - vt)^2 + \gamma^2 y^2} \right) \\ \sigma_{zz} &= \frac{1}{2} \frac{\bar{\lambda}_0}{\bar{\mu}_0 + \bar{\lambda}_0} (\sigma_{xx} + \sigma_{yy}) \quad (45) \\ &= \frac{\bar{\lambda}_0 b}{\pi} \frac{c^2}{c_l^2} \frac{-\gamma_l y}{(x - vt)^2 + \gamma_l^2 y^2} \\ &= \frac{b}{\pi} \frac{\bar{\lambda}_0 \bar{\mu}_0}{2\bar{\mu}_0 + \bar{\lambda}_0} \frac{-\gamma_l y}{(x - vt)^2 + \gamma_l^2 y^2} \\ \sigma_{xy} &= \frac{\bar{\mu}_0 bc^2 (x - vt)}{\pi v^2} \left(\frac{2\gamma_l}{(x - vt)^2 + \gamma_l^2 y^2} - \right. \\ &\quad \left. - \frac{\alpha^2 (\gamma + 1/\gamma)}{(x - vt)^2 + \gamma^2 y^2} \right). \end{aligned}$$

It is important to note that for a screw dislocation, the stress on the plane $x - vt = 0$ becomes infinite at $v = c$. This sets an upper limit on the speed of screw dislocations in the spacetime continuum, and provides an explanation for the speed of light limit. This upper limit also applies to edge dislocations, as the shear stress becomes infinite everywhere at $v = c$, even though the speed of longitudinal deformations c_l is greater than that of transverse deformations c [14, see p. 191] [11, see p. 40].

The non-zero components of the strain tensor in cartesian coordinates are derived from $\varepsilon^{\mu\nu} = \frac{1}{2}(u^{\mu;\nu} + u^{\nu;\mu})$ [1, see Eq.(41)]:

$$\begin{aligned} \varepsilon_{xx} &= \frac{bc^2 y}{\pi v^2} \left(\frac{-\gamma_l}{(x - vt)^2 + (\gamma_l y)^2} + \frac{\alpha^2 \gamma}{(x - vt)^2 + (\gamma y)^2} \right) \\ \varepsilon_{yy} &= \frac{bc^2 y}{\pi v^2} \left(\frac{\gamma_l^3}{(x - vt)^2 + (\gamma_l y)^2} - \frac{\alpha^2 \gamma}{(x - vt)^2 + (\gamma y)^2} \right) \quad (46) \\ \varepsilon_{xy} &= \frac{bc^2 (x - vt)}{2\pi v^2} \left(\frac{2\gamma_l}{(x - vt)^2 + (\gamma_l y)^2} - \right. \\ &\quad \left. - \frac{\alpha^2 (\gamma + 1/\gamma)}{(x - vt)^2 + (\gamma y)^2} \right) \end{aligned}$$

in an isotropic continuum.

Non-zero components involving time are given by

$$\begin{aligned} \varepsilon_{tx} = \varepsilon_{xt} &= \frac{1}{2} \left(\frac{\partial u_x}{\partial(ct)} + \frac{\partial u_t}{\partial x} \right) \\ \varepsilon_{ty} = \varepsilon_{yt} &= \frac{1}{2} \left(\frac{\partial u_y}{\partial(ct)} + \frac{\partial u_t}{\partial y} \right) \\ \varepsilon_{tx} &= \frac{b}{2\pi} \frac{c}{v} \left(\frac{\gamma l y}{(x-vt)^2 + \gamma_l^2 y^2} - \right. \\ &\quad \left. - \alpha^2 \frac{\gamma y}{(x-vt)^2 + \gamma^2 y^2} \right) \\ \varepsilon_{ty} &= -\frac{b}{2\pi} \frac{c}{v} \left(\frac{\gamma_l(x-vt)}{(x-vt)^2 + \gamma_l^2 y^2} - \right. \\ &\quad \left. - \frac{\alpha^2}{\gamma^2} \frac{\gamma(x-vt)}{(x-vt)^2 + \gamma^2 y^2} \right) \end{aligned} \tag{47}$$

where $u_t = 0$ has been used. This assumes that the edge dislocation is fully formed and moving with velocity v as described. Using (20), the non-zero stress components involving time are given by

$$\begin{aligned} \sigma_{tx} &= \frac{b\bar{\mu}_0}{\pi} \frac{c}{v} \left(\frac{\gamma l y}{(x-vt)^2 + \gamma_l^2 y^2} - \right. \\ &\quad \left. - \alpha^2 \frac{\gamma y}{(x-vt)^2 + \gamma^2 y^2} \right) \\ \sigma_{ty} &= -\frac{b\bar{\mu}_0}{\pi} \frac{c}{v} \left(\frac{\gamma_l(x-vt)}{(x-vt)^2 + \gamma_l^2 y^2} - \right. \\ &\quad \left. - \frac{\alpha^2}{\gamma^2} \frac{\gamma(x-vt)}{(x-vt)^2 + \gamma^2 y^2} \right). \end{aligned} \tag{48}$$

4.3 Edge dislocation strain energy density

As we have seen in Section 3.3, the screw dislocation is massless as $\varepsilon = 0$ and hence $\mathcal{E}_{||} = 0$ for the screw dislocation: it is a pure distortion, with no dilatation. In this section, we evaluate the strain energy density of the edge dislocation.

As seen in [1, see Section 8.1], the strain energy density of the spacetime continuum is separated into two terms: the first one expresses the dilatation energy density (the mass longitudinal term) while the second one expresses the distortion energy density (the massless transverse term):

$$\mathcal{E} = \mathcal{E}_{||} + \mathcal{E}_{\perp} \tag{49}$$

where

$$\mathcal{E}_{||} = \frac{1}{2} \bar{\kappa}_0 \varepsilon^2 \equiv \frac{1}{32\bar{\kappa}_0} (\rho c^2)^2 \equiv \frac{1}{2\bar{\kappa}_0} t_s^2 \tag{50}$$

where ε is the volume dilatation and ρ is the mass energy density of the edge dislocation, and

$$\mathcal{E}_{\perp} = \bar{\mu}_0 e^{\alpha\beta} e_{\alpha\beta} \equiv \frac{1}{4\bar{\mu}_0} t^{\alpha\beta} t_{\alpha\beta}. \tag{51}$$

where from [1, see Eq. (36)] the energy-momentum stress tensor $T^{\alpha\beta}$ is decomposed into a stress deviation tensor $t^{\alpha\beta}$ and a scalar t_s , according to

$$t^{\alpha\beta} = T^{\alpha\beta} - t_s g^{\alpha\beta} \tag{52}$$

where $t_s = \frac{1}{4} T^{\alpha}_{\alpha}$. Then the dilatation strain energy density of the edge dislocation is given by the (massive) longitudinal dilatation energy density (50) and the distortion (massless) strain energy density of the edge dislocation is given by the transverse distortion energy density (51).

4.3.1 Stationary edge dislocation energy density

We first consider the case of the stationary edge dislocation of Section 4.1. The volume dilatation ε for the stationary edge dislocation is given by

$$\varepsilon = \varepsilon^{\alpha}_{\alpha} = \varepsilon_{xx} + \varepsilon_{yy} \tag{53}$$

where the non-zero diagonal elements of the strain tensor are obtained from (40). Substituting for ε_{xx} and ε_{yy} from (40), we obtain

$$\varepsilon = -\frac{b}{\pi} \frac{\bar{\mu}_0}{2\bar{\mu}_0 + \bar{\lambda}_0} \frac{y}{x^2 + y^2}. \tag{54}$$

In cylindrical polar coordinates, (54) is expressed as

$$\varepsilon = -\frac{b}{\pi} \frac{\bar{\mu}_0}{2\bar{\mu}_0 + \bar{\lambda}_0} \frac{\sin \theta}{r}. \tag{55}$$

We can disregard the negative sign in (54) and (55) as it can be eliminated by using the **FS/RH** convention instead of the **SF/RH** convention for the Burgers vector [14, see p. 22]).

As mentioned in Section 4.1, the volume dilatation ε can be calculated from the edge dislocation displacement (longitudinal) equation (16), viz.

$$\nabla^2 u_{||}^y = -\frac{\bar{\mu}_0 + \bar{\lambda}_0}{\bar{\mu}_0} \varepsilon^{,y}.$$

For the x -component, this equation gives

$$\nabla^2 u_x = \frac{\partial^2 u_x}{\partial x^2} + \frac{\partial^2 u_x}{\partial y^2} = -\frac{\bar{\mu}_0 + \bar{\lambda}_0}{\bar{\mu}_0} \varepsilon_{,x}. \tag{56}$$

Substituting for u_x from (38), we obtain

$$\nabla^2 u_x = -\frac{2b}{\pi} \frac{\bar{\mu}_0 + \bar{\lambda}_0}{2\bar{\mu}_0 + \bar{\lambda}_0} \frac{xy}{(x^2 + y^2)^2} = -\frac{\bar{\mu}_0 + \bar{\lambda}_0}{\bar{\mu}_0} \varepsilon_{,x}. \tag{57}$$

Hence

$$\varepsilon_{,x} = \frac{2b}{\pi} \frac{\bar{\mu}_0}{2\bar{\mu}_0 + \bar{\lambda}_0} \frac{xy}{(x^2 + y^2)^2} \tag{58}$$

and

$$\varepsilon = \frac{2b}{\pi} \frac{\bar{\mu}_0}{2\bar{\mu}_0 + \bar{\lambda}_0} \int \frac{xy}{(x^2 + y^2)^2} dx. \tag{59}$$

Evaluating the integral [40], we obtain

$$\varepsilon = -\frac{b}{\pi} \frac{\bar{\mu}_0}{2\bar{\mu}_0 + \bar{\lambda}_0} \frac{y}{x^2 + y^2} \quad (60)$$

in agreement with (54).

Similarly for the y -component, substituting for u_y from (38), the equation

$$\nabla^2 u_y = \frac{\partial^2 u_y}{\partial x^2} + \frac{\partial^2 u_y}{\partial y^2} = -\frac{\bar{\mu}_0 + \bar{\lambda}_0}{\bar{\mu}_0} \varepsilon_{,y} \quad (61)$$

gives

$$\varepsilon_{,y} = -\frac{b}{\pi} \frac{\bar{\mu}_0}{2\bar{\mu}_0 + \bar{\lambda}_0} \frac{x^2 - y^2}{(x^2 + y^2)^2}. \quad (62)$$

Evaluating the integral [40]

$$\varepsilon = -\frac{b}{\pi} \frac{\bar{\mu}_0}{2\bar{\mu}_0 + \bar{\lambda}_0} \int \frac{x^2 - y^2}{(x^2 + y^2)^2} dy, \quad (63)$$

we obtain

$$\varepsilon = -\frac{b}{\pi} \frac{\bar{\mu}_0}{2\bar{\mu}_0 + \bar{\lambda}_0} \frac{y}{x^2 + y^2} \quad (64)$$

again in agreement with (54).

The mass energy density is calculated from (4)

$$\rho c^2 = 4\bar{\kappa}_0 \varepsilon = 2(2\bar{\lambda}_0 + \bar{\mu}_0) \varepsilon \quad (65)$$

where (3) has been used. Substituting for ε from (54), the mass energy density of the stationary edge dislocation is given by

$$\rho c^2 = \frac{4b}{\pi} \frac{\bar{\kappa}_0 \bar{\mu}_0}{2\bar{\mu}_0 + \bar{\lambda}_0} \frac{y}{x^2 + y^2}. \quad (66)$$

In cylindrical polar coordinates, (66) is expressed as

$$\rho c^2 = \frac{4b}{\pi} \frac{\bar{\kappa}_0 \bar{\mu}_0}{2\bar{\mu}_0 + \bar{\lambda}_0} \frac{\sin \theta}{r}. \quad (67)$$

Using (54) in (50), the stationary edge dislocation longitudinal dilatation strain energy density is then given by

$$\mathcal{E}_{||} = \frac{b^2}{2\pi^2} \frac{\bar{\kappa}_0 \bar{\mu}_0^2}{(2\bar{\mu}_0 + \bar{\lambda}_0)^2} \frac{y^2}{(x^2 + y^2)^2}. \quad (68)$$

In cylindrical polar coordinates, (68) is expressed as

$$\mathcal{E}_{||} = \frac{b^2}{2\pi^2} \frac{\bar{\kappa}_0 \bar{\mu}_0^2}{(2\bar{\mu}_0 + \bar{\lambda}_0)^2} \frac{\sin^2 \theta}{r^2}. \quad (69)$$

The distortion strain energy density is calculated from (51). The expression is expanded using the non-zero elements of the strain tensor (40) to give

$$\mathcal{E}_{\perp} = \bar{\mu}_0 (e_{xx}^2 + e_{yy}^2 + e_{xy}^2 + e_{yx}^2). \quad (70)$$

As seen previously in (33),

$$e^{\alpha\beta} = \varepsilon^{\alpha\beta} - e_s g^{\alpha\beta} \quad (71)$$

where $e_s = \frac{1}{4} \varepsilon$ is the volume dilatation calculated in (54) and

$$e^{\alpha\beta} e_{\alpha\beta} = \left(\varepsilon^{\alpha\beta} - \frac{1}{4} \varepsilon g^{\alpha\beta} \right) \left(\varepsilon_{\alpha\beta} - \frac{1}{4} \varepsilon g_{\alpha\beta} \right). \quad (72)$$

For $g^{\alpha\beta} = \eta^{\alpha\beta}$, the off-diagonal elements of the metric tensor are 0, the diagonal elements are 1 and (70) becomes

$$\mathcal{E}_{\perp} = \bar{\mu}_0 \left[\left(\varepsilon_{xx} - \frac{1}{4} \varepsilon \right)^2 + \left(\varepsilon_{yy} - \frac{1}{4} \varepsilon \right)^2 + 2\varepsilon_{xy}^2 \right]. \quad (73)$$

Expanding the quadratic terms and making use of (53), (73) becomes

$$\mathcal{E}_{\perp} = \bar{\mu}_0 \left(\varepsilon_{xx}^2 + \varepsilon_{yy}^2 - \frac{3}{8} \varepsilon^2 + 2\varepsilon_{xy}^2 \right) \quad (74)$$

and finally

$$\mathcal{E}_{\perp} = \bar{\mu}_0 \left(\frac{5}{8} \varepsilon^2 - 2\varepsilon_{xx}\varepsilon_{yy} + 2\varepsilon_{xy}^2 \right). \quad (75)$$

Substituting from (40) and (54) in the above,

$$\begin{aligned} \mathcal{E}_{\perp} = & \frac{5}{8} \frac{b^2 \bar{\mu}_0}{\pi^2} \left(\frac{\bar{\mu}_0}{2\bar{\mu}_0 + \bar{\lambda}_0} \right)^2 \frac{y^2}{(x^2 + y^2)^2} + \frac{b^2 \bar{\mu}_0}{2\pi^2} \\ & \frac{y^2 \left[(3\bar{\mu}_0 + 2\bar{\lambda}_0)(\bar{\mu}_0 + 2\bar{\lambda}_0)x^4 - 2\bar{\mu}_0^2 x^2 y^2 - \bar{\mu}_0^2 y^4 \right]}{(2\bar{\mu}_0 + \bar{\lambda}_0)^2 (x^2 + y^2)^4} + \\ & + \frac{b^2 \bar{\mu}_0}{2\pi^2} \left(\frac{\bar{\mu}_0 + \bar{\lambda}_0}{2\bar{\mu}_0 + \bar{\lambda}_0} \right)^2 \frac{x^2 (x^2 - y^2)^2}{(x^2 + y^2)^4}. \end{aligned} \quad (76)$$

which becomes

$$\begin{aligned} \mathcal{E}_{\perp} = & \frac{b^2}{2\pi^2} \frac{\bar{\mu}_0}{(2\bar{\mu}_0 + \bar{\lambda}_0)^2} \frac{1}{(x^2 + y^2)^4} \\ & \left\{ \frac{5}{4} \bar{\mu}_0^2 y^2 (x^2 + y^2)^2 - \right. \\ & - y^2 \left[(3\bar{\mu}_0 + 2\bar{\lambda}_0)(\bar{\mu}_0 + 2\bar{\lambda}_0)x^4 - 2\bar{\mu}_0^2 x^2 y^2 - \bar{\mu}_0^2 y^4 \right] + \\ & \left. + (\bar{\mu}_0 + \bar{\lambda}_0)^2 x^2 (x^2 - y^2)^2 \right\}. \end{aligned} \quad (77)$$

In cylindrical polar coordinates, (77) is expressed as

$$\begin{aligned} \mathcal{E}_{\perp} = & \frac{b^2}{2\pi^2} \frac{\bar{\mu}_0}{(2\bar{\mu}_0 + \bar{\lambda}_0)^2} \left\{ \frac{5}{4} \bar{\mu}_0^2 \frac{\sin^2 \theta}{r^2} - \frac{\sin^2 \theta}{r^2} \right. \\ & \left[(3\bar{\mu}_0 + 2\bar{\lambda}_0)(\bar{\mu}_0 + 2\bar{\lambda}_0) \cos^4 \theta - \right. \\ & - 2\bar{\mu}_0^2 \cos^2 \theta \sin^2 \theta - \bar{\mu}_0^2 \sin^4 \theta \left. \right] + \\ & \left. + (\bar{\mu}_0 + \bar{\lambda}_0)^2 \frac{\cos^2 \theta}{r^2} (\cos^2 \theta - \sin^2 \theta)^2 \right\} \end{aligned} \quad (78)$$

or

$$\begin{aligned} \mathcal{E}_\perp = & \frac{b^2}{2\pi^2} \frac{\bar{\mu}_0}{(2\bar{\mu}_0 + \bar{\lambda}_0)^2} \left\{ \frac{5}{4} \bar{\mu}_0^2 \frac{\sin^2 \theta}{r^2} - \right. \\ & - \left[(3\bar{\mu}_0 + 2\bar{\lambda}_0)(\bar{\mu}_0 + 2\bar{\lambda}_0) \cos^4 \theta \frac{\sin^2 \theta}{r^2} - \right. \\ & - 2\bar{\mu}_0^2 \cos^2 \theta \frac{\sin^4 \theta}{r^2} - \bar{\mu}_0^2 \frac{\sin^6 \theta}{r^2} \left. \right] + \\ & \left. + (\bar{\mu}_0 + \bar{\lambda}_0)^2 \cos^2 2\theta \frac{\cos^2 \theta}{r^2} \right\}. \end{aligned} \quad (79)$$

4.3.2 Moving edge dislocation energy density

We next consider the general case of the moving edge dislocation in the spacetime continuum of Section 4.2, with cartesian coordinates (x, y, z) . We first evaluate the volume dilatation ε for the moving edge dislocation. The volume dilatation is given by

$$\varepsilon = \varepsilon^\alpha_\alpha = \varepsilon_{xx} + \varepsilon_{yy} \quad (80)$$

where the non-zero diagonal elements of the strain tensor are obtained from (46). Substituting for ε_{xx} and ε_{yy} from (46) in (80), we notice that the transverse terms cancel out, and we are left with the following longitudinal term:

$$\varepsilon = \frac{bc^2y}{\pi v^2} \frac{\gamma_l^3 - \gamma_l}{(x - vt)^2 + \gamma_l^2 y^2} \quad (81)$$

This equation can be further reduced to

$$\varepsilon = \frac{bc^2}{\pi v^2} \frac{v^2}{c_l^2} \frac{\gamma_l y}{(x - vt)^2 + \gamma_l^2 y^2} \quad (82)$$

and finally, using $c^2/c_l^2 = \bar{\mu}_0/(2\bar{\mu}_0 + \bar{\lambda}_0)$ (see (9) and (44)),

$$\varepsilon(x_i, t) = \frac{b}{2\pi} \frac{2\bar{\mu}_0}{2\bar{\mu}_0 + \bar{\lambda}_0} \frac{\gamma_l y}{(x - vt)^2 + \gamma_l^2 y^2}. \quad (83)$$

As seen previously, the mass energy density is calculated from (65):

$$\rho c^2 = 4\bar{\kappa}_0 \varepsilon = 2(2\bar{\lambda}_0 + \bar{\mu}_0) \varepsilon. \quad (84)$$

Substituting for ε from (83), the mass energy density of an edge dislocation is given by

$$\rho(x_i, t) c^2 = \frac{b}{2\pi} \frac{8\bar{\kappa}_0 \bar{\mu}_0}{2\bar{\mu}_0 + \bar{\lambda}_0} \frac{\gamma_l y}{(x - vt)^2 + \gamma_l^2 y^2}. \quad (85)$$

Using (83) in (50), the edge dislocation longitudinal dilatation strain energy density is then given by

$$\mathcal{E}_\parallel = \frac{1}{2} \bar{\kappa}_0 \left(\frac{b}{2\pi} \frac{2\bar{\mu}_0}{2\bar{\mu}_0 + \bar{\lambda}_0} \frac{\gamma_l y}{(x - vt)^2 + \gamma_l^2 y^2} \right)^2. \quad (86)$$

The distortion strain energy density is calculated from (51). The expression is expanded using the non-zero elements of the strain tensor (46) and (47) and, from (71) and (72), we obtain [1, see Eqs.(114–115)]

$$\begin{aligned} \mathcal{E}_\perp = & \bar{\mu}_0 \left[\left(\varepsilon_{xx} - \frac{1}{4} \varepsilon \right)^2 + \left(\varepsilon_{yy} - \frac{1}{4} \varepsilon \right)^2 \right. \\ & \left. - 2\varepsilon_{tx}^2 - 2\varepsilon_{ty}^2 + 2\varepsilon_{xy}^2 \right]. \end{aligned} \quad (87)$$

Expanding the quadratic terms and making use of (53) as in (74), (87) becomes

$$\mathcal{E}_\perp = \bar{\mu}_0 \left(\varepsilon_{xx}^2 + \varepsilon_{yy}^2 - \frac{3}{8} \varepsilon^2 - 2\varepsilon_{tx}^2 - 2\varepsilon_{ty}^2 + 2\varepsilon_{xy}^2 \right). \quad (88)$$

Substituting from (46), (47) and (82),

$$\begin{aligned} \mathcal{E}_\perp = & \bar{\mu}_0 \left(\frac{b}{2\pi} \frac{c^2}{v^2} \right)^2 \left\{ -\frac{3}{8} \left(2 \frac{v^2}{c_l^2} \frac{\gamma_l y}{(x - vt)^2 + \gamma_l^2 y^2} \right)^2 + \right. \\ & + 4 \left(\frac{-\gamma_l y}{(x - vt)^2 + \gamma_l^2 y^2} + \frac{\alpha^2 \gamma y}{(x - vt)^2 + \gamma^2 y^2} \right)^2 + \\ & + 4 \left(\frac{\gamma_l^3 y}{(x - vt)^2 + \gamma_l^2 y^2} - \frac{\alpha^2 \gamma y}{(x - vt)^2 + \gamma^2 y^2} \right)^2 - \\ & - 2 \frac{v^2}{c^2} \left(\frac{\gamma_l y}{(x - vt)^2 + \gamma_l^2 y^2} - \alpha^2 \frac{\gamma y}{(x - vt)^2 + \gamma^2 y^2} \right)^2 - \\ & - 2 \frac{v^2}{c^2} \left(\frac{-\gamma_l (x - vt)}{(x - vt)^2 + \gamma_l^2 y^2} + \frac{\alpha^2}{\gamma^2} \frac{\gamma (x - vt)}{(x - vt)^2 + \gamma^2 y^2} \right)^2 + \\ & \left. + 2 \left(\frac{2\gamma_l (x - vt)}{(x - vt)^2 + \gamma_l^2 y^2} - \frac{\alpha^2 (\gamma + 1/\gamma) (x - vt)}{(x - vt)^2 + \gamma^2 y^2} \right)^2 \right\} \end{aligned} \quad (89)$$

which simplifies to

$$\begin{aligned} \mathcal{E}_\perp = & \bar{\mu}_0 \frac{b^2}{2\pi^2} \frac{c^4}{v^4} \left\{ \frac{\alpha^4 (3 + \gamma^2)}{(x - vt)^2 + \gamma^2 y^2} - \right. \\ & - 2\alpha^2 \frac{\left(3 + \frac{1}{\gamma^2} \right) \gamma_l \gamma (x - vt)^2 + \left(2\gamma_l^2 - \frac{v^2}{c^2} \right) \gamma_l \gamma y^2}{\left((x - vt)^2 + \gamma_l^2 y^2 \right) \left((x - vt)^2 + \gamma^2 y^2 \right)} + \\ & \left. + \frac{\left(3 + \gamma^2 \right) \gamma_l^2 (x - vt)^2 + 2 \left(\alpha^2 + \gamma_l^4 - \frac{3}{8} \frac{v^4}{c_l^4} \right) \gamma_l^2 y^2}{\left((x - vt)^2 + \gamma_l^2 y^2 \right)^2} \right\}. \end{aligned} \quad (90)$$

We consider the above equations for the moving edge dislocation in the limit as $v \rightarrow 0$. Then the terms

$$\frac{\gamma y}{(x - vt)^2 + \gamma^2 y^2} \rightarrow \frac{\sin \theta}{r} \quad (91)$$

and

$$\frac{x - vt}{(x - vt)^2 + \gamma^2 y^2} \rightarrow \frac{\cos \theta}{r} \quad (92)$$

in cylindrical polar coordinates. Similarly for the same terms with γ_l instead of γ .

The volume dilatation obtained from (83) is then given in cylindrical polar coordinates (r, θ, z) by

$$\varepsilon \rightarrow \frac{b}{2\pi} \frac{2\bar{\mu}_0}{2\bar{\mu}_0 + \bar{\lambda}_0} \frac{\sin \theta}{r}. \quad (93)$$

The mass energy density is obtained from (85) to give

$$\rho c^2 \rightarrow \frac{b}{2\pi} \frac{8\bar{\kappa}_0\bar{\mu}_0}{2\bar{\mu}_0 + \bar{\lambda}_0} \frac{\sin \theta}{r}. \quad (94)$$

From (86), the edge dislocation dilatation strain energy density is then given by

$$\mathcal{E}_{\parallel} \rightarrow \frac{b^2}{2\pi^2} \frac{\bar{\kappa}_0\bar{\mu}_0^2}{(2\bar{\mu}_0 + \bar{\lambda}_0)^2} \frac{\sin^2 \theta}{r^2}. \quad (95)$$

These equations are in agreement with (55), (67) and (69) respectively.

The edge dislocation distortion strain energy density in the limit as $v \rightarrow 0$ is obtained from (89) by making use of (91) and (92) as follows:

$$\begin{aligned} \mathcal{E}_{\perp} \rightarrow & \bar{\mu}_0 \frac{b^2}{4\pi^2} \frac{c^4}{v^4} \left\{ -\frac{3}{2} \frac{v^4}{c_l^4} \frac{\sin^2 \theta}{r^2} + \right. \\ & + 4 \left(-\frac{\sin \theta}{r} + \alpha^2 \frac{\sin \theta}{r} \right)^2 + 4 \left(\gamma_l^2 \frac{\sin \theta}{r} - \alpha^2 \frac{\sin \theta}{r} \right)^2 - \\ & - 2 \frac{v^2}{c^2} \left(\frac{\sin \theta}{r} - \alpha^2 \frac{\sin \theta}{r} \right)^2 - \\ & - 2 \frac{v^2}{c^2} \left(-\gamma_l \frac{\cos \theta}{r} + \frac{\alpha^2}{\gamma} \frac{\cos \theta}{r} \right)^2 + \\ & \left. + 2 \left(2\gamma_l \frac{\cos \theta}{r} - \alpha^2 \left(\gamma + \frac{1}{\gamma} \right) \frac{\cos \theta}{r} \right)^2 \right\}. \end{aligned} \quad (96)$$

Simplifying,

$$\begin{aligned} \mathcal{E}_{\perp} \rightarrow & \bar{\mu}_0 \frac{b^2}{4\pi^2} \frac{c^4}{v^4} \left\{ -\frac{3}{2} \frac{v^4}{c_l^4} \frac{\sin^2 \theta}{r^2} + \right. \\ & + 4(-1 + \alpha^2)^2 \frac{\sin^2 \theta}{r^2} + 4(\gamma_l^2 - \alpha^2)^2 \frac{\sin^2 \theta}{r^2} - \\ & - 2 \frac{v^2}{c^2} (1 - \alpha^2)^2 \frac{\sin^2 \theta}{r^2} - \\ & - 2 \frac{v^2}{c^2} \left(-\gamma_l + \frac{\alpha^2}{\gamma} \right)^2 \frac{\cos^2 \theta}{r^2} + \\ & \left. + 2 \left(2\gamma_l - \alpha^2 \left(\gamma + \frac{1}{\gamma} \right) \right)^2 \frac{\cos^2 \theta}{r^2} \right\}. \end{aligned} \quad (97)$$

Using the definitions of γ^2 , γ_l^2 and α^2 from (27), (42) and (43) respectively, using the first term of the Taylor expansion for

γ and γ_l as $v \rightarrow 0$, and neglecting the terms multiplied by $-2v^2/c^2$ in (97) as they are of order v^6/c^6 , (97) becomes

$$\begin{aligned} \mathcal{E}_{\perp} \rightarrow & \bar{\mu}_0 \frac{b^2}{4\pi^2} \frac{c^4}{v^4} \left\{ \left[-\frac{3}{2} \frac{v^4}{c_l^4} + \frac{v^4}{c^4} + \right. \right. \\ & \left. \left. + 4 \left(1 - \frac{v^2}{c_l^2} - 1 + \frac{v^2}{2c^2} \right)^2 \right] \frac{\sin^2 \theta}{r^2} + \right. \\ & \left. + 4 \left[1 - \frac{1}{2} \frac{v^2}{c_l^2} - 1 + \frac{v^2}{2c^2} \right]^2 \frac{\cos^2 \theta}{r^2} \right\}. \end{aligned} \quad (98)$$

Squaring and simplifying, we obtain

$$\begin{aligned} \mathcal{E}_{\perp} \rightarrow & \bar{\mu}_0 \frac{b^2}{4\pi^2} \frac{c^4}{v^4} \left\{ \left(\frac{5}{2} \frac{v^4}{c_l^4} + 2 \frac{v^4}{c^4} + 4 \frac{v^4}{c_l^2 c^2} \right) \frac{\sin^2 \theta}{r^2} + \right. \\ & \left. + \left(\frac{v^4}{c_l^4} + \frac{v^4}{c^4} - 2 \frac{v^4}{c_l^2 c^2} \right) \frac{\cos^2 \theta}{r^2} \right\} \end{aligned} \quad (99)$$

and further

$$\begin{aligned} \mathcal{E}_{\perp} \rightarrow & \bar{\mu}_0 \frac{b^2}{2\pi^2} \left\{ \left(1 + 2 \frac{c^2}{c_l^2} + \frac{5}{4} \frac{c^4}{c_l^4} \right) \frac{\sin^2 \theta}{r^2} + \right. \\ & \left. + \frac{1}{2} \left(1 - 2 \frac{c^2}{c_l^2} + \frac{c^4}{c_l^4} \right) \frac{\cos^2 \theta}{r^2} \right\}. \end{aligned} \quad (100)$$

Using $c^2/c_l^2 = \bar{\mu}_0/(2\bar{\mu}_0 + \bar{\lambda}_0)$ (see (9) and (44)), (100) becomes

$$\begin{aligned} \mathcal{E}_{\perp} \rightarrow & \bar{\mu}_0 \frac{b^2}{2\pi^2} \left\{ \left(1 + \frac{2\bar{\mu}_0}{2\bar{\mu}_0 + \bar{\lambda}_0} + \right. \right. \\ & \left. \left. + \frac{5}{4} \frac{\bar{\mu}_0^2}{(2\bar{\mu}_0 + \bar{\lambda}_0)^2} \right) \frac{\sin^2 \theta}{r^2} + \frac{1}{2} \left(1 - \right. \right. \\ & \left. \left. - \frac{2\bar{\mu}_0}{2\bar{\mu}_0 + \bar{\lambda}_0} + \frac{\bar{\mu}_0^2}{(2\bar{\mu}_0 + \bar{\lambda}_0)^2} \right) \frac{\cos^2 \theta}{r^2} \right\}. \end{aligned} \quad (101)$$

This equation represents the impact of the time terms included in the calculation of (87) and the limit operation $v \rightarrow 0$ used in (89).

5 Curved dislocations

In this section, we consider the equations for generally curved dislocations generated by infinitesimal elements of a dislocation. These allow us to handle complex dislocations that are encountered in the spacetime continuum.

5.1 The Burgers displacement equation

The Burgers displacement equation for an infinitesimal element of a dislocation $d\mathbf{l} = \boldsymbol{\xi} dl$ in vector notation is given by [14, see p. 102]

$$\begin{aligned} \mathbf{u}(\mathbf{r}) = & \frac{\mathbf{b}}{4\pi} \int_A \frac{\hat{\mathbf{R}} \cdot d\mathbf{A}}{R^2} - \frac{1}{4\pi} \oint_C \frac{\mathbf{b} \times d\mathbf{l}'}{R} + \\ & + \frac{1}{4\pi} \frac{\bar{\mu}_0 + \bar{\lambda}_0}{2\bar{\mu}_0 + \bar{\lambda}_0} \nabla \left[\oint_C \frac{(\mathbf{b} \times \mathbf{R}) \cdot d\mathbf{l}'}{R} \right] \end{aligned} \quad (102)$$

where \mathbf{u} is the displacement vector, \mathbf{r} is the vector to the displaced point, \mathbf{r}' is the vector to the dislocation infinitesimal element $d\mathbf{l}'$, $\mathbf{R} = \mathbf{r}' - \mathbf{r}$, \mathbf{b} is the Burgers vector, and closed loop C bounds the area A .

In tensor notation, (102) is given by

$$u_\mu(r^\nu) = -\frac{1}{8\pi} \int_A b_\mu \frac{\partial}{\partial x'^\alpha} (\nabla'^2 R) dA^\alpha - \frac{1}{8\pi} \oint_C b^\beta \epsilon_{\mu\beta\gamma} \nabla'^2 R dx'^\gamma - \frac{1}{4\pi} \frac{\bar{\mu}_0 + \bar{\lambda}_0}{2\bar{\mu}_0 + \bar{\lambda}_0} \oint_C b_\beta \epsilon^{\beta\alpha\gamma} \frac{\partial^2 R}{\partial x'^\mu \partial x'^\alpha} dx'_\gamma \quad (103)$$

where $\epsilon^{\alpha\beta\gamma}$ is the permutation symbol, equal to 1 for cyclic permutations, -1 for anti-cyclic permutations, and 0 for permutations involving repeated indices. As noted by Hirth [14, see p. 103], the first term of this equation gives a discontinuity $\Delta \mathbf{u} = \mathbf{b}$ over the surface A , while the two other terms are continuous except at the dislocation line. This equation is used to calculate the displacement produced at a point \mathbf{r} by an arbitrary curved dislocation by integration over the dislocation line.

5.2 The Peach and Koehler stress equation

The Peach and Koehler stress equation for an infinitesimal element of a dislocation is derived by differentiation of (103) and substitution of the result in (20) [14, see p. 103–106]. In this equation, the dislocation is defined continuous except at the dislocation core, removing the discontinuity over the surface A and allowing to express the stresses in terms of line integrals alone.

$$\sigma_{\mu\nu} = -\frac{\bar{\mu}_0}{8\pi} \oint_C b^\alpha \epsilon_{\beta\alpha\mu} \frac{\partial}{\partial x'^\beta} (\nabla'^2 R) dx'_\nu - \frac{\bar{\mu}_0}{8\pi} \oint_C b^\alpha \epsilon_{\beta\alpha\nu} \frac{\partial}{\partial x'^\beta} (\nabla'^2 R) dx'_\mu - \frac{\bar{\mu}_0}{4\pi} \frac{\bar{\mu}_0 + \bar{\lambda}_0}{2\bar{\mu}_0 + \bar{\lambda}_0} \oint_C b_\alpha \epsilon^{\beta\alpha\gamma} \left(\frac{\partial^3 R}{\partial x'^\beta \partial x'^\mu \partial x'^\nu} - \delta_{\mu\nu} \frac{\partial}{\partial x'^\beta} (\nabla'^2 R) \right) dx'_\gamma. \quad (104)$$

This equation is used to calculate the stress field of an arbitrary curved dislocation by line integration.

6 Framework for quantum physics

In a solid, dislocations represent the fundamental displacement processes that occur in its atomic structure. A solid viewed in electron microscopy or other microscopic imaging techniques is a tangle of screw and edge dislocations [10, see p. 35 and accompanying pages]. Similarly, dislocations in the spacetime continuum are taken to represent the fundamental displacement processes that occur in its structure. These fundamental displacement processes should thus correspond to

basic quantum phenomena and provide a framework for the description of quantum physics in *STCED*.

We find that dislocations have fundamental properties that reflect those of particles at the quantum level. These include self-energy and interactions mediated by the strain energy density of the dislocations. The role played by virtual particles in Quantum Electrodynamics is replaced by the interaction of the energy density of the dislocations. This theory is not perturbative as in QED, but rather calculated from analytical expressions. The analytical equations can become very complicated, and in some cases, perturbative techniques are used to simplify the calculations, but the availability of analytical expressions permit a better understanding of the fundamental processes involved.

Although the existence of virtual particles in QED is generally accepted, there are physicists who still question this interpretation of QED perturbation expansions. Weingard [41] “argues that if certain elements of the orthodox interpretation of states in QM are applicable to QED, then it must be concluded that virtual particles cannot exist. This follows from the fact that the transition amplitudes correspond to superpositions in which virtual particle type and number are not sharp. Weingard argues further that analysis of the role of measurement in resolving the superposition strengthens this conclusion. He then demonstrates in detail how in the path integral formulation of field theory no creation and annihilation operators need appear, yet virtual particles are still present. This analysis shows that the question of the existence of virtual particles is really the question of how to interpret the propagators which appear in the perturbation expansion of vacuum expectation values (scattering amplitudes).” [42]

The basic Feynman diagrams can be seen to represent screw dislocations as photons, edge dislocations as particles, and their interactions. The exchange of virtual particles in interactions can be taken as the forces resulting from the overlap of the dislocations’ strain energy density, with suitably modified diagrams. The perturbative expansions are also replaced by finite analytical expressions.

6.1 Quantization

The Burgers vector as defined by expression (5) has similarities to the Bohr-Sommerfeld quantization rule

$$\oint_C p dq = nh \quad (105)$$

where q is the position canonical coordinate, p is the momentum canonical coordinate and h is Planck’s constant. This leads us to consider the following quantization rule for the *STC*: at the quantum level, we assume that the spacetime continuum has a granularity characterized by a length b_0 corresponding to the smallest elementary Burgers dislocation-displacement vector possible in the *STC*. The idea that the existence of a shortest length in nature would lead to a natural cut-off to generate finite integrals in QED has been raised

before [43]. The smallest elementary Burgers dislocation-displacement vector introduced here provides a lower bound as shown in the next section. Then the magnitude of a Burgers vector can be expressed as a multiple of the elementary Burgers vector:

$$b = nb_0. \tag{106}$$

We find that b is usually divided by 2π in dislocation equations, and hence we define

$$\tilde{b} = \frac{b}{2\pi}, \tag{107}$$

and similarly for the elementary Burgers dislocation-displacement vector b_0 ,

$$\tilde{b}_0 = \frac{b_0}{2\pi}. \tag{108}$$

6.2 Screw dislocations in quantum physics

Screw dislocations in the spacetime continuum are identified with massless, transverse deformations, specifically photons. Consider the displacement of a stationary screw dislocation as derived in Section 3.1:

$$u_z = \frac{b}{2\pi} \theta = \tilde{b} \theta. \tag{109}$$

Taking the derivative with respect to time, we obtain

$$\dot{u}_z = v_z = \frac{b}{2\pi} \dot{\theta} = \frac{b}{2\pi} \omega. \tag{110}$$

The speed of the transverse displacement is c , the speed of light. Substituting for $\omega = 2\pi\nu$, (110) becomes

$$c = b\nu. \tag{111}$$

Hence

$$b = \lambda, \tag{112}$$

the wavelength of the screw dislocation. This result is illustrated in Fig. 5. It is important to note that this relation applies only to screw dislocations.

The strain energy density of the screw dislocation is given by the transverse distortion energy density derived in Section 3.3. For a stationary screw dislocation, substituting (107) into (35),

$$\mathcal{E}_\perp = \frac{\bar{\mu}_0 \tilde{b}^2}{2} \frac{1}{r^2}. \tag{113}$$

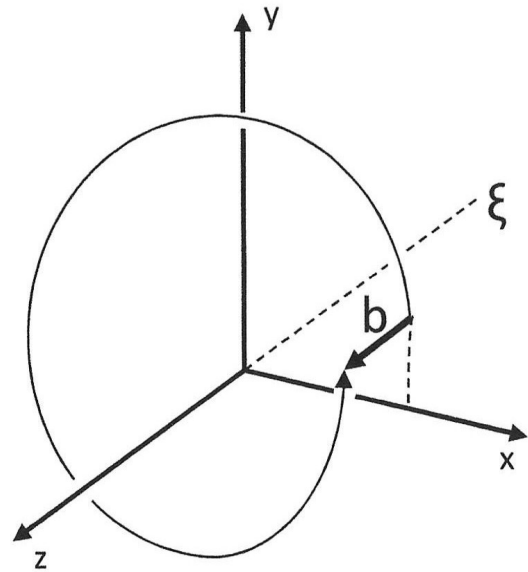
The total strain energy of the screw dislocation is then given by

$$W_\perp = \int_V \mathcal{E}_\perp dV \tag{114}$$

where the volume element dV in cylindrical polar coordinates is given by $rdr d\theta dz$. Substituting for \mathcal{E}_\perp from (113), (114) becomes

$$W_\perp = \int_V \frac{\bar{\mu}_0 \tilde{b}^2}{2r^2} r dr d\theta dz. \tag{115}$$

Fig. 5: A wavelength of a screw dislocation.



From (106), \tilde{b} can be taken out of the integral to give

$$W_\perp = \frac{\bar{\mu}_0 \tilde{b}^2}{2} \int_b^\Lambda \frac{1}{r} dr \int_\theta d\theta \int_z dz \tag{116}$$

where Λ is a cut-off parameter corresponding to the radial extent of the dislocation, limited by the average distance to its nearest neighbours.

The strain energy per wavelength is then given by

$$\frac{W_\perp}{\lambda} = \frac{\bar{\mu}_0 \tilde{b}^2}{2} \log \frac{\Lambda}{b} \int_0^{2\pi} d\theta \tag{117}$$

and finally

$$\frac{W_\perp}{\lambda} = \frac{\bar{\mu}_0 b^2}{4\pi} \log \frac{\Lambda}{b}. \tag{118}$$

The implications of the total strain energy of the screw dislocation are discussed further in comparison to Quantum Electrodynamics (QED) in Section 7.

6.3 Edge dislocations in quantum physics

The strain energy density of the edge dislocation is derived in Section 4.3. The dilatation (massive) strain energy density of the edge dislocation is given by the longitudinal strain energy density (50) and the distortion (massless) strain energy density of the edge dislocation is given by the transverse strain energy density (51).

For the stationary edge dislocation of (79), using (107)

into (79), we have

$$\begin{aligned} \mathcal{E}_\perp = & \frac{2\bar{b}^2\bar{\mu}_0}{(2\bar{\mu}_0 + \bar{\lambda}_0)^2} \left\{ \frac{5}{4}\bar{\mu}_0^2 \frac{\sin^2 \theta}{r^2} - \right. \\ & - \left[(3\bar{\mu}_0 + 2\bar{\lambda}_0)(\bar{\mu}_0 + 2\bar{\lambda}_0) \cos^4 \theta \frac{\sin^2 \theta}{r^2} - \right. \\ & - 2\bar{\mu}_0^2 \cos^2 \theta \frac{\sin^4 \theta}{r^2} - \bar{\mu}_0^2 \frac{\sin^6 \theta}{r^2} \left. \right] + \\ & \left. + (\bar{\mu}_0 + \bar{\lambda}_0)^2 \cos^2 2\theta \frac{\cos^2 \theta}{r^2} \right\}. \end{aligned} \quad (119)$$

The distortion strain energy of the edge dislocation is then given by

$$W_\perp = \int_V \mathcal{E}_\perp dV \quad (120)$$

where the volume element dV in cylindrical polar coordinates is given by $rdr d\theta dz$. Substituting for \mathcal{E}_\perp from (119) and taking \bar{b} out of the integral, (120) becomes

$$\begin{aligned} W_\perp = & \frac{2\bar{b}^2\bar{\mu}_0}{(2\bar{\mu}_0 + \bar{\lambda}_0)^2} \int_z \int_\theta \int_{b_0}^\Lambda \left\{ \frac{5}{4}\bar{\mu}_0^2 \frac{\sin^2 \theta}{r^2} - \right. \\ & - \left[(3\bar{\mu}_0 + 2\bar{\lambda}_0)(\bar{\mu}_0 + 2\bar{\lambda}_0) \cos^4 \theta \frac{\sin^2 \theta}{r^2} - \right. \\ & - 2\bar{\mu}_0^2 \cos^2 \theta \frac{\sin^4 \theta}{r^2} - \bar{\mu}_0^2 \frac{\sin^6 \theta}{r^2} \left. \right] + \\ & \left. + (\bar{\mu}_0 + \bar{\lambda}_0)^2 \cos^2 2\theta \frac{\cos^2 \theta}{r^2} \right\} r dr d\theta dz \end{aligned} \quad (121)$$

where again Λ is a cut-off parameter corresponding to the radial extent of the dislocation, limited by the average distance to its nearest neighbours.

Evaluating the integral over r ,

$$\begin{aligned} W_\perp = & \frac{2\bar{b}^2\bar{\mu}_0}{(2\bar{\mu}_0 + \bar{\lambda}_0)^2} \log \frac{\Lambda}{b_0} \int_z \int_0^{2\pi} \left\{ \frac{5}{4}\bar{\mu}_0^2 \sin^2 \theta - \right. \\ & - \left[(3\bar{\mu}_0 + 2\bar{\lambda}_0)(\bar{\mu}_0 + 2\bar{\lambda}_0) \cos^4 \theta \sin^2 \theta - \right. \\ & - 2\bar{\mu}_0^2 \cos^2 \theta \sin^4 \theta - \bar{\mu}_0^2 \sin^6 \theta \left. \right] + \\ & \left. + (\bar{\mu}_0 + \bar{\lambda}_0)^2 \cos^2 2\theta \cos^2 \theta \right\} d\theta dz. \end{aligned} \quad (122)$$

Evaluating the integral over θ [40], we obtain (123) at the top of the next page. Applying the limits of the integration, both the coefficients of $\bar{\lambda}_0^2$ and $\bar{\mu}_0\bar{\lambda}_0$ are equal to 0 and only the coefficient of $\bar{\mu}_0^2$ is non-zero. Equation (123) then becomes

$$W_\perp = \frac{2\bar{b}^2\bar{\mu}_0}{(2\bar{\mu}_0 + \bar{\lambda}_0)^2} \log \frac{\Lambda}{b_0} \int_0^\ell \frac{9\pi}{4} \bar{\mu}_0^2 dz. \quad (124)$$

where ℓ is the length of the edge dislocation.

Evaluating the integral over z , we obtain the stationary edge dislocation transverse strain energy per unit length

$$\frac{W_\perp}{\ell} = \frac{9\pi}{2} \bar{b}^2 \bar{\mu}_0 \left(\frac{\bar{\mu}_0}{2\bar{\mu}_0 + \bar{\lambda}_0} \right)^2 \log \frac{\Lambda}{b_0}. \quad (125)$$

We find that the stationary edge dislocation transverse strain energy per unit length (where we have added the label E)

$$\frac{W_\perp^E}{\ell} = \frac{9}{8\pi} \bar{b}^2 \bar{\mu}_0 \left(\frac{\bar{\mu}_0}{2\bar{\mu}_0 + \bar{\lambda}_0} \right)^2 \log \frac{\Lambda}{b_0} \quad (126)$$

is similar to the stationary screw dislocation transverse strain energy per unit length

$$\frac{W_\perp^S}{\ell} = \frac{1}{4\pi} \bar{b}^2 \bar{\mu}_0 \log \frac{\Lambda}{b_0} \quad (127)$$

except for the proportionality constant.

Similarly, the longitudinal strain energy of the stationary edge dislocation is given by

$$W_\parallel^E = \int_V \mathcal{E}_\parallel dV. \quad (128)$$

Substituting for \mathcal{E}_\parallel from (69), this equation becomes

$$W_\parallel^E = \int_V \frac{b^2}{2\pi^2} \frac{\bar{\kappa}_0 \bar{\mu}_0^2}{(2\bar{\mu}_0 + \bar{\lambda}_0)^2} \frac{\sin^2 \theta}{r^2} dV. \quad (129)$$

Similarly to the previous derivation, this integral gives

$$\frac{W_\parallel^E}{\ell} = \frac{1}{2\pi} \bar{b}^2 \bar{\kappa}_0 \left(\frac{\bar{\mu}_0}{2\bar{\mu}_0 + \bar{\lambda}_0} \right)^2 \log \frac{\Lambda}{b_0}. \quad (130)$$

The total strain energy of the stationary screw and edge dislocations have similar functional forms, with the difference residing in the proportionality constants. This is due to the simpler nature of the stationary dislocations and their cylindrical polar symmetry. This similarity is not present for the general case of moving dislocations as evidenced in equations (37), (86) and (90).

For the moving edge dislocation in the limit as $v \rightarrow 0$, substituting for (101) in (120) and using (107), we have

$$\begin{aligned} W_\perp^E \rightarrow & 2\bar{b}^2\bar{\mu}_0 \int_z \int_\theta \int_{b_0}^\Lambda r dr d\theta dz \\ & \left\{ \left(1 + \frac{2\bar{\mu}_0}{2\bar{\mu}_0 + \bar{\lambda}_0} + \frac{5}{4} \frac{\bar{\mu}_0^2}{(2\bar{\mu}_0 + \bar{\lambda}_0)^2} \right) \frac{\sin^2 \theta}{r^2} + \right. \\ & \left. + \frac{1}{2} \left(1 - \frac{2\bar{\mu}_0}{2\bar{\mu}_0 + \bar{\lambda}_0} + \frac{\bar{\mu}_0^2}{(2\bar{\mu}_0 + \bar{\lambda}_0)^2} \right) \frac{\cos^2 \theta}{r^2} \right\} \end{aligned} \quad (131)$$

where again Λ is a cut-off parameter corresponding to the radial extent of the dislocation, limited by the average distance to its nearest neighbours.

$$\begin{aligned}
 W_{\perp} = & \frac{2\bar{b}^2\bar{\mu}_0}{(2\bar{\mu}_0 + \bar{\lambda}_0)^2} \log \frac{\Lambda}{b_0} \int_z \left[\frac{5}{4} \bar{\mu}_0^2 \left(\frac{\theta}{2} - \frac{1}{4} \sin 2\theta \right) - \right. \\
 & - (3\bar{\mu}_0 + 2\bar{\lambda}_0)(\bar{\mu}_0 + 2\bar{\lambda}_0) \left(\frac{\theta}{16} + \frac{1}{64} \sin 2\theta - \frac{1}{64} \sin 4\theta - \frac{1}{192} \sin 6\theta \right) + \\
 & + 2\bar{\mu}_0^2 \left(\frac{\theta}{16} - \frac{1}{64} \sin 2\theta - \frac{1}{64} \sin 4\theta + \frac{1}{192} \sin 6\theta \right) + \\
 & + \bar{\mu}_0^2 \left(\frac{5\theta}{16} - \frac{15}{64} \sin 2\theta + \frac{3}{64} \sin 4\theta - \frac{1}{192} \sin 6\theta \right) + \\
 & \left. + (\bar{\mu}_0 + \bar{\lambda}_0)^2 \left(\frac{\theta}{4} + \frac{3}{16} \sin 2\theta + \frac{1}{16} \sin 4\theta + \frac{1}{48} \sin 6\theta \right) \right]_0^{2\pi} dz
 \end{aligned} \tag{123}$$

Evaluating the integral over r ,

$$\begin{aligned}
 W_{\perp}^E \rightarrow & 2\bar{b}^2\bar{\mu}_0 \log \frac{\Lambda}{b_0} \int_z \int_0^{2\pi} d\theta dz \\
 & \left\{ \left(1 + \frac{2\bar{\mu}_0}{2\bar{\mu}_0 + \bar{\lambda}_0} + \frac{5}{4} \frac{\bar{\mu}_0^2}{(2\bar{\mu}_0 + \bar{\lambda}_0)^2} \right) \sin^2 \theta + \right. \\
 & \left. + \frac{1}{2} \left(1 - \frac{2\bar{\mu}_0}{2\bar{\mu}_0 + \bar{\lambda}_0} + \frac{\bar{\mu}_0^2}{(2\bar{\mu}_0 + \bar{\lambda}_0)^2} \right) \cos^2 \theta \right\}.
 \end{aligned} \tag{132}$$

Evaluating the integral over θ [40] and applying the limits of the integration, we obtain

$$\begin{aligned}
 W_{\perp}^E \rightarrow & 2\bar{b}^2\bar{\mu}_0 \log \frac{\Lambda}{b_0} \int_0^{\ell} dz \\
 & \left\{ \left(1 + \frac{2\bar{\mu}_0}{2\bar{\mu}_0 + \bar{\lambda}_0} + \frac{5}{4} \frac{\bar{\mu}_0^2}{(2\bar{\mu}_0 + \bar{\lambda}_0)^2} \right) (\pi) + \right. \\
 & \left. + \frac{1}{2} \left(1 - \frac{2\bar{\mu}_0}{2\bar{\mu}_0 + \bar{\lambda}_0} + \frac{\bar{\mu}_0^2}{(2\bar{\mu}_0 + \bar{\lambda}_0)^2} \right) (\pi) \right\}
 \end{aligned} \tag{133}$$

and evaluating the integral over z , we obtain the moving edge dislocation transverse strain energy per unit length in the limit as $v \rightarrow 0$

$$\begin{aligned}
 \frac{W_{\perp}^E}{\ell} \rightarrow & \frac{3}{4\pi} \bar{b}^2\bar{\mu}_0 \left(1 + \frac{2}{3} \frac{\bar{\mu}_0}{2\bar{\mu}_0 + \bar{\lambda}_0} + \right. \\
 & \left. + \frac{7}{6} \frac{\bar{\mu}_0^2}{(2\bar{\mu}_0 + \bar{\lambda}_0)^2} \right) \log \frac{\Lambda}{b_0}
 \end{aligned} \tag{134}$$

where ℓ is the length of the edge dislocation.

6.4 Strain energy of moving dislocations

In the general case of moving dislocations, the derivation of the screw dislocation transverse strain energy and the edge dislocation transverse and longitudinal strain energies is more difficult. In this section, we provide an overview discussion of the topic.

6.4.1 Screw dislocation transverse strain energy

The transverse strain energy of a moving screw dislocation, which also corresponds to its total strain energy, is given by

$$W_{\perp}^S = \int_V \mathcal{E}_{\perp}^S dV \tag{135}$$

where the strain energy density \mathcal{E}_{\perp}^S is given by (113), viz.

$$\mathcal{E}_{\perp}^S = \frac{1}{2} \bar{b}^2 \bar{\mu}_0 \frac{\gamma^2}{(x - vt)^2 + \gamma^2 y^2} \tag{136}$$

and V is the 4-dimensional volume of the screw dislocation. The volume element dV in cartesian coordinates is given by $dx dy dz d(ct)$.

Substituting for \mathcal{E}_{\perp}^S , (135) becomes

$$W_{\perp}^S = \int_V \frac{1}{2} \bar{b}^2 \bar{\mu}_0 \frac{\gamma^2}{(x - vt)^2 + \gamma^2 y^2} dx dy dz d(ct). \tag{137}$$

As before, \bar{b} is taken out of the integral from (106), and the integral over z is handled by considering the strain energy per unit length of the dislocation:

$$\frac{W_{\perp}^S}{\ell} = \frac{\bar{b}^2 \bar{\mu}_0}{2} \int_{ct} \int_y \int_x \frac{\gamma^2}{(x - vt)^2 + \gamma^2 y^2} dx dy d(ct) \tag{138}$$

where ℓ is the length of the dislocation and as before, Λ is a cut-off parameter corresponding to the radial extent of the dislocation, limited by the average distance to its nearest neighbours.

Evaluating the integral over x [40],

$$\begin{aligned}
 \frac{W_{\perp}^S}{\ell} = & \frac{\bar{b}^2 \bar{\mu}_0}{2} \gamma^2 \int_{ct} \int_y dy d(ct) \\
 & \left[\frac{1}{\gamma y} \arctan \left(\frac{x - vt}{\gamma y} \right) \right]_{\sqrt{y^2 - b^2}}^{\sqrt{\Lambda^2 - y^2}}
 \end{aligned} \tag{139}$$

where the limits corresponding to the maximum cut-off parameter Λ and minimum cut-off parameter b are stated explicitly. Applying the limits of the integration, we obtain

$$\frac{W_{\perp}^S}{\ell} = \frac{\bar{b}^2 \bar{\mu}_0}{2} \gamma^2 \int_{ct} \int_y dy d(ct) \left\{ \frac{1}{\gamma y} \arctan \left(\frac{\sqrt{\Lambda^2 - y^2} - vt}{\gamma y} \right) - \frac{1}{\gamma y} \arctan \left(\frac{\sqrt{y^2 - b^2} - vt}{\gamma y} \right) \right\}. \tag{140}$$

This integration over y is not elementary and likely does not lead to a closed analytical form. If we consider the following simpler integral, the solution is given by

$$\int_y \frac{1}{\gamma y} \arctan \left(\frac{x - vt}{\gamma y} \right) dy = -\frac{i}{2} \left[\text{Li}_2 \left(-i \frac{x - vt}{\gamma y} \right) - \text{Li}_2 \left(i \frac{x - vt}{\gamma y} \right) \right] \tag{141}$$

where $\text{Li}_n(x)$ is the polylogarithm function. As pointed out in [44], “[t]he polylogarithm arises in Feynman diagram integrals (and, in particular, in the computation of quantum electrodynamics corrections to the electrons gyromagnetic ratio), and the special cases $n = 2$ and $n = 3$ are called the dilogarithm and the trilogarithm, respectively.” This is a further indication that the interaction of strain energies are the physical source of quantum interaction phenomena described by Feynman diagrams as will be seen in Section 7.

6.4.2 Edge dislocation longitudinal strain energy

The longitudinal strain energy of a moving edge dislocation is given by

$$W_{\parallel}^E = \int_V \mathcal{E}_{\parallel}^E dV \tag{142}$$

where the strain energy density \mathcal{E}_{\perp}^E is given by (86), viz.

$$\mathcal{E}_{\parallel}^E = \frac{1}{2} \bar{\kappa}_0 \bar{b}^2 \left(\frac{2\bar{\mu}_0}{2\bar{\mu}_0 + \bar{\lambda}_0} \frac{\gamma_1 y}{(x - vt)^2 + \gamma_1^2 y^2} \right)^2 \tag{143}$$

and V is the 4-dimensional volume of the edge dislocation. The volume element dV in cartesian coordinates is given by $dx dy dz d(ct)$.

Substituting for $\mathcal{E}_{\parallel}^E$, (142) becomes

$$W_{\parallel}^E = \int_V \frac{1}{2} \bar{\kappa}_0 \bar{b}^2 \left(\frac{2\bar{\mu}_0}{2\bar{\mu}_0 + \bar{\lambda}_0} \frac{\gamma_1 y}{(x - vt)^2 + \gamma_1^2 y^2} \right)^2 dx dy dz d(ct). \tag{144}$$

As before, \bar{b} is taken out of the integral from (106), and the integral over z is handled by considering the strain energy per

unit length of the dislocation:

$$\frac{W_{\parallel}^E}{\ell} = 2 \bar{\kappa}_0 \bar{b}^2 \frac{\bar{\mu}_0^2}{(2\bar{\mu}_0 + \bar{\lambda}_0)^2} \int_{ct} \int_y \int_x \frac{(\gamma_1 y)^2}{((x - vt)^2 + \gamma_1^2 y^2)^2} dx dy d(ct) \tag{145}$$

where ℓ is the length of the dislocation and as before, Λ is a cut-off parameter corresponding to the radial extent of the dislocation, limited by the average distance to its nearest neighbours.

The integrand has a functional form similar to that of (138), and a similar solution behaviour is expected. Evaluating the integral over x [40],

$$\frac{W_{\parallel}^E}{\ell} = 2 \bar{\kappa}_0 \bar{b}^2 \frac{\bar{\mu}_0^2}{(2\bar{\mu}_0 + \bar{\lambda}_0)^2} \int_{ct} \int_y dy d(ct) \left[\frac{1}{2} \frac{x - vt}{(x - vt)^2 + (\gamma_1 y)^2} + \frac{1}{2\gamma_1 y} \arctan \left(\frac{x - vt}{\gamma_1 y} \right) \right] \frac{\sqrt{\Lambda^2 - y^2}}{\sqrt{y^2 - b^2}} \tag{146}$$

where the limits corresponding to the maximum cut-off parameter Λ and minimum cut-off parameter b are stated explicitly. Applying the limits of the integration, we obtain

$$\frac{W_{\parallel}^E}{\ell} = 2 \bar{\kappa}_0 \bar{b}^2 \frac{\bar{\mu}_0^2}{(2\bar{\mu}_0 + \bar{\lambda}_0)^2} \int_{ct} \int_y dy d(ct) \left\{ \frac{1}{2} \frac{\sqrt{\Lambda^2 - y^2} - vt}{(\sqrt{\Lambda^2 - y^2} - vt)^2 + (\gamma_1 y)^2} - \frac{1}{2} \frac{\sqrt{y^2 - b^2} - vt}{(\sqrt{y^2 - b^2} - vt)^2 + (\gamma_1 y)^2} + \frac{1}{2\gamma_1 y} \arctan \left(\frac{\sqrt{\Lambda^2 - y^2} - vt}{\gamma_1 y} \right) - \frac{1}{2\gamma_1 y} \arctan \left(\frac{\sqrt{y^2 - b^2} - vt}{\gamma_1 y} \right) \right\}. \tag{147}$$

This integration over y is again found to be intractable, including that of (140), and likely does not lead to a closed analytical form. In the arctan Λ integral of (140) and (147), we can make the approximation $\sqrt{\Lambda^2 - y^2} \simeq \Lambda$ and evaluate this term as seen in (141):

$$\int_y \frac{1}{\gamma_1 y} \arctan \left(\frac{\Lambda - vt}{\gamma_1 y} \right) dy = -\frac{i}{2} \left[\text{Li}_2 \left(-i \frac{\Lambda - vt}{\gamma_1 y} \right) - \text{Li}_2 \left(i \frac{\Lambda - vt}{\gamma_1 y} \right) \right] \tag{148}$$

where $\text{Li}_n(x)$ is the polylogarithm function as seen previously.

6.4.3 Edge dislocation transverse strain energy

The transverse strain energy of a moving edge dislocation is given by

$$W_{\perp}^E = \int_V \mathcal{E}_{\perp}^E dV \quad (149)$$

where the strain energy density \mathcal{E}_{\perp}^E is given by (90), viz.

$$\begin{aligned} \mathcal{E}_{\perp}^E = 2\bar{\mu}_0 \bar{b}^2 \frac{c^4}{v^4} & \left\{ \frac{\alpha^4 (3 + \gamma^2)}{(x - vt)^2 + \gamma^2 y^2} - \right. \\ & - 2\alpha^2 \frac{\left(3 + \frac{1}{\gamma^2}\right) \gamma_l \gamma (x - vt)^2 + \left(2\gamma_l^2 - \frac{v^2}{c^2}\right) \gamma_l \gamma y^2}{\left((x - vt)^2 + \gamma_l^2 y^2\right) \left((x - vt)^2 + \gamma^2 y^2\right)} + \\ & \left. + \frac{(3 + \gamma^2) \gamma_l^2 (x - vt)^2 + 2\left(\alpha^2 + \gamma_l^4 - \frac{3}{8} \frac{v^4}{c_l^4}\right) \gamma_l^2 y^2}{\left((x - vt)^2 + \gamma_l^2 y^2\right)^2} \right\} \quad (150) \end{aligned}$$

and V is the 4-dimensional volume of the edge dislocation. The volume element dV in cartesian coordinates is given by $dx dy dz d(ct)$.

Substituting for \mathcal{E}_{\perp}^E as before, taking \bar{b} out of the integral from (106), and handling the integral over z by considering the strain energy per unit length of the dislocation, (149) becomes

$$\begin{aligned} \frac{W_{\perp}^E}{\ell} = 2\bar{\mu}_0 \bar{b}^2 \frac{c^4}{v^4} & \int_{ct} \int_y \int_x dx dy d(ct) \\ & \left\{ \frac{\alpha^4 (3 + \gamma^2)}{(x - vt)^2 + \gamma^2 y^2} - \right. \\ & - 2\alpha^2 \frac{\left(3 + \frac{1}{\gamma^2}\right) \gamma_l \gamma (x - vt)^2 + \left(2\gamma_l^2 - \frac{v^2}{c^2}\right) \gamma_l \gamma y^2}{\left((x - vt)^2 + \gamma_l^2 y^2\right) \left((x - vt)^2 + \gamma^2 y^2\right)} + \\ & \left. + \frac{(3 + \gamma^2) \gamma_l^2 (x - vt)^2 + 2\left(\alpha^2 + \gamma_l^4 - \frac{3}{8} \frac{v^4}{c_l^4}\right) \gamma_l^2 y^2}{\left((x - vt)^2 + \gamma_l^2 y^2\right)^2} \right\} \quad (151) \end{aligned}$$

where ℓ is the length of the dislocation and as before, Λ is a cut-off parameter corresponding to the radial extent of the dislocation, limited by the average distance to its nearest neighbours.

Again, the integrand has functional forms similar to that of (138) and (145). A similar, but more complex, solution behaviour is expected, due to the additional complexity of (151).

7 Dislocation interactions in quantum physics

As mentioned in Section 6, the basic Feynman diagrams can be seen to represent screw dislocations as photons, edge dislocations as particles, and their interactions. More specifically, the external legs of Feynman diagrams that are on mass-shell representing real particles correspond to dislocations, while the virtual off mass-shell particles are replaced by the interaction of the strain energy densities. The exchange of virtual

particles in QED interactions can be taken as the perturbation expansion representation of the forces resulting from the overlap of the strain energy density of the dislocations. The Feynman diagram propagators are replaced by the dislocation strain energy density interaction expressions.

The properties of Burgers vectors and dislocations [14, see pp.25-26] have rules similar to those of Feynman diagrams, but not equivalent as virtual particles are replaced by dislocation strain energy density interactions. A Burgers vector is invariant along a dislocation line. Two Burgers circuits are equivalent if one can be deformed into the other without crossing dislocation lines. The resultant Burgers vector within equivalent Burgers circuits is the same.

Dislocation nodes are points where multiple dislocations meet. If all the dislocation vectors ξ_i are taken to be positive away from a node, then

$$\sum_{i=1}^N \xi_i = 0 \quad (152)$$

for the N dislocations meeting at the node. Burgers vectors are conserved at dislocation nodes.

In this section, we consider the interactions of dislocations which are seen to result from the force resulting from the overlap of their strain energy density in the *STC* [14, see p. 112].

7.1 Parallel dislocation interactions

From Hirth [14, see pp. 117-118], the energy of interaction per unit length between parallel dislocations (including screw and edge dislocation components) is given by

$$\begin{aligned} \frac{W_{12}}{\ell} = & -\frac{\bar{\mu}_0}{2\pi} (\mathbf{b}_1 \cdot \boldsymbol{\xi}) (\mathbf{b}_2 \cdot \boldsymbol{\xi}) \log \frac{R}{R_{\Lambda}} - \\ & -\frac{\bar{\mu}_0}{\pi} \frac{\bar{\mu}_0 + \bar{\lambda}_0}{2\bar{\mu}_0 + \bar{\lambda}_0} (\mathbf{b}_1 \times \boldsymbol{\xi}) \cdot (\mathbf{b}_2 \times \boldsymbol{\xi}) \log \frac{R}{R_{\Lambda}} - \\ & -\frac{\bar{\mu}_0}{\pi} \frac{\bar{\mu}_0 + \bar{\lambda}_0}{2\bar{\mu}_0 + \bar{\lambda}_0} \frac{[(\mathbf{b}_1 \times \boldsymbol{\xi}) \cdot \mathbf{R}][(\mathbf{b}_2 \times \boldsymbol{\xi}) \cdot \mathbf{R}]}{R^2} \quad (153) \end{aligned}$$

where $\boldsymbol{\xi}$ is parallel to the z axis, $(\mathbf{b}_i \cdot \boldsymbol{\xi})$ are the screw components, $(\mathbf{b}_i \times \boldsymbol{\xi})$ are the edge components, R is the separation between the dislocations, and R_{Λ} is the distance from which the dislocations are brought together, resulting in the decrease in energy of the “system”.

The components of the interaction force per unit length between the parallel dislocations are obtained by differentiation:

$$\begin{aligned} \frac{F_R}{\ell} = & -\frac{\partial(W_{12}/\ell)}{\partial R} \\ \frac{F_{\theta}}{\ell} = & -\frac{1}{R} \frac{\partial(W_{12}/\ell)}{\partial \theta}. \quad (154) \end{aligned}$$

Substituting from (153), (154) becomes

$$\begin{aligned} \frac{F_R}{\ell} &= \frac{\bar{\mu}_0}{2\pi R} (\mathbf{b}_1 \cdot \boldsymbol{\xi}) (\mathbf{b}_2 \cdot \boldsymbol{\xi}) + \\ &+ \frac{\bar{\mu}_0}{\pi R} \frac{\bar{\mu}_0 + \bar{\lambda}_0}{2\bar{\mu}_0 + \bar{\lambda}_0} (\mathbf{b}_1 \times \boldsymbol{\xi}) \cdot (\mathbf{b}_2 \times \boldsymbol{\xi}) \\ \frac{F_\theta}{\ell} &= \frac{\bar{\mu}_0}{\pi R^3} \frac{\bar{\mu}_0 + \bar{\lambda}_0}{2\bar{\mu}_0 + \bar{\lambda}_0} [(\mathbf{b}_1 \cdot \mathbf{R}) [(\mathbf{b}_2 \times \mathbf{R}) \cdot \boldsymbol{\xi}] + \\ &+ (\mathbf{b}_2 \cdot \mathbf{R}) [(\mathbf{b}_1 \times \mathbf{R}) \cdot \boldsymbol{\xi}]]. \end{aligned} \quad (155)$$

7.2 Curved dislocation interactions

In this section, we extend the investigation of curved dislocations initiated in Section 5, to the interaction energy and interaction force between curved dislocations [14, see pp. 106-110]. The derivation considers the interaction between two dislocation loops, but has much more extensive applications, being extendable to the interaction energy between two arbitrarily positioned segments of dislocation lines.

If a dislocation loop 1 is brought in the vicinity of another dislocation loop 2, the stresses originating from loop 2 do work $-W_{12}$ on loop 1 where W_{12} is the interaction energy between the two dislocation loops. The work done on loop 1 represents a decrease in the strain energy of the total system. In that case, if W_{12} is negative, the energy of the system decreases and an attractive force exists between the loops [14, see p. 106].

The interaction energy between the two dislocation loops is given by [14, see p. 108]

$$\begin{aligned} W_{12} &= -\frac{\bar{\mu}_0}{2\pi} \oint_{C_1} \oint_{C_2} \frac{(\mathbf{b}_1 \times \mathbf{b}_2) \cdot (d\mathbf{l}_1 \times d\mathbf{l}_2)}{R} + \\ &+ \frac{\bar{\mu}_0}{4\pi} \oint_{C_1} \oint_{C_2} \frac{(\mathbf{b}_1 \cdot d\mathbf{l}_1) (\mathbf{b}_2 \cdot d\mathbf{l}_2)}{R} + \\ &+ \frac{\bar{\mu}_0}{2\pi} \frac{\bar{\mu}_0 + \bar{\lambda}_0}{2\bar{\mu}_0 + \bar{\lambda}_0} \oint_{C_1} \oint_{C_2} \frac{(\mathbf{b}_1 \times d\mathbf{l}_1) \cdot \mathbf{T} \cdot (\mathbf{b}_2 \times d\mathbf{l}_2)}{R} \end{aligned} \quad (156)$$

where \mathbf{T} is given by

$$T_{ij} = \frac{\partial^2 R}{\partial x_i \partial x_j}. \quad (157)$$

The force produced by an external stress acting on a dislocation loop is given by [14, see p. 109]

$$d\mathbf{F} = (\mathbf{b} \cdot \boldsymbol{\sigma}) \times d\mathbf{l} \quad (158)$$

where $\boldsymbol{\sigma}$ is the stress tensor in the medium, \mathbf{b} is the Burgers vector, and $d\mathbf{l}$ is the dislocation element. This equation can be used with (104) to determine the interaction force between dislocation segments.

As each element $d\mathbf{l}$ of a dislocation loop is acted upon by the forces caused by the stress of the other elements of the

dislocation loop, the work done against these corresponds to the self-energy of the dislocation loop. The self-energy of a dislocation loop can be calculated from (156) to give [14, see p. 110]

$$\begin{aligned} W_{self} &= \frac{\bar{\mu}_0}{8\pi} \oint_{C_1=C} \oint_{C_2=C} \frac{(\mathbf{b} \cdot d\mathbf{l}_1) (\mathbf{b} \cdot d\mathbf{l}_2)}{R} + \\ &+ \frac{\bar{\mu}_0}{4\pi} \frac{\bar{\mu}_0 + \bar{\lambda}_0}{2\bar{\mu}_0 + \bar{\lambda}_0} \oint_{C_1=C} \oint_{C_2=C} \frac{(\mathbf{b} \times d\mathbf{l}_1) \cdot \mathbf{T} \cdot (\mathbf{b} \times d\mathbf{l}_2)}{R} \end{aligned} \quad (159)$$

where \mathbf{T} is as defined in (157).

More complicated expressions can be obtained for interactions between two non-parallel straight dislocations [14, see pp. 121-123] and between a straight segment of a dislocation and a differential element of another dislocation [14, see pp. 124-131]. This latter derivation can be used for more arbitrary dislocation interactions.

7.3 Physical application of dislocation interactions

In Quantum Electrodynamics, these correspond to particle-particle and particle-photon interactions, which are taken to be mediated by virtual particles. This is in keeping with the QED picture, but as shown above, particle-particle and particle-photon interactions physically result from the overlap of their strain energy density which results in an interaction force. Again, this improved understanding of the physical nature of dislocation interactions demonstrates that the interactions do not need to be represented by virtual particle exchange as discussed in Section 6.

This theory provides a straightforward physical explanation of particle-particle and particle-photon interactions that is not based on perturbation theory, but rather on a direct evaluation of the interactions.

7.4 Photons and screw dislocation interactions

Screw dislocations interact via the force resulting from the overlap of the strain energy density of the dislocations in the *STC* [14, see p. 112].

As seen in Section 6.2, screw dislocations in the spacetime continuum are identified with the massless, transverse deformations, photons. As pointed out in [45], it has been known since the 1960s that photons can interact with each other in atomic media much like massive particles do. A review of collective effects in photon-photon interactions is given in [46].

In QED, photon-photon interactions are known as photon-photon scattering, which is thought to be mediated by virtual particles. This is in keeping with the QED picture, but as shown in this work, photon-photon interactions physically result from the overlap of their strain energy density. This improved understanding of the physical nature of photon-photon interactions demonstrates that the interaction does not need to

be represented by virtual particle exchanges, in that the nature of the physical processes involved is now understood.

From (153), the energy of interaction per unit length between parallel screw dislocations (photons) is given by

$$\frac{W_{12}^{ss}}{\ell} = -\frac{\bar{\mu}_0}{2\pi} (\mathbf{b}_1 \cdot \boldsymbol{\xi}) (\mathbf{b}_2 \cdot \boldsymbol{\xi}) \log \frac{R}{R_\Lambda} \quad (160)$$

where $\boldsymbol{\xi}$ is parallel to the z axis, $(\mathbf{b}_i \cdot \boldsymbol{\xi})$ are the screw components, R is the separation between the dislocations, and R_Λ is the distance from which the dislocations are brought together, resulting in the reduction in the energy of the 2-photon “system”.

From (155), the components of the interaction force per unit length between the parallel screw dislocations are given by:

$$\frac{F_R^{ss}}{\ell} = \frac{\bar{\mu}_0}{2\pi R} (\mathbf{b}_1 \cdot \boldsymbol{\xi}) (\mathbf{b}_2 \cdot \boldsymbol{\xi}) \quad (161)$$

$$\frac{F_\theta^{ss}}{\ell} = 0.$$

The interaction force is radial in nature, independent of the angle θ , as expected.

8 Physical explanations of QED phenomena

As we have seen in previous sections, spacetime continuum dislocations have fundamental properties that reflect those of phenomena at the quantum level. In particular, the improved understanding of the physical nature of interactions mediated by the strain energy density of the dislocations. The role played by virtual particles in Quantum Electrodynamics is replaced by the work done by the forces resulting from the dislocation stresses, and the resulting interaction of the strain energy density of the dislocations. In this section, we examine the physical explanation of QED phenomena provided by this theory, including self-energy and mass renormalization.

8.1 Dislocation self-energy and QED self energies

Dislocation self energies are found to be similar in structure to Quantum Electrodynamics self energies. They are also divergent if integrated over all of spacetime, with the divergence being logarithmic in nature. However, contrary to QED, dislocation self energies are bounded by the density of dislocations present in the spacetime continuum, which results in an upperbound to the integral of half the average distance between dislocations. As mentioned by Hirth [14], this has little impact on the accuracy of the results due to the logarithmic dependence.

The dislocation self-energy is related to the dislocation self-force. The dislocation self-force arises from the force on an element in a dislocation caused by other segments of the *same* dislocation line. This process provides an explanation for the QED self-energies without the need to resort to

the emission/absorption of virtual particles. It can be understood, and is particular to, dislocation dynamics as dislocations are defects that extend in the spacetime continuum [14, see p. 131]. Self-energy of a straight-dislocation segment of length L is given by [14, see p. 161]:

$$W_{self} = \frac{\bar{\mu}_0}{4\pi} \left((\mathbf{b} \cdot \boldsymbol{\xi})^2 + \frac{\bar{\mu}_0 + \bar{\lambda}_0}{2\bar{\mu}_0 + \bar{\lambda}_0} |(\mathbf{b} \times \boldsymbol{\xi})|^2 \right) L \left(\log \frac{L}{b} - 1 \right), \quad (162)$$

where there is no interaction between two elements of the segment when they are within $\pm b$, or equivalently

$$W_{self} = \frac{\bar{\mu}_0}{4\pi} \left((\mathbf{b} \cdot \boldsymbol{\xi})^2 + \frac{\bar{\mu}_0 + \bar{\lambda}_0}{2\bar{\mu}_0 + \bar{\lambda}_0} |(\mathbf{b} \times \boldsymbol{\xi})|^2 \right) L \log \frac{L}{eb}, \quad (163)$$

where $e = 2.71828\dots$. These equations provide analytic expressions for the non-perturbative calculation of quantum self energies and interaction energies, and eliminate the need for the virtual particle interpretation.

In particular, the pure screw (photon) self-energy

$$W_{self}^S = \frac{\bar{\mu}_0}{4\pi} (\mathbf{b} \cdot \boldsymbol{\xi})^2 L \log \frac{L}{eb} \quad (164)$$

and the pure edge (particle) self-energy

$$W_{self}^E = \frac{\bar{\mu}_0}{4\pi} \frac{\bar{\mu}_0 + \bar{\lambda}_0}{2\bar{\mu}_0 + \bar{\lambda}_0} |(\mathbf{b} \times \boldsymbol{\xi})|^2 L \log \frac{L}{eb} \quad (165)$$

are obtained from (163), while (163) is also the appropriate equation to use for the dual wave-particle “system”.

8.2 Dislocation strain energy and QED mass renormalization

This approach also resolves and eliminates the mass renormalization problem. This problem arises in QED due to the incomplete description of particle energies at the quantum level. This paper shows that the strain energy density of an edge dislocation, which corresponds to a particle, consists of a longitudinal dilatation mass density term and a transverse distortion energy density term, as shown in (49), (50), and (51).

QED, in its formulation, only uses the transverse distortion strain energy density in its calculations. This is referred to as the bare mass m_0 . However, there is no dilatation mass density term used in QED, and hence no possibility of properly deriving the mass. The bare mass m_0 is thus renormalized by replacing it with the actual experimental mass m . Using the longitudinal dilatation mass density term as in this paper will provide the correct mass m and eliminate the need for mass renormalization.

9 Discussion and conclusion

This paper provides a framework for the physical description of physical processes at the quantum level based on dislocations in the spacetime continuum within the theory of the Elastodynamics of the Spacetime Continuum (*STCED*).

We postulate that the spacetime continuum has a granularity characterized by a length b_0 corresponding to the smallest elementary Burgers dislocation-displacement vector possible. One inference that comes out of this paper is that the basic structure of spacetime consists of a lattice of cells of size b_0 , rather than the “quantum foam” currently preferred in the literature. The “quantum foam” view may well be a representation of the disturbances and fragmentation of the b_0 lattice due to dislocations and other defects in the spacetime continuum.

There are two types of dislocations: Edge dislocations correspond to dilatations (longitudinal displacements) which have an associated rest-mass energy, and are identified with particles. Screw dislocations correspond to distortions (transverse displacements) which are massless and are identified with photons when not associated with an edge dislocation. Arbitrary mixed dislocations can be decomposed into a screw component and an edge component, giving rise to wave-particle duality.

We consider both stationary and moving dislocations, and find that stationary dislocations are simpler to work with due to their cylindrical polar symmetry, but are of limited applicability. Moving screw dislocations are found to be Lorentz invariant. Moving edge dislocations involve both the speed of light corresponding to transverse displacements and the speed of longitudinal displacements c_l . However, the speed of light c upper limit also applies to edge dislocations, as the shear stress becomes infinite everywhere at $v = c$, even though the speed of longitudinal deformations c_l is greater than that of transverse deformations c .

We calculate the strain energy density of both stationary and moving screw and edge dislocations. The strain energy density of the screw dislocation is given by the transverse distortion energy density, and does not have a mass component. On the other hand, the dilatation strain energy density of the edge dislocation is given by the (massive) longitudinal dilatation energy density, and the distortion (massless) strain energy density of the edge dislocation is given by the transverse distortion energy density. This provides a solution to the mass renormalization problem in QED. Quantum Electrodynamics only uses the equivalent of the transverse distortion strain energy density in its calculations, and hence has no possibility of properly deriving the mass, which is in the longitudinal dilatation massive strain energy density term that is not used in QED.

The theory provides an alternative model for Quantum Electrodynamics processes, without the mathematical formalism of QED. In this framework, self-energies and interac-

tions are mediated by the strain energy density of the dislocations. The role played by virtual particles in Quantum Electrodynamics is replaced by the interaction of the strain energy densities of the dislocations. This theory is not perturbative as in QED, but rather calculated from analytical expressions. The analytical equations can become very complicated, and in some cases, perturbative techniques will need to be used to simplify the calculations, but the availability of analytical expressions permits a better understanding of the fundamental physical processes involved.

We provide examples of dislocation-dislocation interactions, applicable to photon-photon, photon-particle, and particle-particle interactions, and of dislocation self-energy calculations, applicable to photons and particles. These equations provide analytical expressions for the non-perturbative calculation of quantum self energies and interaction energies, and provides a physical process replacement for the virtual particle interpretation used in QED.

The theory proposed in this paper is formulated in a formalism based on Continuum Mechanics and General Relativity. This formalism is different from that used in Quantum Mechanics and Quantum Electrodynamics, and is currently absent of quantum states and uncertainties as is commonplace in quantum physics. Both formalisms are believed to be equivalent representations of the same physical phenomena. It may well be that as the theory is developed further, the formalism of orthonormal basis function sets in Hilbert spaces will be introduced to facilitate the solution of problems.

As shown in [47], it is a characteristic of Quantum Mechanics that conjugate variables are Fourier transform pairs of variables. The Heisenberg Uncertainty Principle thus arises because the momentum p of a particle is proportional to its de Broglie wave number k . Consequently, we need to differentiate between the measurement limitations that arise from the properties of Fourier transform pairs of conjugate variables, and any inherent limitations that may or may not exist at the quantum level, independently of the measurement process. Quantum theory currently assumes that the inherent limitations are the same as the measurement limitations. As shown in [47], quantum measurement limitations affect our perception of the quantum environment only, and are not inherent limitations of the quantum level, i.e. there exists a physical world, independently of an observer or a measurement, as seen here. See also the comments in [48, pp. 3–15].

This framework lays the foundation to develop a theory of the physical description of physical processes at the quantum level, based on dislocations in the spacetime continuum, within the theory of the Elastodynamics of the Spacetime Continuum. The basis of this framework is given in this initial paper. This framework allows the theory to be fleshed out in subsequent investigations. Disclinations in the spacetime continuum are expected to introduce new physical processes at the quantum level, to be worked out in future investigations. Additional spacetime continuum fundamental

processes based on ongoing physical defect theory investigations will emerge as they are applied to *STCED*, and will lead to further explanation of current quantum physics challenges.

Submitted on June 30, 2015 / Accepted on July 1, 2015

References

1. Millette P. A. Elastodynamics of the Spacetime Continuum. *The Abraham Zelmanov Journal*, 2012, v. 5, 221–277.
2. Millette P. A. On the Decomposition of the Spacetime Metric Tensor and of Tensor Fields in Strained Spacetime. *Progress in Physics*, 2012, v. 8 (4), 5–8.
3. Millette P. A. The Elastodynamics of the Spacetime Continuum as a Framework for Strained Spacetime. *Progress in Physics*, 2013, v. 9 (1), 55–59.
4. Millette P. A. Derivation of Electromagnetism from the Elastodynamics of the Spacetime Continuum. *Progress in Physics*, 2013, v. 9 (2), 12–15.
5. Millette P. A. Strain Energy Density in the Elastodynamics of the Spacetime Continuum and the Electromagnetic Field. *Progress in Physics*, 2013, v. 9 (2), 82–86.
6. Millette P. A. Dilatation–Distortion Decomposition of the Ricci Tensor. *Progress in Physics*, 2013, v. 9 (4), 32–33.
7. Millette P. A. Wave-Particle Duality in the Elastodynamics of the Spacetime Continuum (STCED). *Progress in Physics*, 2014, v. 10 (4), 255–258.
8. Segel L. A. *Mathematics Applied to Continuum Mechanics*. Dover Publications, New York, 1987.
9. Landau L. D., Lifshitz E. M., Kosevich A. M. and Pitaevskii L. P. *Theory of Elasticity*, 3rd ed., revised and enlarged. Butterworth-Heinemann, Oxford, 1986, pp. 108–132.
10. Hull D. and Bacon D. J. *Introduction to Dislocations*, 5th ed. Elsevier Ltd., Amsterdam, 2011.
11. Weertman J. and Weertman J. R. *Elementary Dislocation Theory*. Oxford University Press, Oxford, 1992.
12. Nabarro F. R. N., ed. *Dislocations in Solids, Volume I, The Elastic Theory*. North-Holland Publishing Co., New York, 1979.
13. Kosevich A. M. Crystal Dislocations and the Theory of Elasticity. in Nabarro F. R. N., ed. *Dislocations in Solids, Volume I, The Elastic Theory*. North-Holland Publishing Co., New York, 1979, pp. 33–141.
14. Hirth R. M. and Lothe J. *Theory of Dislocations*, 2nd ed. Krieger Publishing Co., Florida, 1982.
15. Edelen, D. G. B. and Lagoudas D. C. *Gauge Theory and Defects in Solids*. North-Holland Publishing, Amsterdam, 1988.
16. Kleinert H. *Gauge Fields in Condensed Matter, Vol. II Stresses and Defects*. World Scientific Publishing, Singapore, 1989.
17. Puntigam R. A., Soleng, H. H. Volterra Distortions, Spinning Strings, and Cosmic Defects. *Class. Quantum Grav.*, 1997, v. 14, 1129–1149. arXiv: gr-qc/9604057.
18. Maluf J. W., Goya, A. Space-Time Defects and Teleparallelism. arXiv: gr-qc/0110107.
19. Sabbata V. de, Sivaram C. *Spin and Torsion in Gravitation*. World Scientific, Singapore, 1994.
20. Rugiero M. L., Tartaglia A. Einstein-Cartan theory as a theory of defects in space-time. arXiv: gr-qc/0306029.
21. Tartaglia A. Defects in Four-Dimensional Continua: a Paradigm for the Expansion of the Universe? arXiv: gr-qc/0808.3216.
22. Unzicker A. Teleparallel Space-Time with Defects yields Geometrization of Electrodynamics with quantized Charges. arXiv: gr-qc/9612061.
23. Unzicker A. What can Physics learn from Continuum Mechanics?. arXiv: gr-qc/0011064.
24. Hossenfelder S. Phenomenology of Space-time Imperfection I: Nonlocal Defects. arXiv: hep-ph/1309.0311.
25. Hossenfelder S. Phenomenology of Space-time Imperfection II: Local Defects. arXiv: hep-ph/1309.0314.
26. Hossenfelder S. Theory and Phenomenology of Spacetime Defects. arXiv: hep-ph/1401.0276.
27. Orowan E. *Z. Phys.*, 1934, v. 89, 605, 634.
28. Polanyi M. *Z. Phys.*, 1934, v. 89, 660.
29. Taylor G. I. *Proc. Roy. Soc.*, 1934, v. A145, 362.
30. Burgers J. M. *Proc. Kon. Ned. Akad. Wetenschap.*, 1939, v. 42, 293, 378.
31. Flügge W. *Tensor Analysis and Continuum Mechanics*. Springer-Verlag, New York, 1972.
32. Woodside D. A. Uniqueness theorems for classical four-vector fields in Euclidean and Minkowski spaces. *Journal of Mathematical Physics*, 1999, v. 40, 4911–4943.
33. Misner C. W., Thorne K. S., Wheeler J. A. (1973). *Gravitation*, W. H. Freeman and Co., San Francisco, pp. 137–138.
34. Eshelby J. D. Energy Relations and the Energy-Momentum Tensor in Continuum Mechanics. in Kanninen M. F., Adler W. F., Rosenfield A. R. and Jaffee R. I., eds. *Inelastic Behavior of Solids*. McGraw-Hill, New York, 1970, pp. 77–115.
35. Eshelby J. D. The Elastic Energy-Momentum Tensor. *Journal of Elasticity*, 1975, v. 5, 321–335.
36. Eshelby J. D. The Energy-Momentum Tensor of Complex Continua. in Kröner, E. and Anthony K.-H., eds. *Continuum Models of Discrete Systems*. University of Waterloo Press, Waterloo, 1980, pp. 651–665.
37. Morse M. M., Feshbach H. (1953, 1981). *Methods of Theoretical Physics, Part I*. Feshbach Publishing, Minneapolis, pp. 322–323.
38. Maugin G. *Material Inhomogeneities in Elasticity*. Chapman & Hall / CRC, Boca Raton, 1993.
39. Eshelby J. D. Aspects of the Theory of Dislocations. in Hopkins H. G. and Sewell M. J., eds. *Mechanics of Solids – The Rodney Hill 60th Anniversary Volume*. Pergamon Press, Oxford, 1982, pp. 185–225.
40. Wolfram Mathematica Online Integrator. integrals.wolfram.com, June 2015.
41. Weingard R. Virtual Particles and the Interpretation of Quantum Field Theory. in Brown H. R. and Harré R. *Philosophical Foundations of Quantum Field Theory*. Clarendon Press, Oxford, 1988, pp. 43–58.
42. Brown H. R. and Harré R. *Philosophical Foundations of Quantum Field Theory*. Clarendon Press, Oxford, 1988, p. 3.
43. Hansson J. On the Origin of Elementary Particle Masses. *Progress in Physics*, 2014, v. 10, 45–47.
44. Wolfram MathWorld Polylogarithm. mathworld.wolfram.com/Polylogarithm.html, June 2015.
45. Lukin M. D. Nonlinear Optics and Quantum Entanglement of Ultra-Slow Single Photons. arXiv: quant-ph/9910094.
46. Marklund M., Shukla P. K. Nonlinear Collective Effects in Photon-Photon and Photon-Plasma Interactions. *Rev. Mod. Phys.*, 2006, v. 78, 591–637. arXiv: hep-ph/0602123.
47. Millette P. A. The Heisenberg Uncertainty Principle and the Nyquist-Shannon Sampling Theorem. *Progress in Physics*, 2013, v. 9 (3), 9–14. arXiv: quant-ph/1108.3135.
48. Auyang S. Y. *How is Quantum Field Theory Possible?* Oxford University Press, Oxford, 1995.

A Planck Vacuum Pilot Model for Inelastic Electron-Proton Scattering

William C. Daywitt

National Institute for Standards and Technology (retired), Boulder, Colorado. E-mail: wcdawitt@me.com

This paper describes the scattering of an incident electron from a proton initially at rest, under the assumptions: that the structureless electron interacts directly with the proton and its structure; that the energy and “size” of the electron are determined by its de Broglie radii; and that the shape of the inelastic scattering curve depends upon how deeply the electron core penetrates the proton structure. Deep inelastic scattering ends when the electron is small enough (energetic enough) to penetrate and destroy the proton core and its derived mass.

1 Introduction

The current theory describing electron-proton (e-p) scattering is the Standard Model theory, where the incident electron interacts with the proton via the exchange of a single virtual photon [1, p. 160]. The present paper offers an alternative theory that is based on the emerging Planck vacuum (PV) theory, where the electron interacts directly with the proton [2–5].

In the PV theory both the electron and proton particles are assumed to possess an invisible (vacuum) substructure, while in addition the proton possesses a visible free-space structure due to its positive charge acting on the degenerate PV quasi-continuum (Appendix A). The particle/PV forces and potentials, and their corresponding Compton and de Broglie radii, are associated with this vacuum substructure. The term “structure” by itself refers in what follows exclusively to the free-space proton structure.

2 Electron energy and size

The electron core ($-e_*$, m_e) exerts the two-term coupling force

$$\frac{(-e_*)(-e_*)}{r^2} - \frac{m_e c^2}{r} \quad (1)$$

on the PV state, where the first ($-e_*$) belongs to the electron and the second ($-e_*$) to the separate Planck particles making up the PV continuum. This force difference vanishes

$$\frac{e_*^2}{r_e^2} - \frac{m_e c^2}{r_e} = 0 \quad (2)$$

at the electron Compton radius $r_e (= e_*^2/m_e c^2)$. Treating this vanishing force as a Lorentz invariant constant then leads to the important Compton-(de Broglie) relations for the electron [6]

$$r_e \cdot m_e c^2 = r_d \cdot cp = r_L \cdot E = e_*^2 \quad (= c\hbar) \quad (3)$$

where $p (= m_e \gamma v)$ and $E (= m_e \gamma c^2)$ are the relativistic momentum and energy of the electron, and e_* is the massless bare charge. The radii $r_d (= r_e/\beta\gamma)$ and $r_L (= r_e/\gamma)$ are the electron de Broglie radii in the space and time directions on the Minkowski space-time diagram, where $\beta = v/c < 1$ and $\gamma = 1/\sqrt{1-\beta^2}$.

From (3) the size of the electron is taken to be the de Broglie radii

$$r_d = \frac{r_e}{\beta\gamma} \approx \frac{r_e}{\gamma} = r_L \quad (4)$$

where the approximation applies to the high energy ($\beta \approx 1$) calculations of the present paper. With (4) inserted into (3),

$$cp = \frac{e_*^2}{r_d} \approx \frac{e_*^2}{r_L} = E \quad (5)$$

leading to

$$E = cp = \frac{e_*^2}{r_d} \quad (6)$$

Thus to reduce the electron size to the proton Compton radius ($r_d = r_p$) requires an electron energy equal to $E = e_*^2/r_p$.

The comparisons to follow utilize

$$E = \frac{e_*^2}{r_d} = \frac{e_*^2 r_p}{r_p r_d} = m_p c^2 \frac{r_p}{r_d} \quad (7)$$

to convert electron energies to r_d/r_p ratios. The Lorentz invariance of (2) ensures that equations (3) and (7) apply in any inertial reference frame.

3 Proton structure

The proton substructure arises from the two-term coupling force [7]

$$\frac{(e_*)(-e_*)}{r^2} + \frac{m_p c^2}{r} \quad (8)$$

the proton core (e_* , m_p) exerts on the PV state, where the force vanishes at the proton Compton radius $r_p (= e_*^2/m_p c^2)$.

The proton also possesses a free-space structure (in contradistinction to the electron) in the form of a spherical rest-frame “collar” surrounding the proton core (Appendix A). This collar may affect the formation of the proton de Broglie radii; if, indeed, these radii even exist for the proton. Either way, the following scattering calculations employ only the proton Compton radius from the vanishing of (8).

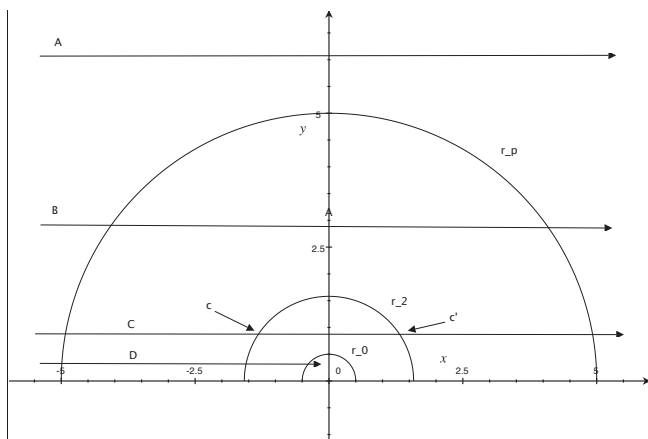


Fig. 1: A highly schematic cross section of the proton structure and four electron-core “trajectories”. The radii r_p and $r_2 (= r_p/3.15)$ represent respectively the proton Compton radius of the substructure and the outer radius of the free-space proton structure.

4 e-p scattering

A highly schematic diagram of the proton cross section is presented in Fig. 1, where r_p is the substructure Compton radius for reference, $r_2 (= r_p/3.15)$ is the outer radius of the proton structure on whose surface resides the apparent charge e of the proton, and r_0 is the radius of the proton core. The latter radius is assumed to be no larger than $r_p/39000$ [7]. Also shown are four electron-core “trajectories” A, B, C, and D, where A and B are propagating in free space and thus represent two elastic e-p scatterings.

Trajectory C ($r_0 < r_d < r_2$) goes through the proton structure, where the electron continuously loses energy (due to excitations of that structure) between its entry and exit points c and c' . Furthermore, since the electron possesses a de Broglie radius (with a corresponding de Broglie wavelength $2\pi r_d$), it exhibits a wave-like nature throughout the trajectory. This wave-like nature, and the finite length ($c-c'$) of the traversed section, produce a resonance within the measured scattering data.

Finally, when the electron energy is great enough ($r_d \ll r_0$) to allow the electron core to penetrate the proton core, this highly energized electron destroys the proton core, leading to the destruction of the proton mass and Compton radius, with a resulting hadron debris field (see Fig. 8.13 in [1, p. 199]).

Fig. 2 shows the experimental scattering data for a beam of 4.879 GeV electrons ($r_d = r_p/5.2$ in (7)) from a proton at rest. The elastic peak at the far right of the figure is represented by B in Fig. 1 with $r_d = r_2$. (This elastic peak is shifted down from the incident electron energy 4.879 GeV to approximately 4.55 GeV ($r_d = r_p/4.9$) by recoil effects.) From the far right to approximately 2.9 GeV on the left the scattering is represented by C in Fig. 1, where the destruction of the proton core has not yet taken place. The three inelastic

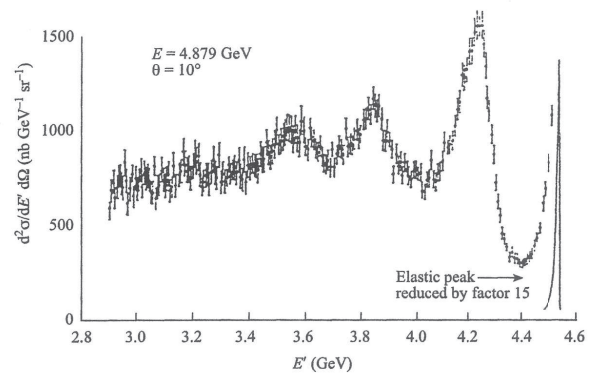


Fig. 2: Elastic and inelastic electron scattering from protons, where E' represents the energy of the scattered electron [9, p. 14] [10]. The scattering angle is 10° . Electron loss increases from right to left.

resonance peaks from left to right in the figure correspond to $r_d \approx r_p/(3.8, 4.1, 4.5)$ from (7).

Fig. 3 shows a repetition of Fig. 2 in a different format, for various scattering angles of the electron. Once more, the destruction of the proton core has not taken place, but the idea of the resonance scattering in the second and fourth paragraphs above is reinforced by the set of five three-peaked curves in the figure. The curves become monotonic when the trajectory between c and c' is deep enough to prevent constructive and destructive interference between reflections at c and c' . Furthermore, when the trajectory is deeper still, D ($r_d \leq r_0$), the electron core will scatter off the proton core.

Again, the proton core is destroyed when $E \gg m_p c^2$ ($r_d \ll r_0$). In this case the incident electron energy is sufficient to overcome the loss sustained in crossing the structure interval ($r_2 - r_0 \approx r_2$) to penetrate the proton core.

Appendix A: Structure

This appendix is a brief review of why the proton is structured and the electron is not [7].

The electron and proton are assumed to exert the two coupling forces

$$F(r) = \pm \left(\frac{e_*^2}{r^2} - \frac{mc^2}{r} \right) \quad (A1)$$

on the PV state, where the plus and minus signs refer to the electron and proton respectively. In effect the negative charge of the electron core ($-e_*, m_e$) in (1) repels the negative PV charges ($-e_*$) away from this core; while the positive charge in the proton core (e_*, m_p) attracts the PV charges. These oppositely charged Coulomb forces (the first terms in (A1)), close to their respective cores, are the fundamental cause of the structureless electron and the structured proton.

The potential energies associated with (A1) are defined by [7]

$$V(r) - V_0 = \int_{0^+}^r F(r') dr' \quad \text{with} \quad V(r_c) = 0 \quad (A2)$$

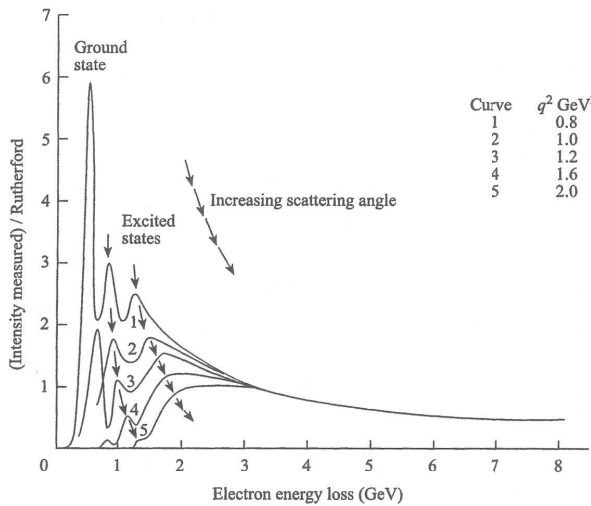


Fig. 3: Inelastic e-p scattering as a function of electron scattering angle [9, p. 17] [11]. Electron loss increases from left to right

where $r_c (= e_*^2/mc^2)$ is the Compton radius of either particle and the 0^+ accounts for the finite (but small) size of the cores. This definition leads to

$$V_p(r) \geq 0 \quad \text{and} \quad V_e(r) \leq 0 \quad (\text{A3})$$

where V_p and V_e are the proton/ and electron/PV coupling potentials.

It is shown in the Klein paradox [8, p. 127] that a sufficiently strong positive potential acting on the vacuum state can force a portion of that state into free space, where that part of the vacuum can then be attacked by free-space particles. Thus the positive and negative potentials in (A3) imply that the proton core, but not the electron core, forces a small spherical (in the core's rest frame) portion of the vacuum into the free space around the proton core. *This free-space vacuum "collar" is identified in the PV theory as the proton structure.* Furthermore, this structure leads to an apparent spread in the charge e_* of the proton core (Appendix B).

Appendix B: Charge spread

The polarization of the proton structure by the proton core leads to an apparent spread of the proton charge that is roughly expressed in the proton electric field as

$$E_p(r) = \frac{e(r)}{r^2} \quad (\text{B1})$$

where the spread is

$$e(r) = \begin{cases} e_* & , r < r_0 \\ < e_* & , r_0 < r < r_2 \\ e = \alpha^{1/2} e_* & , r_2 \leq r \end{cases} \quad (\text{B2})$$

$r_2 = r_p/3.15$, and $\alpha (\approx 1/137)$ is the fine structure constant. The radius r_2 defines the outer extent of the proton structure.

An important characteristic of this result is the large charge gradient

$$\frac{\Delta e}{\Delta r} = \frac{e - e_*}{r_2 - r_0} \approx -\frac{e_*(1 - \sqrt{\alpha})}{r_2} \approx -\frac{0.92e_*}{r_2} \quad (\text{B3})$$

between the core charge e_* and the observed proton charge e at r_2 . This result explains a similar gradient in the QED spread depicted in Fig. 11.6 of [9, p. 319].

Submitted on June 11, 2015 / Accepted on July 2, 2015

References

1. Thomson M. Modern Particle Physics. McGraw-Hill Book Company, U.S.A., 2013.
2. Daywitt W.C. The Planck Vacuum. *Progress in Physics*, 2009, v. 5 (1), 20. See also www.planckvacuum.com.
3. Daywitt W.C. The Source of the Quantum Vacuum. *Progress in Physics*, 2009, v. 5 (1), 27.
4. Daywitt W.C. The Electron and Proton Planck-Vacuum Coupling Forces and the Dirac Equation. *Progress in Physics*, 2014, v. 10, 114.
5. Daywitt W.C. The Strong and Weak Forces and their Relationship to the Dirac Particles and the Vacuum State. *Progress in Physics*, 2015, v. 11, 18.
6. Daywitt W.C. The de Broglie Relations Derived from the Electron and Proton Coupling to the Planck Vacuum State. *Progress in Physics*, 2015, v. 11 (2), 189.
7. Daywitt W.C. The Structured Proton and the Structureless Electron as Viewed in the Planck Vacuum Theory. *Progress in Physics*, 2015, v. 11 (2), 117.
8. Gingrich D.M. Practical Quantum Electrodynamics. CRC, The Taylor & Francis Group, Boca Raton, 2006.
9. Aitchison I.J.R., Hey A.J.G. Gauge Theories in Particle Physics, Vol. 1. Taylor & Francis, New York, London, 2003.
10. Bartel W.B. *et al.* Electroproduction of Pions Near the $\Delta 1236$ Isobar and the Form Factor $G_M^*(q^2)$ of the $(\gamma N \Delta)$ -Vertex. *Phys. Lett.*, 1968, v. 28B, 148.
11. Perkins D. Introduction to High Energy Physics, 1st ed. Addison Wesley Publishing, 1972.

Antiparticles and Charge Conjugation in the Planck Vacuum Theory

William C. Daywitt

National Institute for Standards and Technology (retired), Boulder, Colorado. E-mail: wcdawitt@me.com

This short paper defines charge conjugation in terms of the Planck vacuum substructure rather than the particle equation of motion. As such, the corresponding operator applies to the proton as well as the electron. Results show that, like their electron and proton counterparts, the positron is structureless while the antiproton possesses a structure consisting of a small vacuum “collar” surrounding its charged core.

1 Introduction

At present the Planck vacuum (PV) theory includes a model for both the electron and proton and the PV state to which these two particles are coupled [1]. But there is a problem: while the theory suggests a source for the negative bare charge ($-e_*$) of the electron (the current PV state itself), it is mute when it comes to the positive bare charge (e_*) of the proton. What follows assumes a bifurcated vacuum state that includes both negative and positive bare charges ($\mp e_*$). This bifurcated state is understood to mean that at each point in free space there exists a PV subspace consisting of a charge doublet ($\mp e_*$), to either branch of which a free particle charge can be coupled.

The charge conjugation operator C from the quantum theory is an operator that changes particles into antiparticles, and visa versa [2, p. 118]. An analogous operator is defined below to expand the PV model to include the particle-antiparticle symmetries and a source for the proton charge (e_*).

2 Charge conjugation

The electron and proton cores, $(-e_*, m_e)$ and (e_*, m_p) respectively, exert the two particle/PV coupling forces

$$\pm \left(\frac{e_*^2}{r^2} - \frac{mc^2}{r} \right) \quad (1)$$

on the PV state, where the plus and minus signs in (1) refer to the electron and proton respectively. At their respective Compton radii these forces reduce to

$$F_e = \frac{(-e_*)(-e_*)}{r_e^2} - \frac{m_e c^2}{r_e} = \frac{e_*^2}{r_e^2} - \frac{m_e c^2}{r_e} = 0 \quad (2)$$

and

$$F_p = \frac{(e_*)(-e_*)}{r_p^2} + \frac{m_p c^2}{r_p} = - \left(\frac{e_*^2}{r_p^2} - \frac{m_p c^2}{r_p} \right) = 0 \quad (3)$$

where $r_e (= e_*^2/m_e c^2)$ and $r_p (= e_*^2/m_p c^2)$ are the electron and proton Compton radii. The first ($-e_*$) and second ($-e_*$) in (2) belong to the electron core and PV charges respectively. The charge (e_*) in (3) belongs to the proton core. The vanishing forces F_e and F_p are Lorentz invariant constants; and the two

forces on the right side of (2) are the “weak” forces, while the two on the right side of (3) are the “strong” forces.

If it is assumed that the charge conjugation operator C' applies only to free-particle charges, then from (2) and (3)

$$C' F_e = \frac{(e_*)(-e_*)}{r_e^2} - \frac{m_e c^2}{r_e} = - \left(\frac{e_*^2}{r_e^2} + \frac{m_e c^2}{r_e} \right) \neq 0 \quad (4)$$

and

$$C' F_p = \frac{(-e_*)(-e_*)}{r_p^2} + \frac{m_p c^2}{r_p} = \frac{e_*^2}{r_p^2} + \frac{m_p c^2}{r_p} \neq 0 \quad (5)$$

both of which destroy the electron and proton Compton radii because the equations are nonvanishing. Since the corresponding antiparticles should possess a Compton radius like their particle counterparts, the C' operator is not a valid charge conjugation operator.

If it is assumed, however, that the charge conjugation operator C applies to both the free-space particle charge and the PV charge doublet, then (2) and (3) yield

$$C F_e = \frac{(e_*)(e_*)}{r_e^2} - \frac{m_e c^2}{r_e} = \frac{e_*^2}{r_e^2} - \frac{m_e c^2}{r_e} = 0 \quad (6)$$

and

$$C F_p = \frac{(-e_*)(e_*)}{r_p^2} + \frac{m_p c^2}{r_p} = - \left(\frac{e_*^2}{r_p^2} - \frac{m_p c^2}{r_p} \right) = 0 \quad (7)$$

where both the electron and proton Compton radii are preserved in their antiparticles. Equations (6) and (7) imply that the equations in (1) are also the antiparticle/PV coupling forces. It is clear from the first charges in (6) and (7), (e_*) and ($-e_*$), that the positron is positively charged and that the antiproton carries a negative charge.

3 Comments

The second charges ($-e_*$) in the first terms of (2) and (3), and the second charges (e_*) in the first terms of (6) and (7), suggest that free particles and their antiparticles exist in two separate spaces, corresponding respectively to the negative and positive branches of the PV charge doublet.

In addition to the C operator preserving electron and proton Compton radii, the form of the first terms in (6) and (7)

imply that the positron is structureless and that the antiproton has structure [1, App. A]. This mirrors those same qualities in the electron and proton, the first terms in (2) and (3).

As an aside, it is interesting to apply C to the electron equation of motion. The Dirac equation for the electron can be expressed as [2, p. 74]

$$i\hbar\left(\frac{\partial}{c\partial t} + \boldsymbol{\alpha} \cdot \nabla\right)\psi = m_e c^2 \beta \psi \quad (8)$$

or, using $c\hbar = e_*^2$,

$$\left[i(-e_*)(-e_*)\left(\frac{\partial}{c\partial t} + \boldsymbol{\alpha} \cdot \nabla\right) - m_e c^2 \beta\right]\psi = 0 \quad (9)$$

where the first $(-e_*)$ belongs to the electron and the second to the negative branch of the PV charge doublet. The corresponding positron equation of motion is then obtained from the charge conjugation of (9)

$$\begin{aligned} & C \left[i(-e_*)(-e_*) \left(\frac{\partial}{c\partial t} + \boldsymbol{\alpha} \cdot \nabla \right) - m_e c^2 \beta \right] \psi \\ &= \left[i(e_*)(e_*) \left(\frac{\partial}{c\partial t} + \boldsymbol{\alpha} \cdot \nabla \right) - m_e c^2 \beta \right] \psi_c = 0 \end{aligned} \quad (10)$$

where ψ_c is the positron spinor that obeys the same equation (9) as the electron spinor ψ . Due to the second (e_*) in (10), it is clear that the positron belongs in the positive branch of the PV doublet.

The same calculations in (8)–(10) are not applicable to the proton particle because, due to the vacuum “collar” (of radius $r_p/3.15$) surrounding the proton core (e_*, m_p) , the proton does not obey a Dirac equation of motion. In effect, the proton cannot be modeled as a point charge because of this “collar”, even though its core (e_*, m_p) is orders-of-magnitude smaller than its Compton radius r_p .

Submitted on July 5, 2015 / Accepted on July 13, 2015

References

1. Daywitt W.C. A Planck Vacuum Pilot Model for Inelastic Electron-Proton Scattering. *Progress in Physics*, v. 11 (4), 308, 2015.
2. Gingrich D.M. *Practical Quantum Electrodynamics*. CRC, The Taylor & Francis Group, Boca Raton, 2006.

The Burgers Spacetime Dislocation Constant b_0 and the Derivation of Planck's Constant

Pierre A. Millette

PierreAMillette@alumni.uottawa.ca, Ottawa, Canada

In a previous paper, a framework for the physical description of physical processes at the quantum level based on dislocations in the spacetime continuum within STCED (Spacetime Continuum Elastodynamics) was proposed and it was postulated that the spacetime continuum has a granularity characterized by a length b_0 corresponding to the smallest elementary Burgers dislocation vector possible. Based on the identification of screw dislocations in the spacetime continuum with photons, the relation between the Burgers constant b_0 and Planck's constant h is determined. Planck's constant is expressed in terms of the spacetime continuum constants. The calculated value of b_0 is found to be equivalent to the Planck length within the approximations of the derivation. Numerical values of the spacetime constants $\bar{\kappa}_0$, $\bar{\mu}_0$ and $\bar{\rho}_0$ are derived. A consistent set of the spacetime constants is proposed based on the Burgers spacetime dislocation constant b_0 being equivalent to the Planck length ℓ_P .

1 Introduction

A previous paper [1] provided a framework for the physical description of physical processes at the quantum level based on dislocations in the spacetime continuum within the theory of the Elastodynamics of the Spacetime Continuum (STCED). Dislocations in the spacetime continuum represent the fundamental displacement processes that occur in its structure, corresponding to basic quantum phenomena and quantum physics in STCED.

Spacetime Continuum Elastodynamics (STCED) [2–5] is based on analyzing the spacetime continuum within a continuum mechanical and general relativistic framework. As shown in [2], for an isotropic and homogeneous spacetime continuum, the STC is characterized by the stress-strain relation

$$2\bar{\mu}_0\varepsilon^{\mu\nu} + \bar{\lambda}_0g^{\mu\nu}\varepsilon = T^{\mu\nu} \quad (1)$$

where $T^{\mu\nu}$ is the energy-momentum stress tensor, $\varepsilon^{\mu\nu}$ is the resulting strain tensor, and

$$\varepsilon = \varepsilon^\alpha{}_\alpha \quad (2)$$

is the trace of the strain tensor obtained by contraction. $\bar{\lambda}_0$ and $\bar{\mu}_0$ are the Lamé elastic constants of the spacetime continuum: $\bar{\mu}_0$ is the shear modulus and $\bar{\lambda}_0$ is expressed in terms of $\bar{\kappa}_0$, the bulk modulus:

$$\bar{\lambda}_0 = \bar{\kappa}_0 - \bar{\mu}_0/2 \quad (3)$$

in a four-dimensional continuum.

A dislocation is characterized by its dislocation vector, known as the *Burgers vector*, b^μ in a four-dimensional continuum, defined positive in the direction of a vector ξ^μ tangent to the dislocation line in the spacetime continuum [6, pp. 17–24].

As discussed in [1], the spacetime continuum, at the quantum level, is assumed to have a granularity characterized by

a length b_0 corresponding to the smallest elementary Burgers dislocation vector possible in the STC. Then the magnitude of a Burgers vector can be expressed as a multiple of the elementary Burgers vector:

$$b = nb_0. \quad (4)$$

We find that b is often divided by 2π in dislocation equations, and hence the constant

$$\bar{b} = \frac{b}{2\pi}, \quad (5)$$

is also defined.

In this paper, we explore the relation between the spacetime Burgers dislocation constant b_0 and Planck's constant, and derive the value of the spacetime continuum constants.

2 Screw dislocations in quantum physics

There are two types of dislocations [1]: 1) Edge dislocations corresponding to dilatations, longitudinal displacements with an associated rest-mass energy, are identified with particles, and 2) screw dislocations corresponding to distortions, transverse displacements which are massless, are identified with photons. Arbitrary mixed dislocations can be decomposed into a screw component and an edge component, giving rise to wave-particle duality [5].

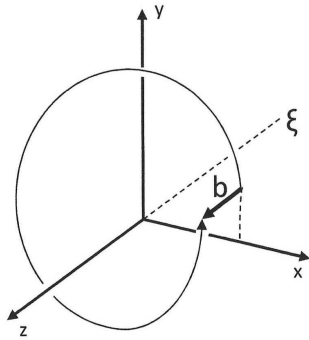
Hence screw dislocations in the spacetime continuum are massless, transverse deformations, and are identified specifically with photons. As shown in [1], the screw dislocation Burgers vector is equal to the wavelength of the screw dislocation

$$b = \lambda. \quad (6)$$

This result is illustrated in Fig. 1.

If we consider a stationary screw dislocation in the spacetime continuum, with cylindrical polar coordinates (r, θ, z) ,

Fig. 1: A wavelength of a screw dislocation.



with the dislocation line along the z -axis (see Fig. 2), then the Burgers vector is along the z -axis and is given by $b_r = b_\theta = 0$, $b_z = b$, the magnitude of the Burgers vector.

The only non-zero component of the deformation is given by [6, pp. 60–61]

$$u_z = \frac{b}{2\pi} \theta = \tilde{b} \tan^{-1} \frac{y}{x}. \tag{7}$$

Similarly, the only non-zero components of the stress and strain tensors are given by

$$\begin{aligned} \sigma_{\theta z} &= \frac{b}{2\pi} \frac{\bar{\mu}_0}{r} \\ \varepsilon_{\theta z} &= \frac{b}{4\pi} \frac{1}{r} \end{aligned} \tag{8}$$

respectively.

The strain energy density of the screw dislocation is given by the transverse distortion energy density [2, Eq. (74)]. The non-zero components of the strain tensor are as defined in (8). Hence

$$\mathcal{E}_\perp = \bar{\mu}_0 (\varepsilon_{\theta z}^2 + \varepsilon_{z\theta}^2). \tag{9}$$

Substituting from (8),

$$\mathcal{E}_\perp = \frac{\bar{\mu}_0 b^2}{8\pi^2} \frac{1}{r^2} = \mathcal{E}. \tag{10}$$

3 Planck’s constant

Based on our identification of screw dislocations in the space-time continuum with photons, we can determine the relation between the Burgers constant b_0 and Planck’s constant h .

Even though the photon is massless, its energy is given by the strain energy density of the screw dislocation, equivalent to the transverse distortion energy density. As shown in [2, Eq. (147)],

$$\hat{p}^2 c^2 = 32\bar{\kappa}_0 \mathcal{E}_\perp, \tag{11}$$

where \hat{p} is the momentum density. For a screw dislocation, substituting for \mathcal{E}_\perp from (10) in (11), we obtain

$$\hat{p}^2 c^2 = 32\bar{\kappa}_0 \frac{\bar{\mu}_0 b^2}{8\pi^2} \frac{1}{r^2}. \tag{12}$$

The kinetic energy density $\hat{p}c$ has to be equivalent to the wave energy density $\widehat{h\nu}$ for the screw dislocation (photon):

$$\hat{p}c = \widehat{h\nu}. \tag{13}$$

The photon’s energy is given by

$$h\nu = \int_V \widehat{h\nu} dV = \widehat{h\nu} V \tag{14}$$

where V is the volume of the screw dislocation. We consider the smallest Burgers dislocation vector possible and replace b with the elementary Burgers dislocation vector b_0 and V with the smallest volume V_0 to derive Planck’s constant. Combining (14), (13) and (12), (14) becomes

$$h = \sqrt{\frac{16\bar{\kappa}_0 \bar{\mu}_0 b_0^2}{(2\pi r)^2} \frac{V_0}{\nu}}. \tag{15}$$

Using (6), the frequency $\nu = c/\lambda$ becomes $\nu = c/b_0$ for the smallest Burgers dislocation vector considered. Substituting into (15), the equation becomes

$$h = \frac{4\sqrt{\bar{\kappa}_0 \bar{\mu}_0} b_0}{2\pi r} \frac{V_0 b_0}{c}. \tag{16}$$

The volume of one wavelength of the screw dislocation can be approximated by a cylinder and, using (6), written as

$$V = \pi r^2 \lambda = \pi r^2 b, \tag{17}$$

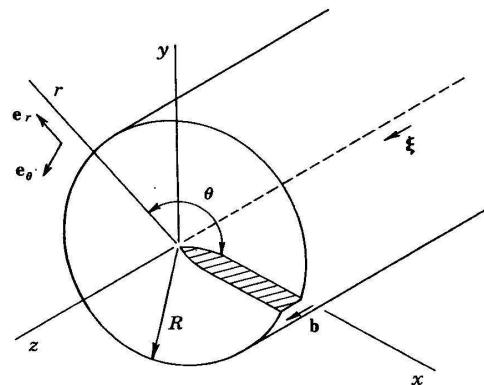
which in the limit as $b \rightarrow b_0$, becomes

$$V_0 = \pi r^2 b_0. \tag{18}$$

Substituting for V_0 into (16), the equation becomes

$$h = \frac{4\sqrt{\bar{\kappa}_0 \bar{\mu}_0} b_0}{2\pi r} \frac{\pi r^2 b_0^2}{c}. \tag{19}$$

Fig. 2: A stationary screw dislocation in cylindrical polar coordinates (r, θ, z) [6, p. 60].



Simplifying,

$$h = \frac{2\sqrt{\bar{\kappa}_0\bar{\mu}_0}}{c}rb_0^3, \quad (20)$$

and in the limit as r approaches b_0 , becomes

$$h = 2\frac{\sqrt{\bar{\kappa}_0\bar{\mu}_0}b_0^4}{c} \quad (21)$$

where the units of h are J-s as expected. This is the basic definition of Planck's constant h in terms of the Lamé spacetime constants and the Burgers spacetime dislocation constant b_0 .

This relation can be further simplified using $\bar{\mu}_0 = 32\bar{\kappa}_0$ from [2, Eq. (150)]. Then

$$h = 8\sqrt{2}\frac{\bar{\kappa}_0b_0^4}{c} = \frac{1}{2\sqrt{2}}\frac{\bar{\mu}_0b_0^4}{c}. \quad (22)$$

Numerically,

$$\bar{\mu}_0b_0^4 = 2\sqrt{2}hc = 5.8 \times 10^{-25} \text{ J m}. \quad (23)$$

The value of the spacetime shear modulus $\bar{\mu}_0$ is not a known physical constant, neither is the value of the spacetime bulk modulus $\bar{\kappa}_0$. However, Macken [8] has derived a value of $\bar{\kappa}_0 = 4.6 \times 10^{113} \text{ J/m}^3$ which as we will see in Section 4 is expected to be a valid estimate. Using $\bar{\mu}_0 = 32\bar{\kappa}_0$ from Millette [2, Eq. (150)], this yields a value of

$$\bar{\mu}_0 = 1.5 \times 10^{115} \text{ J/m}^3. \quad (24)$$

Note that the units can be expressed equivalently as N/m^2 or J/m^3 . Substituting for $\bar{\mu}_0$ in (23), we obtain the value of the elementary Burgers vector

$$b_0 = 1.4 \times 10^{-35} \text{ m}. \quad (25)$$

This value compares very favorably with the Planck length $1.6 \times 10^{-35} \text{ m}$. Given the approximations used in its derivation, this suggests that the elementary Burgers vector b_0 and the Planck length are equivalent.

With these constants, we are now in a position to calculate the remaining unknown spacetime constant, the density of the spacetime continuum $\bar{\rho}_0$. Using the relation [2]

$$c = \sqrt{\frac{\bar{\mu}_0}{\bar{\rho}_0}}, \quad (26)$$

the density of the spacetime continuum is

$$\bar{\rho}_0 = 1.7 \times 10^{98} \text{ kg/m}^3. \quad (27)$$

4 Analytic form of constants b_0 and $\bar{\kappa}_0$

Blair [7, p. 3–4] writes Einstein's field equation as

$$\mathbf{T} = \frac{c^4}{8\pi G}\mathbf{G},$$

where \mathbf{T} is the stress energy tensor, \mathbf{G} is the Einstein curvature tensor and G is the universal gravitational constant. He notes the very large value of the proportionality constant. This leads him to point out that spacetime is an elastic medium that can support waves, but its extremely high stiffness means that extremely small amplitude waves have a very high energy density. He notes that the coupling constant $c^4/8\pi G$ can be considered as a modulus of elasticity for spacetime, and identifies the quantity c^3/G with the characteristic impedance of spacetime [7, p. 45].

From this, Macken [8] derives an “interactive bulk modulus of spacetime”, which we identify with the spacetime continuum bulk modulus, given by

$$\bar{\kappa}_0 = \frac{c^7}{\hbar G^2}. \quad (28)$$

The result obtained for the numerical value of b_0 and its close correspondance to the Planck length suggests that the value of $\bar{\kappa}_0$ proposed in [8] is correct. From Millette [2, Eq. (150)] we then have

$$\bar{\mu}_0 = 32\frac{c^7}{\hbar G^2}. \quad (29)$$

From (23), we can write

$$b_0^4 = 2\sqrt{2}\frac{hc}{\bar{\mu}_0}. \quad (30)$$

Substituting from (29), this relation becomes

$$b_0^4 = \frac{\sqrt{2}\pi}{8}\frac{\hbar^2 G^2}{c^6} \quad (31)$$

and finally

$$b_0 = \left(\frac{\pi}{4\sqrt{2}}\right)^{\frac{1}{4}}\sqrt{\frac{\hbar G}{c^3}} = 0.86\ell_P \quad (32)$$

where ℓ_P is Planck's length, defined as [9]

$$\ell_P = \sqrt{\frac{\hbar G}{c^3}}. \quad (33)$$

Hence, as mentioned in Section 3, this suggests that the elementary Burgers dislocation vector b_0 and the Planck length ℓ_P are equivalent within the approximations of the derivation.

5 Recommended constants

Starting from the statement that the Burgers spacetime dislocation constant b_0 is equivalent to the Planck length ℓ_P , we derive the constant of proportionality of (21). We thus set

$$h = k\frac{\sqrt{\bar{\kappa}_0\bar{\mu}_0}b_0^4}{c} \quad (34)$$

where k is the improved constant of proportionality for the relation. Substituting for $\bar{\kappa}_0$ from (28), for $\bar{\mu}_0$ from (29), and setting $b_0 = \ell_P$ from (33), the equation becomes

$$h = k \sqrt{32} \frac{c^7}{\hbar G^2} \frac{1}{c} \frac{\hbar^2 G^2}{c^6} \quad (35)$$

from which we obtain

$$k = \frac{\pi}{2\sqrt{2}}. \quad (36)$$

Hence, with the Burgers spacetime dislocation constant b_0 equivalent to the Planck length ℓ_P , the basic definition of Planck's constant h in terms of the Lamé spacetime constants and the Burgers spacetime dislocation constant b_0 is given by

$$h = \frac{\pi}{2\sqrt{2}} \frac{\sqrt{\bar{\kappa}_0 \bar{\mu}_0} b_0^4}{c}. \quad (37)$$

In terms of $\bar{\kappa}_0$, we have

$$h = 2\pi \frac{\bar{\kappa}_0 b_0^4}{c} \quad (38)$$

or

$$\bar{\hbar} = \frac{\bar{\kappa}_0 b_0^4}{c} \quad (39)$$

and in terms of $\bar{\mu}_0$, we have

$$h = \frac{\pi}{16} \frac{\bar{\mu}_0 b_0^4}{c}. \quad (40)$$

As stated, the Burgers spacetime dislocation constant b_0 is given by

$$b_0 = \ell_P = \sqrt{\frac{\hbar G}{c^3}} \quad (41)$$

and the spacetime continuum Lamé constants are as per (28) and (29):

$$\begin{aligned} \bar{\kappa}_0 &= \frac{c^7}{\hbar G^2} \\ \bar{\mu}_0 &= 32 \frac{c^7}{\hbar G^2}. \end{aligned} \quad (42)$$

It is recommended that the relations in this section be retained as the official definition of these constants.

6 Discussion and conclusion

We have expressed Planck's constant in terms of the spacetime continuum constants $\bar{\kappa}_0$, $\bar{\mu}_0$, b_0 , and the speed of light c . The calculated value of b_0 compares very favorably with the Planck length and suggests that the elementary Burgers vector b_0 and the Planck length are equivalent within the approximations of the derivation. An estimate of the numerical values of the spacetime constants $\bar{\kappa}_0$, $\bar{\mu}_0$ and $\bar{\rho}_0$ is also obtained, based on Macken's [8] derived value of $\bar{\kappa}_0$ which is

found to be a valid estimate, given the agreement between b_0 and the Planck length ℓ_P .

A consistent set of recommended spacetime constants is obtained based on setting the Burgers spacetime dislocation constant b_0 equivalent to the Planck length ℓ_P .

Submitted on July 15, 2015 / Accepted on July 18, 2015

References

1. Millette P.A. Dislocations in the Spacetime Continuum: Framework for Quantum Physics. *Progress in Physics*, 2015, v. 11 (4), 287–307.
2. Millette P.A. Elastodynamics of the Spacetime Continuum. *The Abraham Zelmanov Journal*, 2012, v. 5, 221–277.
3. Millette P.A. The Elastodynamics of the Spacetime Continuum as a Framework for Strained Spacetime. *Progress in Physics*, 2013, v. 9 (1), 55–59.
4. Millette P.A. Strain Energy Density in the Elastodynamics of the Spacetime Continuum and the Electromagnetic Field. *Progress in Physics*, 2013, v. 9 (2), 82–86.
5. Millette P.A. Wave-Particle Duality in the Elastodynamics of the Spacetime Continuum (STCED). *Progress in Physics*, 2014, v. 10 (4), 255–258.
6. Hirth R.M. and Lothe J. Theory of Dislocations, 2nd ed. Krieger Publishing Co., Florida, 1982.
7. Blair D.G., ed. The Detection of Gravitational Waves. Cambridge University Press, Cambridge, 1991.
8. Macken J.A. The Universe is Only Spacetime, Rev. 7.1. Self-published, Santa Rosa, CA, 2013, p. 4-24.
9. Kaku M. Quantum Field Theory, A Modern Introduction. Oxford University Press, Oxford, 1993, p. 10.

Quantum Gravity Experiments

Reginald T. Cahill

School of Chemical and Physical Sciences, Flinders University. E-mail: reg.cahill@flinders.edu.au

A new quantum gravity experiment is reported with the data confirming the generalisation of the Schrödinger equation to include the interaction of the wave function with dynamical space. Dynamical space turbulence, via this interaction process, raises and lowers the energy of the electron wave function, which is detected by observing consequent variations in the electron quantum barrier tunnelling rate in reverse-biased Zener diodes. This process has previously been reported and enabled the measurement of the speed of the dynamical space flow, which is consistent with numerous other detection experiments. The interaction process is dependent on the angle between the dynamical space flow velocity and the direction of the electron flow in the diode, and this dependence is experimentally demonstrated. This interaction process explains gravity as an emergent quantum process, so unifying quantum phenomena and gravity. Gravitational waves are easily detected.

1 Introduction

The quantum theory of gravity explains the gravitational acceleration of matter as caused by the refraction of quantum waves by the time dependence and spatial inhomogeneities of the dynamical space flow [1]. This has been tested against numerous experimental gravitational phenomena [2]: bore hole g anomalies, flat spiral galaxy rotation curves, black hole systematics and star orbit data [3], lensing of light by stars and galaxies, expanding universe supernova redshift-brightness data without need for dark matter or dark energy [4], anisotropic Brownian motion [5], directional dependence of nuclear decay rates [6]. The key initial experiments detected the dynamical space using light speed anisotropy gas-mode Michelson optical interferometers and EM speed anisotropy in RF coaxial cables. More recently quantum detectors have been discovered that directly detected the space flow [7, 8]. All these different experimental techniques reveal a turbulent space flow speed from direction RA ~ 4.5 hrs, Dec= 80° S, with a speed of ~ 500 km/s. These velocities are moderated over a year by the orbital motion of the Earth.

The dynamical space quantum detectors, which use reverse biased Zener Diodes, Fig. 1 and Fig. 2, have given rise to a new critical test of the quantum theory of gravity, reported herein, namely an orientation dependent effect, which directly tests the modified Schrödinger equation which includes the effects of the dynamical space. This uses collocated quantum detectors which are either in parallel configuration or anti-parallel configuration, Fig. 3.

2 Quantum gravity

Dynamical space is a phenomenon repeatedly detected by a variety of experimental techniques [2]. The Schrödinger equation must be extended to include the dynamical space by using the Euler time derivative $\partial/\partial t \rightarrow \partial/\partial t + \mathbf{v}(\mathbf{r}, t) \cdot \nabla$, where $\mathbf{v}(\mathbf{r}, t)$ is the classical field description of the dynamical space

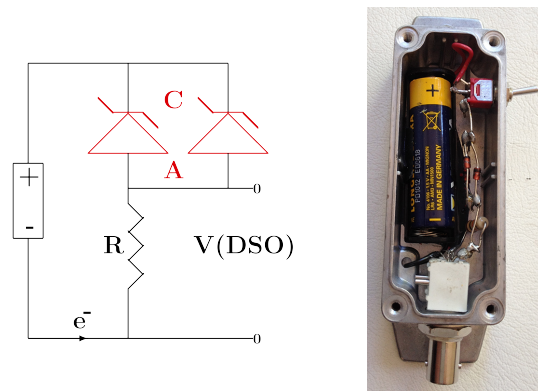


Fig. 1: Left: Circuit of Zener Diode Space Flow Detector, showing 1.5 V AA battery, two 1N4728A zener diodes operating in reverse bias mode, and having a Zener voltage of 3.3 V, and resistor $R = 10 \text{ K}\Omega$. Voltage V across resistor is measured and used to determine the turbulent space flow driven fluctuating tunnelling current through the Zener diodes. Correlated currents from two collocated detectors are shown in Fig. 4. Right: Photo of detector with 5 Zener diodes in parallel.

velocity:

$$i\hbar \frac{\partial \psi(\mathbf{r}, t)}{\partial t} = -\frac{\hbar^2}{2m} \nabla^2 \psi(\mathbf{r}, t) + V(\mathbf{r}, t) \psi(\mathbf{r}, t) - i\hbar \mathbf{v}(\mathbf{r}, t) \cdot \nabla \psi(\mathbf{r}, t). \quad (1)$$

Here $\mathbf{v}(\mathbf{r}, t)$ is the velocity field describing the dynamical space at a classical field level, and the coordinates \mathbf{r} give the relative location of $\psi(\mathbf{r}, t)$ and $\mathbf{v}(\mathbf{r}, t)$, relative to a Euclidean embedding space, and also used by an observer to locate structures. This is not an aether embedded in a non-dynamical space, but a dynamical space which induces an

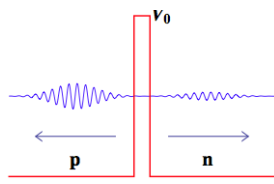


Fig. 2: Electron wave function after barrier quantum transmission and reflection from the LHS, with p and n denoting semiconductor type, showing partially transmitted component and partially reflected component, when the diode is operated in reverse-bias mode, as shown in Fig. 1. Space flow fluctuations raise and lower the energy of the incident wave function, which changes the relative magnitude of these two components.



Fig. 3: Left: Two collocated detectors in parallel configuration, Right: anti-parallel configuration. The corresponding data is shown in Fig. 4. The data in Fig. 5 was obtained with one of the detectors in the parallel configuration shifted by 1cm, and together aligned with the Earth's spin axis.

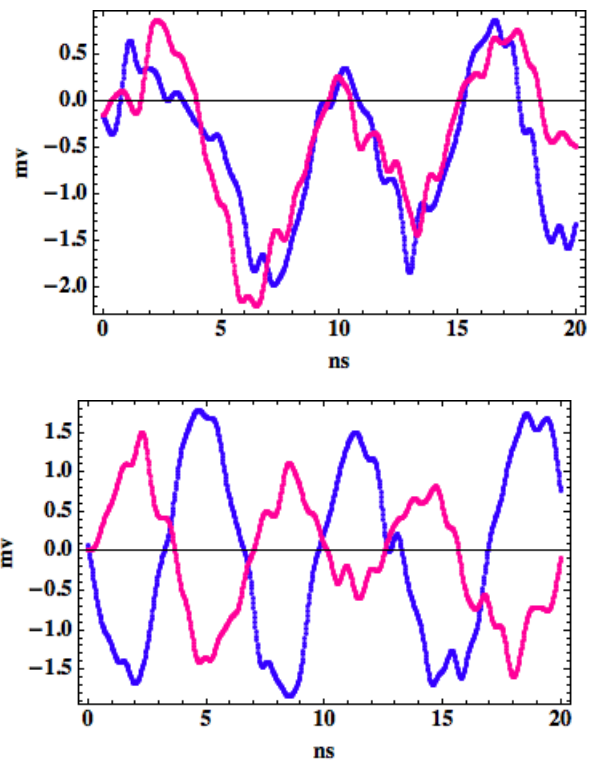


Fig. 4: Correlated current fluctuations, as indicated by voltage across resistor R , and with DSO operated with $1\text{ M}\Omega$ AC input, and no filters. Top: From two collocated parallel detectors, as shown in Fig. 1. Bottom: Anti-correlated current fluctuations from the two collocated but anti-parallel detectors, also shown in Fig. 1. This data confirms the dynamical consequences of the $-i\hbar\mathbf{v} \cdot \nabla\psi$ term in the new Schrödinger equation. This term is the origin of the quantum gravity.

embedding space or coordinate system. The Euler derivative was first introduced by Euler in 1757 when beginning the study of fluids, and ensures that fluid dynamics are relative to the fluid, and not fixed relative to an observer. Hertz in 1890 introduced this Euler derivative into Maxwell's EM theory, but was unaware of the meaning of $\mathbf{v}(\mathbf{r}, t)$. The detection of the dynamical space then mandates the use of the Euler derivative in the Schrödinger equation [1].

A significant effect follows from (1), namely the emergence of gravity as a quantum effect: an Ehrenfest wave-packet analysis reveals the classical limit and shows that the acceleration of a localised wave packet, due to the space terms alone, when $V(\mathbf{r}, t) = 0$, given by $\mathbf{g} = d^2\langle\mathbf{r}\rangle/dt^2$, gives [1]

$$\mathbf{g}(\mathbf{r}, t) = \frac{\partial\mathbf{v}}{\partial t} + (\mathbf{v} \cdot \nabla)\mathbf{v} \tag{2}$$

That derivation showed that the acceleration is independent of the mass m : whence we have the derivation of the Weak Equivalence Principle, discovered experimentally by Galileo.

Note that the emergent quantum-theoretic matter acceleration in (2), is also, and independently, the constituent accel-

eration $\mathbf{a}(\mathbf{r}, t)$ of the space flow velocity field,

$$\begin{aligned} \mathbf{a}(\mathbf{r}, t) &= \lim_{\Delta t \rightarrow 0} \frac{\mathbf{v}(\mathbf{r} + \mathbf{v}(\mathbf{r}, t)\Delta t, t + \Delta t) - \mathbf{v}(\mathbf{r}, t)}{\Delta t} \\ &= \frac{\partial\mathbf{v}}{\partial t} + (\mathbf{v} \cdot \nabla)\mathbf{v}. \end{aligned} \tag{3}$$

which describes the acceleration of a constituent element of space by tracking its change in velocity. This means that space has a structure that permits its velocity to be defined and detected, which experimentally has been done. This then suggests, from (2) and (3), that the simplest dynamical equation for $\mathbf{v}(\mathbf{r}, t)$ is

$$\nabla \cdot \left(\frac{\partial\mathbf{v}}{\partial t} + (\mathbf{v} \cdot \nabla)\mathbf{v} \right) = -4\pi G\rho(\mathbf{r}, t); \quad \nabla \times \mathbf{v} = \mathbf{0} \tag{4}$$

because it then gives $\nabla \cdot \mathbf{g} = -4\pi G\rho(\mathbf{r}, t)$, $\nabla \times \mathbf{g} = \mathbf{0}$, which is Newton's inverse square law of gravity in differential form. Hence the fundamental insight is that Newton's gravitational acceleration field $\mathbf{g}(\mathbf{r}, t)$ for matter is really the acceleration

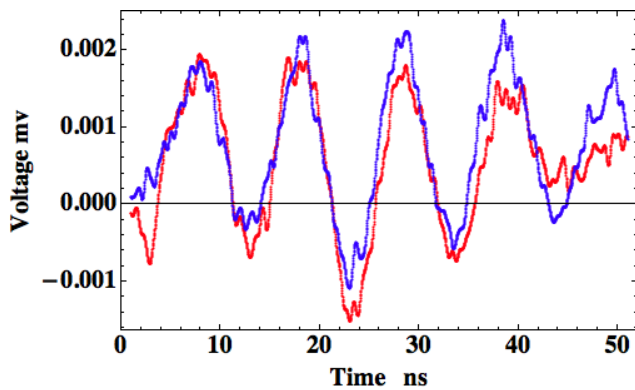


Fig. 5: Correlated current fluctuations, as indicated by voltage across resistor R , and with DSO operated with $1\text{ M}\Omega$ AC input, and no filters. Detectors in parallel configuration, and orientated parallel to Earth axis, but offset by 1 cm, and plotted with a time offset of 20 ns, implying a speed of 500 km/s.

field $\mathbf{a}(\mathbf{r}, t)$ of the structured dynamical space and that quantum matter acquires that acceleration because it is fundamentally a wave effect, and the wave is refracted by the accelerations of space. While (4) is the simplest 3-space dynamical equation, this derivation permits further terms which maintain Newton's inverse square law external to a spherical mass, but which otherwise leads to new observed aspects of gravity, which have previously been ascribed to "dark matter", but which are now revealed to be a dynamical aspect of space.

3 Quantum gravity directional experiment

The presence of the $-i\hbar\mathbf{v}\cdot\nabla$ dynamical space term provides a critical test of the emergent quantum gravity theory. For plane wave electrons, $\psi \sim e^{i(\mathbf{k}\cdot\mathbf{r}-i\omega t)}$, the space interaction term changes the energy of the electrons, for uniform \mathbf{v} ,

$$E = \hbar\omega \rightarrow \hbar\omega + \hbar\mathbf{k}\cdot\mathbf{v} \quad (5)$$

This space induced energy shift changes the potential energy barrier electron quantum tunnelling amplitudes in a reverse-biased Zener diode, Fig. 2. This effect is easily measured by means of the circuit in Fig. 1. A critical implication is that the electron tunnelling current must depend on the angle θ between \mathbf{k} and \mathbf{v} , as in $\mathbf{k}\cdot\mathbf{v} = kv \cos \theta$. To test this effect two collocated detectors were arranged as in Fig. 3, with parallel and anti-parallel configurations. The resulting currents are shown in Fig. 4, and confirm this angle dependence effect.

As well if one of the detectors in the parallel configuration is moved by 1 cm, then a time delay effect of 20 ns is detected, as in Fig. 5. This corresponds to a spatial speed of ~ 500 km/s from a S direction, as detected in numerous other experiments.

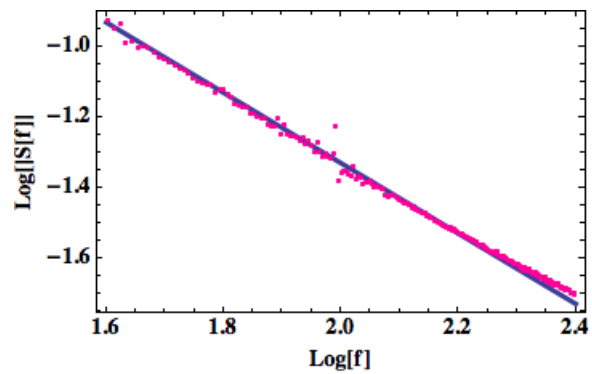


Fig. 6: Typical frequency spectrum data, showing $\text{Log}[S[f]]$ plotted against $\text{Log}[f]$ from the current fluctuation data, showing slope of -1.0 , as the solid plot, revealing a $1/f$ spectrum, typical of Johnson $1/f$ electronic systems "noise", and so explaining the origin of Johnson noise [10], and also demonstrating again the fractal structure of the dynamical space.

Most electronic devices exhibit Johnson noise [10], where the electron current has a characteristic $1/f$ spectrum. The origin of this noise has never been explained until now. The frequency spectrum for one of the current fluctuations in Fig. 4 is shown in Fig. 6, and exhibits a $1/f$ spectrum. This implies that Johnson noise is a consequence of the fractal structure of the space flow.

4 Conclusions

The experimental detection of dynamical space required generalisation of Maxwell's EM Theory, Schrödinger's Quantum Theory and a corresponding generalisation of the Dirac Quantum Theory [9], and the determination of a dynamical theory for space. As a consequence it has been discovered that gravity is an emergent quantum effect. Here we have reported new key tests of this quantum theory of gravity by detecting predicted angle dependencies of quantum barrier electron tunnelling currents. The fluctuating electron currents amount to the detection of wave effects of the dynamical space: gravitational waves [11].

Submitted on August 6, 2015 / Accepted on August 10, 2015

References

1. Cahill R. T. Dynamical Fractal 3-Space and the Generalised Schrödinger Equation: Equivalence Principle and Vorticity Effects, *Progress in Physics*, 2006, v. 1, 27–34.
2. Cahill R. T. Discovery of Dynamical 3-Space: Theory, Experiments and Observations - A Review, *A. J. Spac. Sci.*, 2013, v. 1 (2), 77–93.
3. Cahill R. T. and Kerrigan D. Dynamical Space: Supermassive Black Holes and Cosmic Filaments, *Progress in Physics*, 2011, v. 4, 79–82.
4. Cahill R. T. and Rothall D. Discovery of Uniformly Expanding Universe, *Progress in Physics*, 2012, v. 1, 63–68.
5. Cahill R. T. Dynamical 3-Space: Anisotropic Brownian Motion Experiment, *Progress in Physics*, 2015, v. 11 (3), 204–207.

6. Shnoll S. E., *Cosmophysical Factors in Stochastic Processes*, American Research Press, Rehoboth, NM, 2012. <http://www.ptep-online.com>.
 7. Cahill R. T. Nanotechnology Quantum Detectors for Gravitational Waves: Adelaide to London Correlations Observed, *Progress in Physics*, 2013, v. 4, 57–62.
 8. Cahill R. T. Gravitational Wave Experiments with Zener Diode Quantum Detectors: Fractal Dynamical Space and Universe Expansion with Inflation Epoch, *Progress in Physics*, 2014, v. 10(3), 131–138.
 9. Cahill R. T. Dynamical 3-Space: Neo-Lorentz Relativity, *Physics International*, 2013, v. 4(1), 60–72.
 10. Johnson J. B. The Schottky Effect in Low Frequency Circuits, *Phys. Rev.*, 1925, v. 26, 71–85.
 11. Cahill R. T. Review of Gravitational Wave Detections: Dynamical Space, *Physics International*, 2014, v. 5(1), 49–86.
-

Dispelling Black Hole Pathologies Through Theory and Observation

Robin James Spivey

Biological Sciences, Bangor University, Brambell, Deiniol Road, Bangor, Gwynedd, Great Britain
E-mail: y.gofod@gmail.com

Astrophysical black holes are by now routinely identified with metrics representing eternal black holes obtained as exact mathematical solutions of Einstein's field equations. However, the mere existence and discovery of stationary solutions is no guarantee that they can be attained through dynamical processes. If a straightforward physical caveat is respected throughout a spacetime manifold then the ingress of matter across an event horizon is prohibited, in accordance with Einstein's expectation. As black hole formation and growth would be inhibited, the various pathological traits of black holes such as information loss, closed timelike curves and singularities of infinite mass density would be obviated. Gravitational collapse would not terminate with the formation of black holes possessing event horizons but asymptotically slow as the maximal time dilation between any pair of worldlines tends towards infinity. The remnants might be better described as dark holes, often indistinguishable from black holes except in certain astrophysically important cases. The absence of trapped surfaces circumvents topological censorship, with potentially observable consequences for astronomy, as exemplified by the remarkable electromagnetic characteristics, extreme energetics and abrupt extinction of quasars within low redshift galaxies.

1 Introduction

Quasars are exceptionally luminous objects located at cosmological distances [1]. Rapid fluctuations in their emissions arguably provide the most compelling hints that black holes of some description exist in nature. The empirically determined "M-sigma relation" points to a causal kinematic connection between black hole growth and galactic evolution, with motions of nearby gas and stars providing irrefutable evidence that $10^6 \sim 10^9 M_{\odot}$ black hole candidates are present [2]. This has led many researchers to conclude that the universe is home to a multitude of black holes conforming to one of the stationary, asymptotically flat, black hole metrics – in accordance with the claim of a leading relativist that the "black holes of nature are the most perfect macroscopic objects that are in the universe" [3].

Potentially pre-dating the earliest stars, quasars may have fostered galaxy formation [4]. However, the question of how their central engines operate remains clouded in considerable uncertainty. Furthermore, astronomical observations have not been satisfactorily reconciled with theory. For instance, the abrupt cessation of quasar activity during the early universe calls for some efficient shutdown mechanism [5]. It is now generally believed that virtually all galactic nuclei harbour a supermassive black hole, most galaxies have undergone a period of quasar activity in the past, black holes have at present scarcely lost any mass through Hawking radiation and a healthy fraction of galaxies are still rich in gas. It is therefore puzzling that the temporary revival of quasar activity is not occasionally observed, especially within gas-rich galaxy clusters. A glaring inconsistency arises with the currently in vogue gas-starvation model of quasar extinction.

Karl Schwarzschild provided the first solution to the field equations of general relativity (GR), obtaining a spherically symmetric metric describing an eternal black hole* with an event horizon [6]. After lengthy deliberation, Einstein remained dismissive of the notion that objects with an event horizon might actually exist in nature, pointing out that a clock arriving at an event horizon would totally cease to advance compared to more remotely situated clocks [7]. The more interesting case of dynamic gravitational collapse within GR, abandoning the assumption of stationary geometry, was tackled analytically that same year by Oppenheimer & Snyder [8]. The mathematical results, as valid now as they ever were [9], establish that from the perspective of a distant observer the implosion initially accelerates until the contraction becomes relativistic, whereupon the implosion rate declines – ultimately halting just as the critical radius is approached. From this vantage, an event horizon only forms in an asymptotic sense, after the infinite passage of time.

Oppenheimer & Snyder also commented on their results from the perspective of the infalling matter. They found that as external time approaches infinity, the proper time along the worldline of an infalling particle tends towards some finite value. They then considered what might happen at later proper times of the infalling particle, apparently without pausing to consider whether time could physically continue to advance for the infalling particle: "after this time an observer comoving with the matter would not be able to send a light signal from the star". It is currently fashionable to ignore Einstein's objection regarding infinite time dilation. But is

*The term "black hole" was not coined until some years after Einstein's departure, the alternative "frozen star" had previously been widely used.

that wise? The field of black hole physics is by now plagued by a variety of serious difficulties. Closed timelike curves seem to be unavoidable within rotating black hole spacetimes, with potentially disturbing connotations for causality and hence physics at its most fundamental level. The notion that information might be captured and destroyed by black holes has also troubled theoretical physicists for decades [10, 11]. This “information paradox” recently led to the suggestion that black holes only possess apparent horizons [12] as opposed to genuine event horizons: features traditionally regarded as the defining hallmarks of true black holes [13].

There is also a widespread expectation that naturally occurring black holes lack “hair” and comply with the principle of topological censorship [14], rapidly settling down either to a Kerr-Newman or, more realistically, a Kerr geometry corresponding to an electrically uncharged, rotating black hole. As will be discussed, astronomical observations cast significant doubt on the reliability of this common assumption. Moreover, due to the generality of results obtained in dynamical collapse scenarios such as Oppenheimer & Snyder considered, there is a suspicion that Einstein was right: it may be difficult or impossible to produce stationary black holes through physically realistic processes.

The goal of this work is to argue that these various conceptual problems can vanish, without departing from Einstein’s gravitational theory, if a straightforward physical consideration is respected throughout a spacetime manifold. This caveat does not impinge upon general covariance and the mathematical apparatus of general relativity is unchanged. A discussion then follows of why quasar observations support the contention that black holes lack event horizons and might be better described as *dark holes*.

2 The Schwarzschild black hole

The Schwarzschild metric represents a non-rotating eternal black hole with the spherically symmetric spacetime

$$ds^2 = \left(1 - \frac{r_s}{r}\right) c^2 dt^2 - \left(1 - \frac{r_s}{r}\right)^{-1} dr^2 - r^2(d\theta^2 + \sin^2\theta d\phi^2) \quad (1)$$

where ds is the spacetime interval, t represents the proper time of a stationary clock at spatial infinity, (r, θ, ϕ) are the usual spherical coordinates ($2\pi r$ being the circumference of a circle at radius r). The event horizon is located at $r = r_s = 2Gm/c^2$, known as the Schwarzschild radius of a black hole. The gravitating mass of the black hole, m , is concentrated at the origin.

As is well-known, if the metric is expressed in this way it has a coordinate singularity at $r = r_s$, the (critical) radius of the event horizon, despite the lack of matter there (the spacetime itself is only singular at $r = 0$). The exterior solution, $r > r_s$, accurately approximates the spacetime outside a spherically symmetric star [15]. This region is well-behaved and suffices for the present discussion.

For a particle following a timelike worldline, $ds^2 \equiv c^2 d\tau^2$ where τ is the proper time of the particle and $d\tau \equiv 0$ for null particles (light rays). Therefore, along the worldline of any particle, $ds^2 \geq 0$, and the following inequality must hold:

$$\left(1 - \frac{r_s}{r}\right) c^2 dt^2 \geq \left(1 - \frac{r_s}{r}\right)^{-1} dr^2 + r^2(d\theta^2 + \sin^2\theta d\phi^2). \quad (2)$$

It is convenient to rearrange this expression to obtain

$$\frac{1}{\left(1 - \frac{r_s}{r}\right)^2} \left(\frac{dr}{dt}\right)^2 + \frac{r^2}{1 - \frac{r_s}{r}} \left(\frac{d\theta}{dt}\right)^2 + \frac{r^2 \sin^2\theta}{1 - \frac{r_s}{r}} \left(\frac{d\phi}{dt}\right)^2 \leq c^2. \quad (3)$$

The Schwarzschild metric is asymptotically flat and, for regions far outside the event horizon, $r \gg r_s$, the effects of gravitational time dilation are negligible. One then finds that $(dr/dt)^2 + r^2 (d\theta/dt)^2 + r^2 \sin^2\theta (d\phi/dt)^2 \leq c^2$ which, considering the spherical coordinate system, confirms the expectation that the speed of light is insurmountable in special relativity, with the possible exception of tachyonic particles.

3 Spacetime coherency

Spacetime is a four-dimensional continuum, a differentiable and connected Lorentzian manifold. In general relativity it is dynamically acted upon by gravitation so as to alter the geodesics of motion. General relativity is a global theory: the presence of mass-energy does not merely influence the local spacetime, but the entire spacetime manifold. Thus, gravity’s range is limited only by the size of the universe. General relativity abides by the principle of general covariance allowing its physical laws to be expressed independently of coordinates.

The order in which events occur is observer-dependent in both special and general relativity. Nevertheless, the *relative rate at which time elapses along two worldlines* (i.e. time dilation/contraction) can be uniquely defined whether the separation between the worldlines is timelike, null or spacelike. Time dilation is a non-local, coordinate-independent quantity encoding genuine physics which is necessary for global consistency. For an arbitrary number n of distinct test particles with proper times $\tau_1, \tau_2 \dots \tau_n$, it must hold that

$$\frac{d\tau_1}{d\tau_n} \times \prod_{i=1}^{n-1} \frac{d\tau_{i+1}}{d\tau_i} = 1. \quad (4)$$

If general relativity is applied to the universe then the proper elapsed time, τ , along any worldline cannot exceed the time since the big bang, even if the universe is spatially infinite. Hence, along any worldline, the proper time $\tau < \infty$ and the proper distance $\ell < \infty$. Recognising that proper time τ is an affine parameter along the worldline $x^\alpha(\tau)$, for a specified spacetime manifold the demand of finite proper time along all worldlines within the universe can be formally stated as

$$\forall x^\alpha(\tau) : \tau < \infty. \quad (5)$$

It should be self-evident that this constraint will be satisfied by any physically realistic spacetime manifold. Non-compliance, as would occur once the advancement of proper times along any pair of worldlines could not proceed in tandem, would break the global coherency and connectedness of the spacetime continuum. Such a basic physical requirement must have priority over all “philosophical” concerns, an issue returned to in the discussion. Spacetime is not merely a local union of space and time but a global one. Failure to appreciate that localised physics can have wider implications for a spacetime manifold may be at the root of some persistent confusions in current black hole research.

4 Time dilation between arbitrary particles

For lightlike particles, the Schwarzschild metric provides a relationship involving two time coordinates t and τ

$$\left(\frac{d\tau}{dt}\right)^2 = \alpha c^2 - \frac{1}{\alpha}\left(\frac{dr}{dt}\right)^2 - r^2\left(\frac{d\theta}{dt}\right)^2 - r^2 \sin^2 \theta \left(\frac{d\phi}{dt}\right)^2. \quad (6)$$

The parameter α is defined as $\alpha \equiv 1 - r_s/r$ for the range $r > r_s$ so that α is strictly positive with $0 < \alpha \leq 1$. This expression allows the time dilation relative to Schwarzschild time t , a coordinate independent physical quantity, to be determined for an arbitrarily moving test particle located anywhere outside the event horizon.

Although particles travelling at the speed of light experience no passage of proper time ($d\tau = 0$), photons travelling radially towards the event horizon are eventually brought to a halt since the original metric then reduces to $(dr/dt)^2 = \alpha^2 c^2$ and, in the limit as $r \rightarrow r_s$, one sees that $\alpha \rightarrow 0$. This represents a worst case scenario since, for non-radial motion of the photon, $(dr/dt)^2 < \alpha^2 c^2$. For a purely radial ingoing photon, $dr/dt = -\alpha c$ and so the minimum Schwarzschild time, Δt_{\min} , required for a photon to travel from an initial radius r_0 to a final radius r_* , with $r_0 > r_* > r_s$, is given by

$$\begin{aligned} \Delta t_{\min} &= t_* - t_0 = \int_{r_0}^{r_*} \left(\frac{dt}{dr}\right) dr = \int_{r_*}^{r_0} \frac{dr}{\alpha c} \\ &= \frac{1}{c} \int_{r_*}^{r_0} \frac{r dr}{r - r_s} = \frac{r_0 - r_*}{c} + \frac{r_s}{c} \ln\left(\frac{r_0 - r_s}{r_* - r_s}\right). \end{aligned} \quad (7)$$

Due to the denominator in the logarithm term, as $r_* \rightarrow r_s$, this time interval grows without limit. Hence, regardless of the location at which photons are emitted outside the black hole, gravitational time dilation prohibits them reaching the event horizon in finite time according to the clock of a Schwarzschild observer.

In order to broaden this result, a quantity v is now defined such that

$$v^2 = \frac{1}{\alpha^2}\left(\frac{dr}{dt}\right)^2 + \frac{r^2}{\alpha}\left(\frac{d\theta}{dt}\right)^2 + \frac{r^2 \sin^2 \theta}{\alpha}\left(\frac{d\phi}{dt}\right)^2. \quad (8)$$

With reference to (3), it is apparent that one can write $v^2 \leq c^2$. This is consistent with v representing a physical

velocity whose magnitude, corrected for relative motion and gravitational time dilation, remains bounded by the speed of light. It can then be seen from (6) that

$$(d\tau/dt)^2 = \alpha(c^2 - v^2)$$

and consequently $0 \leq (d\tau/dt)^2 \leq 1$. The time dilation relation between two arbitrary worldlines with proper times τ_1 and τ_2 exploring the exterior Schwarzschild geometry can therefore be obtained from formula (9) where $\alpha_1 = 1 - r_s/r_1$ and $\alpha_2 = 1 - r_s/r_2$ with subscripts referring to worldlines 1 and 2 respectively. Thus, α_1 and α_2 have the same range as α such that consideration is strictly restricted to the region external to the event horizon. Since $v_1^2 \leq c^2$ and $v_2^2 \leq c^2$, neither the numerator nor denominator of (9) can be negative under any circumstances.

If a timelike particle following worldline 2 approaches the event horizon, $r_2 \rightarrow r_s$, then $\alpha_2 \rightarrow 0$ with the numerator of (9) remaining positive. For a timelike observer moving along worldline 1 sufficiently distant from the event horizon that $\alpha_1 \gg \alpha_2$ it is then apparent that $d\tau_2/d\tau_1 \rightarrow 0$, meaning that proper time ceases to advance along worldline 2. Noting that timelike particles take longer to approach the event horizon than light rays and that $d\tau_1/dt$ remains finite for any time-like observer comfortably outside the event horizon, one may conclude that

According to any external observer following a timelike worldline, light rays and timelike particles require infinite proper time to reach the event horizon of a Schwarzschild black hole.

Because (5) must be respected it follows that

Since infalling particles cannot experience the passage of time beyond that corresponding to infinite proper time along all other worldlines, they are incapable of penetrating the event horizon of a Schwarzschild black hole.

These statements are completely independent of the (arbitrary) choice of coordinate system. Furthermore, they do not require that observers be either stationary or infinitely remote. Indeed, observers could be relatively close to the event horizon without violating the assumption that $\alpha_1 \gg \alpha_2$. There is no optical illusion at play associated with the time of flight of photons – the conclusion holds for inanimate clocks lacking the faculty of vision just as well as it does for conventional observers.

Note also that there is no need for any special synchronisation procedure between the two particles: infinite time dilation prevents the ingress of matter across an event horizon as long as external clocks continue to mark time. If $\tau_2 = 0$ at the commencement of worldline 2 and the event horizon is approached as $\tau_2 \rightarrow \tau_h$, a finite proper time, then regardless of where and when worldline 1 commences it is still true that

$$\left(\frac{d\tau_2}{d\tau_1}\right)^2 = \left(\frac{d\tau_2}{dt}\right)^2 \div \left(\frac{d\tau_1}{dt}\right)^2 = \frac{\alpha_2 c^2 - \frac{1}{\alpha_2} \left(\frac{dr_2}{dt}\right)^2 - r_2^2 \left(\frac{d\theta_2}{dt}\right)^2 - r_2^2 \sin^2 \theta_2 \left(\frac{d\phi_2}{dt}\right)^2}{\alpha_1 c^2 - \frac{1}{\alpha_1} \left(\frac{dr_1}{dt}\right)^2 - r_1^2 \left(\frac{d\theta_1}{dt}\right)^2 - r_1^2 \sin^2 \theta_1 \left(\frac{d\phi_1}{dt}\right)^2} = \frac{\alpha_2 (c^2 - v_2^2)}{\alpha_1 (c^2 - v_1^2)}. \quad (9)$$

$\tau_1 \rightarrow \infty$ as $\tau_2 \rightarrow \tau_h$. This is manifestly so because

$$\begin{aligned} \tau_1(\tau_2 \rightarrow \tau_h) &= \int_0^{\tau_h} \left(\frac{d\tau_1}{d\tau_2}\right) d\tau_2 \\ &= \int_0^{\tau_h} \left(\frac{d\tau_2}{d\tau_1}\right)^{-1} d\tau_2 \rightarrow \infty. \end{aligned} \quad (10)$$

Proper times separating events along worldlines are invariant quantities, as are infinitesimal proper times. Thus, the same can be said of the ratio of the rate of passage of proper times along distinct worldlines. If the previous calculation were to be repeated using so-called horizon-penetrating coordinates (e.g. Lemaître, Novikov, Gullstrand-Painlevé, Kruskal-Szekeres, ingoing Eddington-Finkelstein [16]) the same results would of course be obtained by virtue of general covariance. The fact that the time dilation approaches infinity as $r_2 \rightarrow r_s$ has nothing to do with the Schwarzschild coordinate singularity at r_s , the coordinates being regular and well-behaved for all $r > r_s$, a range that was entirely adequate for the purposes of this analysis.

Therefore, contrary to some common assertions, an astronaut could not fall into a black hole without incident. Although τ_2 would remain finite in such circumstances, τ_1 would approach infinity as $\tau_2 \rightarrow \tau_h$. The astronaut encounters no immediate physical impediment at the event horizon but, due to the demand of global coherency and the need for proper times along worldlines to remain finite in (5), the condition $\tau_2 \leq \tau_h$ must be respected. Thus, the worldline of the astronaut would terminate as $\tau_2 \rightarrow \tau_h$, *corresponding to a situation in which the spacetime manifold totally ceases to evolve*. The astronaut simply would not experience proper times later than τ_h which, in effect, would be the moment when his or her worldline reaches future timelike infinity within the Schwarzschild spacetime. Times $\tau_2 > \tau_h$ would necessarily be fictitious and unphysical due to violation of (5).

For all $\tau_2 < \tau_h$, there is no consistency problem. One is not obliged to make an *either or* selection, exclusively choosing between the infalling or remote observer perspectives – they are mutually compatible projections of a globally coherent spacetime manifold. However, if one insists on abandoning coherency to consider the physically impossible case $\tau_2 > \tau_h$, a choice is then mandatory but the results are physically meaningless. That infalling matter indefinitely hovers above the horizon from the perspective of a distant Schwarzschild observer is a well-established result [15, 17]. In order to further clarify matters, it has been extended here to arbitrarily situated and potentially moving external observers who may be in quite close proximity to the event horizon.

The impermeability of the event horizon due to time dilation effects has in recent years been highlighted in the context of the black hole information paradox [18]. Furthermore, several core arguments promulgating that belief that event horizons are traversable have been dispelled [19]. While it is well-known that nothing can escape from a black hole, this analysis suggests that event horizons cannot be traversed in *any* direction whilst offering a readily comprehensible explanation as to why that is. Although angular momentum has been ignored here for simplicity, one would not expect its influence to alter the conclusions. Rotation would only represent an additional barrier, further hindering the arrival of particles at the event horizon of a Kerr black hole.

5 Dynamically formed black holes

A classic general relativity textbook originally published four decades ago argued that eternal black holes provide an excellent approximation to the outcome of gravitational collapse [15]. This advice may have been taken a tad too literally. Clearly, if event horizons are bidirectionally impermeable then the black hole information paradox would be trivially resolved. The interior geometry of the Schwarzschild metric may satisfy the field equations, but the constraint (5) suggests it cannot be arrived at through gravitational collapse, it is merely a hypothetical arrangement. Spacetime coherency issues aside, the equivalent rest mass energy of the Schwarzschild singularity goes no way towards counterbalancing its gravitational potential energy which, by any realistic assessment, is infinitely negative. Therefore, a Schwarzschild black hole and a collapsing star of the same mass forming a dark hole frozen in time have vastly different energies and are hence inequivalent on energy conservation grounds.

If the proper time for an infalling particle is advanced without regard for physics elsewhere then the spacetime can decouple and become non-connected, leading to a host of conceptual difficulties. For physically realistic gravitational collapse, however, it is not that infalling matter would hover in suspension above an event horizon – but that an event horizon would never form, in keeping with the external observer perspective of Oppenheimer & Snyder's analysis. However, in the unlikely event that the universe were host to fully-formed eternal black holes, their event horizons would behave as impenetrable barriers to infalling matter. Due to time-reversal symmetry, the geometry of spacetime in general relativity is as much a function of the future distribution of mass and energy as the past distribution, endowing the theory with a teleological quality. Thus, the event horizons of such hypo-

thetical black holes could in principle expand in anticipation of infalling matter so that time dilation halts the ingress of matter sooner than it might otherwise do. Notice that such expansion need not involve any increase in the gravitational potential of infalling matter since the potential near the event horizon is independent of black hole mass.

Hawking radiation arises due to separation of virtual particle pairs in the vicinity of a black hole event horizon [20], causing eternal black holes to evaporate with a perfect thermal spectrum, devoid of information content. Conversely, frozen stars with their rich, history-dependent structure, are able to radiate in the regular black body manner – thus avoiding information loss [21]. However, this issue is of lesser importance to the present discussion than the need for spacetime to remain coherent and connected. Black hole research has not led to many testable predictions but this consideration can have readily observable astronomical implications.

6 Topological admissibility

Trapped surfaces are defined as surfaces from which light rays initially pointing outwards are obliged to converge inwardly. The existence of a trapped surface is a precondition of several well-known theorems in general relativity. The event horizon of a Schwarzschild black hole is a null surface inside which surfaces equidistant from the horizon are all trapped. According to the Penrose-Hawking singularity theorems [22–24], a trapped surface inevitably leads to a geodesically incomplete spacetime manifold, implying the imminent formation of a singularity. However, if time dilation and global spacetime considerations prohibit the formation of event horizons then trapped surfaces cannot naturally arise and the singularity theorems have no physical relevance. By the same logic, the closed timelike curves of rotating eternal black holes would be avoided. Speculations concerning the physics internal to an event horizon are invulnerable to falsification and hence, strictly speaking, outside the scope of empirical science. However, although the presence of event horizons cannot be directly verified [13], evidence of their non-existence could in principle be obtained.

Like the singularity theorems, the principle of topological censorship [14] assumes the presence of a trapped surface. Therefore, if time dilation guards against event horizon formation, the gravitational collapse of a rapidly spinning cloud of gas would be capable of forming an axisymmetric structure of toroidal topology. Due to its dynamic nature, this scenario also falls outside the scope of earlier constraints on black hole topology [25, 26]. If physically realistic astrophysical black holes can be toroidal, the astronomical implications could be observable from afar.

Amongst the most energetic phenomena of the universe, quasars outshine galaxies by as many as three orders of magnitude. They were most abundant at redshifts of $z \sim 2$ when the universe was less than 20% its present age and are sig-

nificantly more scarce by now [27]. They create bipolar outflows [28], axially aligned relativistic jets penetrating intergalactic space and ultimately forming gigantic radio lobes as their energy is dissipated. Often chaotically turbulent, the jets are comprised of electrically charged particles which can form knots via magnetohydrodynamic processes. The orientation of the jets exhibits long-term stability, hinting at a direct dependency on the angular momentum vector of a supermassive black hole as opposed to that of an accretion disk of relatively low mass which is vulnerable to significant disruption by the assimilation of roving stars. This is another weakness of models seeking to account for jet formation in terms of a magnetised accretion disk.

The discovery of various metrics describing stationary spacetimes in which black holes are completely described by mass, angular momentum and electromagnetic charge alone led to the “no-hair conjecture”. Though the Schwarzschild and Kerr-Newman metrics are lacking in “follicles”, it is very natural to expect macroscopic departures from these metrics during realistic collapse scenarios. Furthermore, since the formation of trapped surfaces would violate spacetime coherency (5), crucial assumptions underpinning the singularity theorems and the principle of topological censorship may not apply.

Providing its assumptions are satisfied, topological censorship requires the central aperture of a toroidal black hole to seal up so rapidly that a ray of light lacks sufficient time to traverse it. Numerical simulations have provided some support for this [29]. However, computational approaches almost invariably adopt horizon-penetrating coordinates and fail to enforce the physical requirement (5). Instead, event horizons are located retrospectively after simulations terminate, without global consistency checks.

Theoretically, metrics describing black holes with toroidal event horizons have been obtained for anti-de Sitter backgrounds with a negatively valued cosmological constant. In such situations, Λ can be arbitrarily small [30]. Thus, toroidal event horizons are only marginally prohibited when considering eternal black holes in asymptotically flat spacetimes. However, if trapped surfaces cannot realistically form during gravitational collapse then topological censorship is bypassed entirely, leaving the toroidal dark hole (TDH) a viable possibility. Most stars capable of undergoing core collapse are massive, hence rapidly reaching the ends of their lifecycles. They are likely to retain sufficient angular momentum from their formation that during implosion their cores will adopt a toroidal geometry, if only transiently. A toroidal core can be supported by degeneracy (electron/neutron) pressure but, for very massive and rapidly rotating stars, direct collapse to a TDH is conceivable. Any of these eventualities could have potentially explosive consequences, scattering ejecta deep into space [31].

The angular momentum of a Kerr black hole is bounded by $|J| \leq GM^2/c$. In the field of black hole thermodynam-

ics, the temperature at which the event horizon radiates is proportional to its surface gravity. This vanishes for an extremal black hole, implying extremality is unattainable by the third law of black hole thermodynamics. However, for a TDH lacking an event horizon, angular momentum should approximately scale with the major radius of the torus. Thus, the Kerr bounds, $-GM^2/c < J < GM^2/c$, could easily be exceeded. Accumulation of angular momentum beyond the Kerr limit may buffer TDH topology, even if accretion is erratic. Evidence has recently emerged of a supermassive black hole within a galactic nucleus rotating at a near extremal rate [32].

Nature possesses only two long range forces and, of the two, electromagnetism is far stronger than gravity. Furthermore, gravity is purely attractive, making it ill-suited as a mechanism for launching relativistic jets of charged particles flowing directly away from a supermassive black hole. Therefore, it is virtually certain that electromagnetism is primarily responsible for jet production. There are no magnetic monopoles in nature but electrically charged particles make up all atoms. That ultrarelativistic jets of charged particles can be sustained for millions of years strongly suggests that the central black hole must itself be electrically charged.

Traditional models have nevertheless taken black holes to be electrically neutral due to common assumptions regarding their topology and the fact that plasma of a surrounding accretion disk can swiftly neutralise any electrical charge accumulating on a spheroidal black hole. A charged (Kerr-Newman) black hole would necessarily possess a magnetosphere due to its rotation but its flux lines would lead directly to the event horizon: oppositely charged particles would be strongly attracted to it, spiralling along the lines of magnetic flux to swiftly neutralise the black hole. Hence, theorists have struggled to explain the extreme energetics of quasars. The popular Blandford-Znajek mechanism [33] appeals to a strongly magnetised accretion disk whose flux lines thread the event horizon of an electrically neutral, Kerr black hole, enabling some coupling to its rotational energy. However, the model has been criticised because one would not expect an accretion disk to become strongly magnetised and the degree of magnetisation required seems infeasibly large [34].

The difficulty is overcome in the TDH case, a strong candidate for the central engine of quasars [31]. It has been previously proposed that a toroidal black hole might be stabilised by quantum gravitational effects [35] but in the present work there is no need for any departure from classical general relativity. If a TDH amasses an electrical charge, e.g. via the proton-electron charge/mass ratio disparity, neutralisation processes involving ambient plasma particles will be suppressed due to topological considerations. Flux lines of the induced dipolar magnetosphere along which charged particles tend to spiral would not lead towards the TDH. Instead, they would locally run parallel to its surface, as depicted in figure 1. Plasma from an orbiting accretion disk would be channelled along the flux lines towards the central aperture,

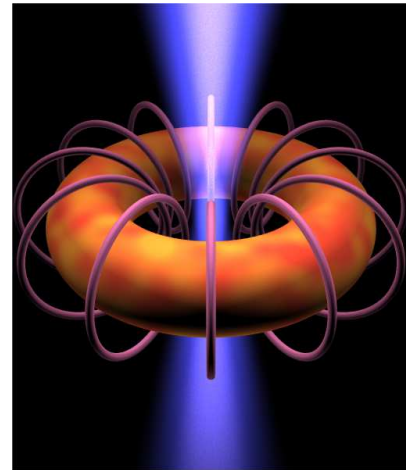


Fig. 1: A rotating toroidal black hole with a non-zero electrical charge generates a magnetic field whose flux lines are capable of resisting a neutralising flow of charged particles from the plasma of an orbiting accretion disk or imploding star. Flux lines point away from the black hole along the rotation axis where, due to extraction of the black hole's rotational energy, biaxial jets may be launched from the central aperture.

the region where the magnetic flux density is highest: the only location where the flux lines lead directly away from the TDH. Conditions for particle ejection are likely to be most favourable at a small displacement along the rotation axis either side of the symmetry plane. There, the magnetic field remains strong and aligned with the observed jets – but gravitational time dilation is less pronounced [31]. The relatively gentle decline in flux with axial displacement can be seen, for example, by considering the magnetic field strength, $B(z)$, of a current, I , flowing along a circular path of radius r at a distance z along the axis from the centre of symmetry:

$$B(z) = \frac{\mu_0 I r^2}{2(z^2 + r^2)^{3/2}} \approx \frac{\mu_0 I}{r(2 + 3z^2/r^2)} \quad \text{for } z \ll r. \quad (11)$$

For a current loop spread over a toroidal surface, the flux density within the central aperture, B_{ap} , whose radius is a can, due to the conservation of charge on the torus and the integrated flux threading the aperture, be approximated by $B_{ap} \approx (r/a)^2 B(0) \approx \mu_0 I r / 2a^2$. Thus, the magnetic field would be strongly amplified when the torus approaches pinch-off, $a \ll r$. Plasma magnetically siphoned into the aperture from the surrounding accretion disk could interact directly with the TDH via this magnetosphere. Furthermore, the lack of an actual event horizon would not preclude an ergoregion [36]. Hence, energy extraction via the Penrose process [37] may also contribute somewhat towards jet production. With lower mass electrons being preferentially ejected, a net charge on the TDH could be reliably maintained, thereby supporting the black hole's magnetosphere. Emitted particles would tend to

emerge in cones around the rotation axis, their convergence assisted by magnetohydrodynamic focusing. A population of neutral atoms and free neutrons in the accretion flow could feed TDH growth and support its long-term rotation against angular momentum losses.

Additional support for this model comes from the observed dichotomy between active and quiescent galaxies and the curious fact that quasars have distinctly finite lifetimes. Given that many galaxies still have ample reserves of gas to sustain accretion disks around supermassive black holes, and that the masses of these black holes cannot have decreased appreciably with time, it is puzzling that quasar activity is in such steep decline in the low redshift universe. One would expect nearby supermassive black holes, in particular those present in galaxy clusters, to at least feast upon stray matter sporadically. Only $\sim 10\%$ of the primordial gas in galaxy clusters has so far been utilised by star formation. For comparison, the figure for the Milky Way is closer to 90% . Nearly all galaxies harbour supermassive black holes so one wonders where are the vestigial traces of radio lobes caused by fleeting flares? Observational data suggests that once a quasar becomes quiescent there is little or no prospect of activity being revived: the galactic nucleus not only seems dormant, but utterly defunct. With regards to this finite lifetime riddle and the apparent lack of even temporary revival of quasar activity in quiescent galaxies, a topological transition offers a very natural and appealing hysteresis mechanism [31, 38, 39]. It has long been appreciated that this is a difficulty for more conventional models [40].

Once a dark hole grows too large, even a steadily supplied accretion disc cannot maintain sufficient influx of angular momentum to sustain the geometry. In addition, the angular momentum of the TDH is continually being sapped by jet generation. Closure of the central aperture is not easily reversed, especially as the ensuing charge neutralisation is rapid when flux lines lead directly to the dark hole. A potential explanation can also be found here for the gamma-ray burst phenomenon, relatively short-lived affairs compared to most supernovae. Such events may correspond to the temporary formation of a TDH/toroidal neutron degenerate structure during the core collapse of a massive spinning star.

7 Discussion

The development of general relativity was one of the greatest triumphs not only of theoretical physics but of all science, providing a description of gravitation compatible with the notion that space and time are part of a unified four dimensional continuum with experimentally verifiable implications. However, as with any intrinsically mathematical theory of physics, its interpretation must be guided by physical considerations and one should not lose sight of the scientific method. Indeed, some existing solutions in general relativity are already widely regarded as unphysical. Examples include the Tipler

cylinder and the Gödel metric, which exhibits closed timelike curves threading all events within its spacetime. It is possible that Einstein's intuition was correct and that all metrics describing eternal black holes should be similarly regarded with a healthy degree of scepticism and replaced with a new dark hole paradigm.

The present work has attempted to reconcile astronomically observed characteristics of quasars, which have inspired suggestions that their central engines may not abide by topological censorship, with a theoretical understanding of why that might be. A global constraint has been highlighted which, if respected everywhere within a spacetime manifold, holds considerable promise for resolving other long-standing problems in black hole research. It requires merely that the advancement of proper time along any worldline never necessitates the physically impossible advancement of proper time along any other worldline. In many circumstances this is trivially satisfied, but the situation changes radically within a spacetime containing pairs of timelike worldlines for which the relative time dilation grows without limit. Some particle worldlines will then reach future timelike infinity in finite proper time, much as light rays/photons do. Worldlines of timelike particles can thereby be truncated. In the case of particles approaching the event horizon of an eternal black hole, this is a consequence of their asymptotically approached apparent velocity – particles moving at the speed of light experience no passage of time. On the other hand, if a spacetime manifold is initially free of event horizons or singularities, it will always remain free of them. A picture emerges of general relativity as a remarkably benign theory of gravitation gracefully accommodating all eventualities. Analytical solutions to the field equations of general relativity are confined to highly idealised situations. More complex and realistic scenarios can only be studied numerically. Nevertheless, the basic conclusions drawn here concerning the non-formation of event horizons for spherically symmetric situations are likely to carry through to more general circumstances.

The present proposal differs significantly from the *gravastar* model [41] which invokes new physics, replacing the interior black hole region with a de Sitter spacetime blending into the exterior Schwarzschild geometry via a carefully-tailored transition layer [42]. It is also distinct from the *eternally collapsing object* (ECO) scenario [43, 44] in that gravitational collapse can be stabilised without recourse to radiation pressure. Furthermore, there is no need to invoke the presence of some “firewall” or exotic new physics at or near the horizon in order to overcome the information paradox [45].

For several decades now, black holes with event horizons have been seriously entertained despite the lack of a single mathematical example of an event horizon forming in finite universal time and their dismissal by the architect of general relativity. There is a deep-seated expectation amongst relativists that all observers should enjoy equal status but one

must not overlook the fact that general relativity is a theory in which global relationships exist between observers. By tracing the progress of an infalling observer beyond the event horizon, as Oppenheimer & Snyder did, one forsakes concern for external observers. In such situations, the worldlines of external observers must magically transcend what is, for them, future timelike infinity – and indeed, therefore, future timelike infinity for the entire spacetime manifold. Thus, the original notion of a “democracy” amongst observers is naïve if one interprets it in a purely local manner, eschewing the original spirit of relativity.

The proper times along all worldlines should remain finite in any physically realistic spacetime manifold. Whilst self-evidently true, this has profound repercussions for gravitational collapse. Global relationships within a spacetime manifold override local considerations. This can arrest dynamical collapse, prohibiting both the initial formation of event horizons and the ingestion of matter across pre-existing event horizons. Hence, any theorems reliant on the presence of trapped surfaces may have no physical bearing. Prevailing expectations that gravitational collapse inevitably leads to singularities and event horizons appear to be in error and fears that black holes destroy information misplaced. Furthermore, if topological censorship is circumvented, then electrically-charged toroidal dark holes could form the central engines of quasars, consistent with astronomical observations. Thus, quasars may already provide intriguing hints that nature’s black holes lack event horizons, and that various physically disturbing pathologies associated with traditional black hole models are obviated in realistic situations – without need for any adjustment to Einstein’s theory of gravitation.

Submitted on August 23, 2015 / Accepted on August 25, 2015

References

- Schmidt M. 3C 273: a star-like object with large red-shift. *Nature*, 1963, v. 197 (4872), 1040.
- Ferrarese L. and Merritt D. A fundamental relation between supermassive black holes and their host galaxies. *ApJ*, 2000, v. 539 (1), L9.
- Chandrasekhar S. The mathematical theory of black holes. 1983. Oxford University Press (International Series of Monographs on Physics. Volume 69), 663.
- Silk J. and Rees M. J. Quasars and galaxy formation. *Astron. Astrophys*, 1998, v. 331, L1.
- Hopkins P. F. and Hernquist L. Quasars are not light bulbs: testing models of quasar lifetimes with the observed Eddington ratio distribution. *ApJ*, 2009, v. 698 (2), 1550.
- Schwarzschild K. On the gravitational field of a mass point according to Einstein’s theory, 1916. (Translation by Antoci S. and Loinger A. arXiv:physics/9905030v1).
- Einstein A. On a stationary system with spherical symmetry consisting of many gravitating masses. *Annals of Mathematics*, 1939, v. 40, 4.
- Oppenheimer J. R. and Snyder H. On continued gravitational contraction. *Phys. Rev.*, 1939, v. 56 (5), 455.
- Novikov I.D. and Frolov V.P. Black holes in the universe. *Physico-USpekhi*, 2001, v. 44 (3), 291.
- Preskill J. Do black holes destroy information? 1992, arXiv: hep-th/9209058.
- Hawking S. W. Information loss in black holes. *Phys. Rev. D*, 2005, v. 72 (8), 084013.
- Hawking S. W. Black holes and the information paradox. Proceedings 17th Int. Conf. Dublin, 2004, *Gen. Rel. & Grav.*, doi:10.1142/9789812701688_0006; arXiv: 1401.5761 (2014); doi:10.1038/nature.2014.14583.
- Abramowicz M. A., Kluzniak W. and Lasota J. P., No observational proof of the black-hole event-horizon, *Astron. Astrophys*, 2002, v. 396, L31.
- Friedman J. L., Schleich K. and Witt D. M. Topological censorship. *Phys. Rev. Lett.*, 1993, v. 71 (10), 1486.
- Misner C. W., Thorne K. S. and Wheeler J. A. *Gravitation*. Macmillan. 1973.
- Finkelstein D. Past-future asymmetry of the gravitational field of a point particle. *Phys. Rev.*, 1958, v. 110 (4), 965.
- Landau L. D. and Lifshitz E. M. The classical theory of fields (Vol. 2), 1975, Butterworth-Heinemann.
- Vachaspati T., Stojkovic D. and Krauss L. M. Observation of incipient black holes and the information loss problem. *Phys. Rev. D*, 2007, v. 76 (2), 024005.
- Weller D. Five fallacies used to link black holes to Einstein’s relativistic space-time. *Progress in Physics*, 2011, v. 1, 93.
- Hawking S. W. Black hole explosions. *Nature*, 1974, v. 248 (5443), 30.
- Chafin C. E. Globally causal solutions for gravitational collapse. 2014. arXiv :1402.1524v1
- Penrose R. Gravitational collapse and space-time singularities. *Phys. Rev. Lett.*, 1965, v. 14 (3), 57.
- Hawking S. W. The occurrence of singularities in cosmology. III. Causality and singularities. *Proc. Roy. Soc. A*, 1967, v. 300 (1461), 187.
- Hawking S. W. and Penrose R. The singularities of gravitational collapse and cosmology. *Proc. Roy. Soc. A*, 1970, v. 314 (1519), 529.
- Hawking S. W. Gravitational radiation from colliding black holes. *Phys. Rev. Lett.*, 1971, v. 26, 1344.
- Hawking S. W. Black holes in general relativity. *Commun. Math. Phys.*, 1972, v. 25, 152.
- Shaver P. A., Wall J. V., Kellermann K. I., Jackson C. A. and Hawkins M. R. S. Decrease in the space density of quasars at high redshift. *Nature*, 1996, v. 384, 439.
- Ganguly R. and Brotherton M. S. On the fraction of quasars with outflows. *ApJ*, 2008, v. 672 (1), 102.
- Shapiro S. L., Teukolsky S. A. and Winicour J. Toroidal black holes and topological censorship. *Phys. Rev. D*, 1995, v. 52 (12), 6982.
- Galloway G. J., Schleich K., Witt D. M. and Woolgar E. Topological censorship and higher genus black holes. *Phys. Rev. D*, 1999, v. 60 (10), 104039.
- Spivey R. J. (2000). Quasars: a supermassive rotating toroidal black hole interpretation. *MNRAS*, 2000, v. 316 (4), 856.
- Risaliti G., Harrison F. A., Madsen K. K., Walton D. J., Boggs S. E., Christensen F. E., ... and Zhang W. W. A rapidly spinning supermassive black hole at the centre of NGC 1365. *Nature*, 2013, v. 494 (7438), 449.
- Blandford R. D. and Znajek R. L. Electromagnetic extraction of energy from Kerr black holes. *MNRAS*, 1977, v. 179 (3), 433.
- Ghosh P. and Abramowicz M. A. Electromagnetic extraction of rotational energy from disc-fed black holes: the strength of the Blandford-Znajek process. *MNRAS* 1997, v. 292 (4), 887.

35. Bambi C. and Modesto L. Can an astrophysical black hole have a topologically non-trivial event horizon? *Phys. Lett. B*, 2011, v. 706 (1), 13.
36. Butterworth E. M. and Ipsier J. R. On the structure and stability of rapidly rotating fluid bodies in general relativity. *ApJ*, 1976, v. 204, 200.
37. Penrose R. and Floyd R.M. Extraction of rotational energy from a black hole. *Nature*, 1971, v. 229 (6), 177.
38. Pompilio F., Harun-or-Rashid S. M. and Roos M. A toroidal black hole for the AGN phenomenon. arXiv: astro-ph/0008475; *Astron. & Astrophys.*, 2000, v. 362, 885.
39. Harun-or-Rashid S. M. Cosmological parameters and black holes, Univ. Helsinki PhD thesis, 2002, arXiv: astro-ph/0210253.
40. Hopkins P. F., Hernquist L., Martini P., Cox T. J., Robertson B., Di Matteo T. and Springel v. A physical model for the origin of quasar lifetimes. *ApJ Lett.*, 2005, v. 625 (2), L71.
41. Mazur P. O. and Mottola E., Gravitational vacuum condensate stars, *Proc. Nat. Acad. Sci.*, 2004, v. 101, 9545.
42. Martin-Moruno P., Garcia N. M., Lobo F. S. and Visser M. Generic thin-shell gravastars. *JCAP*, 2012, v. 3, 034.
43. Mitra A. Radiation pressure supported stars in Einstein gravity: eternally collapsing objects. *MNRAS*, 2006, v. 369 (1), 492.
44. Mitra A. and Glendenning N. K. Likely formation of general relativistic radiation pressure supported stars or “eternally collapsing objects”. *MNRAS Lett.*, 2010, v. 404 (1), L50.
45. Almheiri A., Marolf D., Polchinski J. and Sully J. Black holes: complementarity or firewalls? *JHEP*, 2013 v. 2, 1.

LETTERS TO PROGRESS IN PHYSICS

Reservations on Cahill’s Quantum Gravity Experiment

Anton L. Vrba

Ryde, Isle of Wight, Great Britain. E-mail: vrba@iow.onl

Cahill reports in *Progr. Phys.*, 2015, v.11(4), 317–320 [1] on the correlations of the random noise generated by two Zener diodes, when they are linearly displaced or differently orientated. His conclusions that this could be a detection, and evidence, of quantum gravity variations are exciting, however in my opinion premature.

Semiconductor diodes have provided means for generating noise [2] used in a variety of applications including cryptography, signal jamming, sound masking, and instrument calibration. The diode noise is usually amplified by factors greater than 100 [3] to obtain a signals around the -50 dBm levels, which are of same order magnitude that Cahill reports.

Referring to Cahill’s Figure 1, we can observe the internal arrangement of the apparatus consisting of a parallel connected array of five diodes, which are serially connected to the sensing resistor, switch and battery — these components, in that particular arrangement, form an EM-sensing loop having a substantial cross-section. There is no local amplification, and buffering, of the noise signal contrary to Zener-diode based noise generators. Figure 3, presumably, depicts the experimental configurations. In my Fig. 1 (guided by Cahill’s Figure 3 right hand side) I reconstructed the experimental electrical circuit diagrams of the inverted arrangement on a common plane formed by the electrical loops defined by the battery, Zener diode and resistor. From this figure it is evident that any EM-induced currents, marked I_m , would induce signals, marked V_m . These are of opposite polarity in the inverted apparatus, as Cahill observed.

In my opinion, the experiment needs to be performed with apparatus that reduce the effects of EM-induced interference to a minimum, achieved by a symmetrical arrangement of the diode array around the sensing resistor, as well as a soft steel enclosure to ensure magnetic and electrical shielding. For those wishing to duplicate the experiment, I propose arranging the components as sketched in Fig. 2, with the edition of a decoupling filter, comprising of a resistor R1 and the four capacitors marked C, that reduces the effect of induced EM interference in the electrical loop formed by the battery circuit. The noise-signal, generated by the four Zener diodes Z1–4, is detected over R2. All components should be nicely, and compactly, sandwiched between two printed circuit boards to ensure symmetry around the longitudinal axis of R2. An EM-induced current in, say, the loop Z1-C-R2 would be of the same magnitude as induced in R2-C-Z2 and thus canceling across R2.

Submitted on August 23, 2015 / Accepted on August 26, 2015

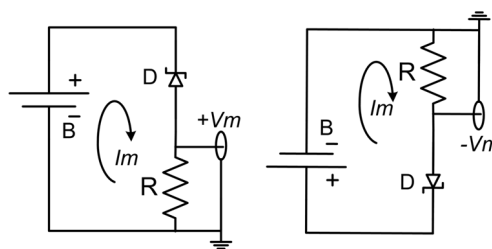


Fig. 1: Inverted Experimental Configuration

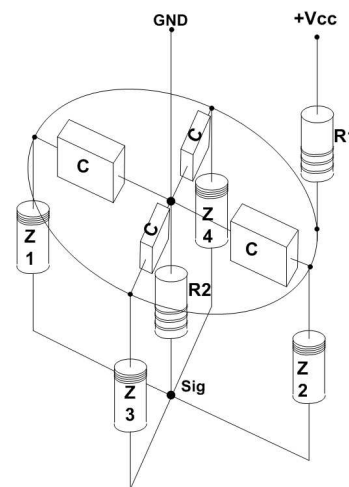


Fig. 2: Proposed Component Arrangement

References

1. Cahill R. T. Quantum gravity experiments. *Progress in Physics*, 2015, v. 11(4), 317–320.
2. Somlo P.I. Zener-diode noise generators. *Electronic Letters*, 1975, v. 11(14), 290. <http://users.cosylab.com/~msekoranja/tmp/04236738.pdf>
3. Appl. Note 3469 “Building a Low-Cost White-Noise Generator”, Maxim Integrated Products, Inc. <http://www.maximintegrated.com/an3469> accessed 8/25/2015

A Model of Dust-like Spherically Symmetric Gravitational Collapse without Event Horizon Formation

Miquel Piñol

Unidad de Medicina Intensiva, Hospital La Fe, 46026, Valencia, Spain. E-mail: miquel.pinyol@gmail.com

Some dynamical aspects of gravitational collapse are explored in this paper. A time-dependent spherically symmetric metric is proposed and the corresponding Einstein field equations are derived. An ultrarelativistic dust-like stress-momentum tensor is considered to obtain analytical solutions of these equations, with the perfect fluid consisting of two purely radial fluxes — the inwards flux of collapsing matter and the outwards flux of thermally emitted radiation. Thermal emission is calculated by means of a simplistic but illustrative model of uninteracting collapsing shells. Our results show an asymptotic approach to a maximal space-time deformation without the formation of event horizons. The size of the body is slightly larger than the Schwarzschild radius during most of its lifetime, so that there is no contradiction with either observations or previous theorems on black holes. The relation of the latter with our results is scrutinized in detail.

1 Introduction

The aim of this paper is to discuss several open problems of conceptual interest concerning black holes and, in particular, to elaborate a simple model of dust-like spherically symmetric gravitational collapse with account of both the inwards flux of the collapsing matter and the outwards flux of emitted thermal radiation. We illustrate how the latter may avoid the formation of event horizons. The metric considered in this work is time-dependent, unlike the Schwarzschild one. Spherical polar coordinates will be used and there will be no need for analytical extensions (such as the one given by the Kruskal-Szekeres chart) because the occurrence of an event horizon at the Schwarzschild radius will be avoided.

In Sec. 2 the main historical events concerning the development of the well-known concept of black hole are reviewed and its precise significance is shortly but precisely detailed. In Sec. 3 some open problems of the common black hole model are pointed out and their relationship with the corresponding historical findings is emphasized. Section 4 deals with the development of the metric of the present model: First of all, in subsec. 4.1 a time-dependent spherically symmetric metric in spherical polar coordinates is presented and the corresponding Einstein field equations are specified. Secondly, a dust-like energy momentum tensor for a purely radial motion with account of an ultrarelativistic collapsing matter and thermally emitted radiation is obtained in subsec. 4.2. Temporal evolution of the metric components is studied in subsec. 4.3, with the absence of emitted thermal radiation being detailed as a particular case. Fourthly, in subsec. 4.4 it is shown that there should exist a limit where the inwards flux of collapsing matter and the outwards flux of thermal radiation become *compensated*. It is also shown the asymptotic character of the approximation to this limit. Some additional considerations about the total mass and the edge of the collapsing body will

be made in subsec. 4.5. Finally, our results are discussed in Sec. 5, paying a special attention to the plausibility of the different hypothesis and the implications of their alternatives.

2 Important historical results concerning black holes

Several historical results in General Relativity led to the concept of black hole. The following list includes some of the most important ones:

1. K. Schwarzschild found in 1916 an exact solution of the Einstein field equations describing the field created by a point particle [1]. (According to Birkhoff's theorem, this solution is also valid for any spherically symmetric body at a distance larger than its radius [2].)
2. J. R. Oppenheimer and G. M. Volkoff discovered in 1939 the existence of upper limit for the mass of neutron stars, above which gravitational collapse could not be avoided [3].
3. In 1967 J. Wheeler used the term "black hole" to name a "gravitationally completely collapsed star" [5].
4. S. Hawking and R. Penrose proved in 1970 that, under certain circumstances, singularities could not be avoided. This is known as the Hawking-Penrose theorem of singularity [6].
All these results concerning black holes arise basically from Einstein's General Relativity. On the other hand, there exist two important features in the description of black holes which require from both Thermodynamics and Quantum Field Theory (QFT):
5. J. Bekenstein defined the entropy of black holes in 1972 and, based on thermodynamic grounds, deduced the need for black-hole radiation [7].
6. In 1974 S. Hawking justified Bekenstein's speculations about the existence of black-hole radiation from the

point of view of QFT. Hawking model implies the creation of particles of negative mass near the event horizon of black holes. The conservation of information is not clearly ensured by this model [8].

3 Some open problems in gravitational collapse

In this section we discuss if the previous historical results genuinely imply the actual existence of black holes as physical objects. It is widely believed that these findings prove the existence of black holes. The argument supporting black hole formation is the following:

1. There exist stars which are massive enough to exceed the Oppenheimer-Volkoff limit at the end of their “vital cycle”. Those stars must finally enter collapse.
2. According to the Hawking-Penrose theorem of singularity, all the mass inside an event horizon must reach a single central point, that is, form a singularity.
3. The solution of the Einstein field equations for the metric of a “point mass” is the Schwarzschild metric, that describes a black hole.

Entering collapse, however, does not immediately lead to the formation of an event horizon and, while the event horizon is not formed, the Hawking-Penrose theorem of singularity is not properly applicable (notice that one of its conditions of application is equivalent either to the existence of an event horizon, or to an expanding Universe taken as a whole). Hence, *a priori* entering collapse must not necessarily lead to a complete collapse.

Certainly, the period of time involved in the process of collapse may be proven to be infinite from the point of view of any external observer (that is, from our perspective on Earth). On the other hand, a “free falling observer” would measure a finite period of time for the collapse, at least if nothing destroys it before reaching its goal [4, 10]. A well-known feature of General Relativity is that space and time are relative but events are absolute. Consequently, it is necessary to reconcile the observations from both reference frames.

It is usually assumed that the free falling observer actually reaches the singularity in a finite time, and the infinite-lasting collapse measured by the external observer is justified in the following way: the free falling body has already reached the central singularity, but as the light emitted from the body inside the black hole never escapes from it, we cannot see it falling; furthermore, the light emitted near the event horizon of the black hole comes to us with a great delay, making us believe that it is still falling.

In fact, there are compelling reasons that make us doubt about the previous explanation: The Schwarzschild metric is symmetric under temporal inversion, which suggests that trajectories in the corresponding space-time should be also reversible, in contrast to the most common interpretation of black holes and their event horizon. Furthermore, General

Relativity is not only intended to explain what an observer “sees” in a given reference frame, but what truly “occurs” in there. Additionally, S. Hawking defended the incompatibility of event horizons with Quantum Mechanics [9].

Solution of this apparent paradox requires a careful analysis of what an external observer would exactly see when looking at a body free falling towards a black hole. On the one hand, it would see the free-falling body approaching asymptotically to the event horizon of the black hole, without ever crossing it. On the other hand, according to Hawking’s law of black hole radiation, the observer should also see the whole black hole evaporating in a very large, but finite period of time. The evaporation of the whole mass of the black hole must logically include that of the free-falling body as well. Were it not to be like this, that is, if the crossing of the event horizon had to be accomplished before the emission of thermal radiation, it would never emit thermal radiation and the laws of Thermodynamics would be infringed. As the temporal order of causally-related events is always the same for all reference frames, we must conclude that the free falling observer should also observe its own complete evaporation before having reached the event horizon. If it had reached the singularity in a finite period of time, its complete evaporation must have occurred in a finite and *lesser* period of time.

Not only should these considerations be valid for the free-falling body approaching a black hole, but also for the process of collapse itself [28]. Consequently, collapsing bodies should never become black holes. On the contrary, they should asymptotically tend to form an event horizon until the time at which they become completely emitted in the form of radiation. An equivalent thesis has already been defended by Mitra [14–18], Robertson and Leiter [19–21], Vachaspati *et al.* [11, 12], and by Piñol and López-Aylagas [13]. In addition, there exist some calculations in string theory which point towards the same direction [22].

Thus, the metric of a collapsing body shall never be in a strict sense Schwarzschild’s one (as it never completely collapses) but a time-dependent metric. In the next section, we solve the Einstein field equations of a time-dependent spherically symmetric metric. Several simplifications are considered to make calculations plausible, but the essential Physics of the problem is respected.

4 Deduction of a metric for gravitational collapse

4.1 Einstein field equations

As we have already pointed out, our goal in this paper is to study the temporal evolution of a spherically symmetric gravitational collapse. Rotations and local inhomogeneities are beyond the scope of the present work. Therefore, the starting point shall be a time-dependent spherically symmetric metric, which in spherical polar coordinates is given by the expression

$$d\tau^2 = e^\nu dt^2 - e^\lambda dr^2 - r^2 d\Omega^2, \quad (1)$$

where $\nu = \nu(r, t)$ and $\lambda = \lambda(r, t)$. Notice that geometrized units have been used ($G = 1, c = 1$). The corresponding Einstein field equations for such metric are the following [23]:

$$8\pi T_0^0 = -e^{-\lambda} \left(\frac{1}{r^2} - \frac{\lambda'}{r} \right) + \frac{1}{r^2}, \tag{2}$$

$$8\pi T_1^1 = -e^{-\lambda} \left(\frac{\nu'}{r} + \frac{1}{r^2} \right) + \frac{1}{r^2}, \tag{3}$$

$$8\pi T_2^2 = -\frac{1}{2} e^{-\lambda} \left(\nu'' + \frac{\nu'^2}{2} + \frac{\nu' - \lambda'}{r} + \frac{\nu' \lambda'}{2} \right) + \frac{1}{2} e^{-\nu} \left(\ddot{\lambda} \frac{\lambda^2}{2} - \frac{\dot{\lambda} \dot{\nu}}{2} \right), \tag{4}$$

$$8\pi T_3^3 = 8\pi T_2^2, \tag{5}$$

$$8\pi T_0^1 = -e^{-\lambda} \frac{\dot{\lambda}}{r}. \tag{6}$$

Subtraction of 3 from 2 yields the identity

$$8\pi (T_0^0 - T_1^1) = \frac{e^{-\lambda}}{r} (\nu' + \lambda'). \tag{7}$$

It will be useful to define a function $\phi(r, t)$

$$-2\phi \equiv \nu + \lambda \tag{8}$$

so that

$$\nu = -\lambda - 2\phi, \quad 8\pi (T_0^0 - T_1^1) = \frac{e^{-\lambda}}{r} (-2\phi'). \tag{9}$$

A mathematical structure for the stress-momentum tensor must be specified in order to solve the previous equations, which will be discussed in next subsection.

4.2 A dust-like stress-momentum tensor of ultrarelativistic particles

The stress-momentum tensor of a perfect fluid may be written in terms of the energy density ρ , the pressure p and the four-velocity u^α as:

$$T_\beta^\alpha = g_{\beta\delta} (\rho + p) u^\alpha u^\delta - \eta_\beta^\alpha p. \tag{10}$$

If the pressure appears to be very small compared to the energy density, in the limit $p \rightarrow 0$ one obtains the stress-momentum tensor of dust:

$$T_\beta^\alpha = g_{\beta\delta} \rho u^\alpha u^\delta. \tag{11}$$

In our model we deal with a dust-like stress-momentum tensor. For the sake of simplicity, we shall consider the perfect fluid splitting into two perfectly radial fluxes: a flux of ingoing collapsing matter and a second flux of outgoing thermal radiation. Both the ingoing collapsing matter and the outgoing thermal radiation are going to be dealt as ultrarelativistic

particles. It has been already established that the matter in a process of gravitational collapse reaches celerities near the speed of light [24]. It is also a well-known fact that, despite photons being “massless”, a photon gas may be assimilated to a gas of ultrarelativistic particles with an effective mass density [25].

It could be expected that the relation between pressure and mass-energy density should be given by the identity $p = \frac{\rho}{3}$ due to the particles being ultrarelativistic. A closer insight into this points out that the above identity would only be properly applicable to an *isotropic* gas and not to the highly *directed* movement considered in the present work. The consideration of two purely “radial” fluxes shall simplify calculations and it is in this sense that a “dust-like” stress-momentum tensor may be used. A similar approach has been already adopted by Borkar and Dhongle [26].

With account of the metric 1 the coefficients of the dust energy-momentum tensor 11 become

$$T_0^0 = e^{-2\phi} e^{-\lambda} \rho (u^0)^2, \tag{12}$$

$$T_1^1 = -e^\lambda \rho (u^1)^2, \tag{13}$$

$$T_0^1 = e^{-2\phi} e^{-\lambda} \rho u^0 u^1. \tag{14}$$

For a purely radial movement (characterized by $d\Omega = 0$) Eq. 1 leads to the relation

$$d\tau^2 = e^{-2\phi} e^{-\lambda} dt^2 - e^\lambda dr^2 \tag{15}$$

which, with account of the identities $\frac{dt}{d\tau} \equiv u^0$ and $\frac{dr}{d\tau} \equiv u^1$, becomes

$$1 = e^{-2\phi} e^{-\lambda} (u^0)^2 - e^\lambda (u^1)^2. \tag{16}$$

Isolating $|u^1| = \sqrt{(u^1)^2}$, we obtain

$$|u^1| = e^{-\phi} e^{-\lambda} u^0 \left[1 - \frac{e^{2\phi} e^\lambda}{(u^0)^2} \right]^{\frac{1}{2}}. \tag{17}$$

In the ultrarelativistic limit $u^0 \rightarrow \infty$ ($u^0 \gg e^{2\phi} e^\lambda$) the component u^1 of the four-velocity becomes

$$|u^1| = e^{-\phi} e^{-\lambda} u^0. \tag{18}$$

Notice that this same relation could have been obtained by imposing the identity $d\tau \sim 0$ in Eq. 15.

Concerning the sign of u^1 , it is clear that $u^1 < 0$ for ingoing matter and $u^1 > 0$ for outgoing thermal radiation, i.e.

$$u_{in}^1 = -e^{-\phi} e^{-\lambda} u^0, \tag{19}$$

$$u_{out}^1 = e^{-\phi} e^{-\lambda} u^0. \tag{20}$$

4.2.1 Stress-momentum tensor of the ingoing matter

If we denote the energy density of the infalling matter by ρ_{in} , according to Eqs. 12, 13, 14 and 19 we have

$$T_{0,in}^0 = e^{-2\phi} e^{-\lambda} \rho_{in} (u^0)^2, \quad (21)$$

$$T_{1,in}^1 = -e^{-2\phi} e^{-\lambda} \rho_{in} (u^0)^2 = -T_{0,in}^0, \quad (22)$$

$$T_{0,in}^1 = -e^{-3\phi} e^{-2\lambda} \rho_{in} (u^0)^2 = -e^{-\phi} e^{-\lambda} T_{0,in}^0. \quad (23)$$

4.2.2 Stress-momentum tensor of the outgoing thermal radiation

Denoting the energy density of the outgoing thermal radiation by ρ_{out} , according to Eqs. 12, 13, 14 and 20 we obtain

$$T_{0,out}^0 = e^{-2\phi} e^{-\lambda} \rho_{out} (u^0)^2, \quad (24)$$

$$T_{1,out}^1 = -e^{-2\phi} e^{-\lambda} \rho_{out} (u^0)^2 = -T_{0,out}^0, \quad (25)$$

$$T_{0,out}^1 = e^{-3\phi} e^{-2\lambda} \rho_{out} (u^0)^2 = e^{-\phi} e^{-\lambda} T_{0,out}^0. \quad (26)$$

4.2.3 Total stress-momentum tensor of the collapsing body

Addition of the stress-momentum tensors of both the infalling matter and the outgoing thermal radiation leads to the total stress-momentum tensor of the collapsing body, which is given by the expressions

$$T_0^0 = e^{-2\phi} e^{-\lambda} (\rho_{in} + \rho_{out}) (u^0)^2, \quad (27)$$

$$T_1^1 = -e^{-2\phi} e^{-\lambda} (\rho_{in} + \rho_{out}) (u^0)^2 = -T_0^0, \quad (28)$$

$$\begin{aligned} T_0^1 &= -e^{-3\phi} e^{-2\lambda} (\rho_{in} - \rho_{out}) (u^0)^2 \\ &= -e^{-\phi} e^{-\lambda} \left(\frac{\rho_{in} - \rho_{out}}{\rho_{in} + \rho_{out}} \right) T_0^0. \end{aligned} \quad (29)$$

Once the mathematical structure of the stress-momentum tensor of the collapsing body is established, we are able to study the temporal evolution of the collapse by solving the Einstein field equations 2-6.

4.3 Temporal evolution of collapse

Substitution of T_0^1 by Eq. 27 in Eq. 6 leads to the following equation:

$$-e^{-\phi} e^{-\lambda} \left(\frac{\rho_{in} - \rho_{out}}{\rho_{in} + \rho_{out}} \right) 8\pi T_0^0 = -e^{-\lambda} \frac{\dot{\lambda}}{r}. \quad (30)$$

From this an expression for the temporal evolution of λ may be isolated:

$$\dot{\lambda} = e^{-\phi} \left(\frac{\rho_{in} - \rho_{out}}{\rho_{in} + \rho_{out}} \right) 8\pi r T_0^0. \quad (31)$$

Initially it is expected that $\rho_{in} \gg \rho_{out}$, as the amount of energy emitted in the form of thermal radiation should reasonably correspond to a very small proportion of the total energy of the collapsing body. In that case, $\left(\frac{\rho_{in} - \rho_{out}}{\rho_{in} + \rho_{out}} \right) \sim 1$ and $\dot{\lambda} \sim e^{-\phi} (8\pi r T_0^0)$, so that λ shall be a strictly increasing function with time and it is expected to acquire considerably large values. In any case, for $\lambda \gg 1$ we have the asymptotic expression

$$8\pi T_0^0 = \frac{1}{r^2} + O(e^{-\lambda}), \quad (32)$$

and therefore,

$$\dot{\lambda} = e^{-\phi} \left(\frac{\rho_{in} - \rho_{out}}{\rho_{in} + \rho_{out}} \right) \frac{1}{r} + O(e^{-\lambda}). \quad (33)$$

On the other hand, we need to estimate as well the value of ϕ . From Eqs. 9 and 28 we obtain

$$\phi' = -\frac{1}{2} e^{\lambda} 8\pi r (T_0^0 - T_1^1) = -e^{\lambda} (8\pi r T_0^0), \quad (34)$$

which combined with Eq. 32 yields

$$\phi' = -\frac{e^{\lambda}}{r} + \left(\frac{1}{r} - \lambda' \right) \sim -\frac{e^{\lambda}}{r}. \quad (35)$$

According to Birkhoff's theorem, outside the radius R of the collapsing body the space-time geometry will be exactly Schwarzschild-like, so that $\phi = 0$ for $r > R$. Inside the collapsing body $T_0^0 > 0$ and consequently $\phi' < 0$. This yields $\phi > 0$ for $r < R$ and $\phi(R, t) = 0$ because of the analytic character of this function.

Equations 33 and 35 are not trivial to resolve analytically. For any time t , however, Eq. 33 and the fact that $\phi > 0$ for any $r < R$ lead to the following inequality:

$$\lambda(t, r) < \lambda(0, r) + \frac{t}{r}. \quad (36)$$

4.4 Asymptotic approach to a pseudo-stability phase

According to the results obtained in the previous section, for any given time t the function $\lambda(r, t)$ is analytic on the domain $r > 0$. Nonetheless, as Eq. 36 is an inequality, no specific values for this function have been provided.

It has been discussed that the ingoing flux of infalling matter is initially expected to be much larger than the outgoing flux of thermal radiation. Despite this, as λ becomes larger, according to Eq. 35 $|\phi'|$ must also increase. On the other hand, as $\phi \geq 0$ the ingoing flux must decrease according to Eq. 23.

As the values of $T_{0,in}^1$ may become as small as wanted, if λ and ϕ were not upper bounded it would not be unreasonable to think that the ingoing flux of infalling matter may eventually become *compensated* by the outgoing flux of thermal radiation. It could be discussed as well that, according to Eq. 26, the flux of outgoing thermal radiation may also become

arbitrarily small, but we proceed first to analyse the details concerning the compensation of fluxes and the consequences of this hypothesis.

The condition for the compensation of both fluxes is naturally given by the equation

$$T_{0,in,s}^1 + T_{0,out,s}^1 = 0. \tag{37}$$

It must not be misunderstood as a transgression of Oppenheimer-Volkoff’s theorem. The star *is not* in equilibrium. It is actually collapsing, as nothing prevents the infalling matter of keeping in collapse. There would simply be an additional flux (arguable in the basis of thermodynamic grounds, and justifiable by the conversion of a portion of the collapsing matter into thermal radiation due to the interaction of their respective fields) that would compensate the energy interchange across a given surface of r -radius.

In that hypothetical state of “stability”, from Eqs. 23 and 26 a relation between the energy densities ρ_{in} and ρ_{out} can be derived

$$\rho_{in,s} = \rho_{out,s} = \frac{1}{2} \rho_s, \tag{38}$$

where the subindex s stands for “stability” (notice that the aforementioned relations are specific of that hypothetical phase). Several considerations concerning the emission of thermal radiation due to collapsing bodies must be made in order to proceed further with the theoretical development.

4.4.1 A model of Hawking-like radiation

According to Hawking [8], the temperature of a black hole is proportional to the inverse of its Schwarzschild radius (R_S) and the thermal radiation emission rate is proportional to the inverse of the square of R_S :

$$\dot{M}_H = -\frac{k}{R_S^2}. \tag{39}$$

We have denoted the thermal emission by \dot{M}_H as it implies a loss in the total mass of the black hole.

In what follows, both the approach and the nomenclature adopted in the study of the mass and its mathematical relation with the components of the stress-momentum tensor and with the functions $\nu(r, t)$ and $\lambda(r, t)$ of the metric 1 are the ones given in Ref. [23]. The total mass of a spherically symmetric body of radius R is given by the following expression:

$$M = \int_0^R 4\pi r^2 T_0^0(r, t) dr. \tag{40}$$

Analogously, the mass contained inside a surface of radius r (concentric to the spherically symmetric body of interest) is given by

$$m(r, t) = \int_0^r 4\pi \tilde{r}^2 T_0^0(\tilde{r}, t) d\tilde{r}. \tag{41}$$

Comparing Eqs. 2 and 41, the following relation can be set between $m(r, t)$ and $\lambda(r, t)$:

$$e^{-\lambda(r,t)} = 1 - \frac{2m(r,t)}{r}, \tag{42}$$

and therefore we have $-e^{-\lambda} \dot{\lambda} = -\frac{2\dot{m}}{r}$ or, equivalently,

$$\dot{\lambda} = \frac{2\dot{m}}{r} e^{\lambda}. \tag{43}$$

Despite the fact that there is solely “one” function $\lambda(r, t)$, it is useful to split $\dot{\lambda}$ into the sum of $\dot{\lambda}_{in}$ (due to the ingoing flux \dot{m}_{in} of collapsing matter) and $\dot{\lambda}_{out}$ (due to the outgoing flux \dot{m}_{out} of thermal radiation). In so doing we obtain

$$\dot{\lambda} = \dot{\lambda}_{in} + \dot{\lambda}_{out} \tag{44}$$

with

$$\dot{\lambda}_{in} = \frac{2\dot{m}_{in}}{r} e^{\lambda}, \quad \dot{\lambda}_{out} = \frac{2\dot{m}_{out}}{r} e^{\lambda}. \tag{45}$$

As pointed out before, the thermal emission of black holes \dot{m}_H is given by Eq. 39. On the other hand, Vachaspati *et al.* showed that the thermal emission of a collapsing shell approaching the Schwarzschild’s radius of a black hole would follow a law of the same style [11]: according to their calculations, the temperature of the collapsing shell turns out to be proportional to the Hawking’s one ($T_V \sim 2.4T_H$, where T_V stands for Vachaspati’s temperature and T_H for Hawking’s temperature).

With account of Eq. 42 the metric 1 becomes

$$d\tau^2 = \left(1 - \frac{2m(r,t)}{r}\right) e^{-2\phi(r,t)} dt^2 - \left(1 - \frac{2m(r,t)}{r}\right)^{-1} dr^2 - r^2 d\Omega^2, \tag{46}$$

where the resemblance with Schwarzschild’s metric results evident. Certainly, there exist two main differences between Eq. 46 and the Schwarzschild’s metric: 1) the mass is not a constant, but a function of the radius. 2) there is an additional factor $e^{-2\phi(r,t)}$ in the coefficient g_{00} .

However, if we 1) deal with motions whose variation in the r -coordinate is small enough and 2) assume a temporal proximity to the hypothetical stationary case that we postulated (i.e., $\dot{m}(r, t) \sim 0$ and $\dot{\phi}(r, t) \sim 0$), then the metric 46 may be *locally* transformed into the Schwarzschild’s one.

In fact, in the *vicinity* of a given radius R_a , where $m(r, t) \sim M_a$ and $\phi(r, t) \sim \Phi_a$, we have

$$d\tau^2 \sim \left(1 - \frac{2M_a}{r}\right) d\tilde{t}^2 - \left(1 - \frac{2M_a}{r}\right)^{-1} dr^2 - r^2 d\Omega^2, \tag{47}$$

with

$$d\tilde{t} \equiv e^{-\Phi_a} dt. \tag{48}$$

At this point it is time to introduce our Hawking-like radiation model. We will conceptually split the collapsing body

into a sequence of concentric spherical shells, each of which asymptotically approaches its corresponding radius $r = 2M_a$ in the coordinate system given by the metric 47. We assume that these collapsing shells do not interact with each other. Along the lines of Ref. [12] it can be deduced that the radiation law obtained for a spherical shell asymptotically approaching in time t the event horizon of a black hole is also valid for any of the concentric shells asymptotically approaching in time \tilde{t} its corresponding $r = 2M_a$ radius in our model. Consequently,

$$\frac{dm_{out}}{d\tilde{t}} = -\frac{k}{r^2} \tag{49}$$

and so

$$\dot{m}_{out} \equiv \frac{dm_{out}}{dt} = \frac{d\tilde{t}}{dt} \frac{dm_{out}}{d\tilde{t}} = -e^{-\phi} \frac{k}{r^2}. \tag{50}$$

From this, we straightforwardly obtain the identity

$$\lambda_{out} = \frac{2e^\lambda}{r} \left(\frac{-e^{-\phi}k}{r^2} \right) = -e^{-\phi} \frac{2k e^\lambda}{r^3}. \tag{51}$$

On the other hand, according to Eqs. 6 and 23 an equivalent expression for λ_{in} is given by

$$\lambda_{in} = e^{-\phi} \left(8\pi r T_{0,in}^0 \right). \tag{52}$$

From Eqs. 12, 21 and 32 we conclude that, asymptotically,

$$8\pi T_{0,in}^0 = \frac{\rho_{in}}{\rho_{in} + \rho_{out}} \frac{1}{r^2} + O(e^{-\lambda}) \tag{53}$$

and therefore, with account of Eq. 38, we obtain

$$\lambda_{in} = e^{-\phi} \left(\frac{\rho_{in}}{\rho_{in} + \rho_{out}} \right) \frac{1}{r} \simeq e^{-\phi} \frac{1}{2r}. \tag{54}$$

The stability phase is naturally defined by the condition

$$\lambda_s = 0 \tag{55}$$

and therefore, from Eqs. 44, 51, 54 and 55 we obtain the relation

$$-e^{-\phi_s} \frac{2k e^{\lambda_s}}{r^3} + e^{-\phi_s} \frac{1}{2r} = 0. \tag{56}$$

Equivalently,

$$e^{\lambda_s} = \frac{1}{4k} r^2, \tag{57}$$

from which a functional dependence of λ on r is obtained for the stability phase

$$\lambda_s(r) = -\ln(4k) + \ln(r^2). \tag{58}$$

Taking into account Eq. 35, from the previous equation we easily obtain an expression for ϕ_s :

$$\phi'_s = -\frac{e^{\lambda_s}}{r} = -\frac{r}{4k}. \tag{59}$$

Integration over r with account of the contour condition $\phi(R, t) = 0 \forall t$ discussed in the previous section yields the identity

$$\phi_s(r) = \int_R^r \phi'_s(\tilde{r}) d\tilde{r} = \frac{1}{8k} (R^2 - r^2), \tag{60}$$

and thus

$$e^{-\phi_s(r)} = e^{\frac{1}{8k}(R^2 - r^2)}. \tag{61}$$

It must be noticed that the existence of the postulated stability phase is self-consistent and that it may be clearly derived from equations 45: both $|\lambda_{in}|$ and $|\lambda_{out}|$ decrease as $\phi(r, t)$ increases by a factor $e^{-\phi(r,t)}$, but only $|\lambda_{out}|$ increases as $\lambda(r, t)$ increases (by a factor $e^{\lambda(r,t)}$). Consequently, even when initially $|\lambda_{out}| \ll |\lambda_{in}|$ at large enough times both quantities should become of the same magnitude.

Nonetheless, a significant issue concerning the behaviour of $\lambda(r, t)$ for small values of r must be remarked. We are going to deal it with detail in the following subsection.

4.4.2 Corrections to the equation of λ_s for small radii

From Eq. 42, as $m(r, t) \geq 0 \forall r, t$, it becomes evident that also $\lambda(r, t)$ must be $\geq 0 \forall r, t$. However, in Eq. 58, it can be checked that it yields $\lambda_s = 0$ at $r = 2\sqrt{k}$ and $\lambda_s < 0$ for $r < 2\sqrt{k}$. Consequently, the mentioned expression cannot be valid for small radii.

As it has been clearly established in subsec. 4.3, if no outwards flux of thermal radiation is taken into account the values of $\lambda(r, t)$ would grow in an unlimited way. Thus, at large times, it would become great enough to imply the T_0^0 component of the stress-momentum tensor to approach the asymptotic expression given in Eq. 32. By contrast, in the previous subsection we have actually taken into account the emission of thermal radiation, and it has been performed with the Hawking-like law specified in Eq. 39, which entails a most prominent emission rate for inner shells. As a consequence, λ_s values decrease at small radii (or, what is the same, it results to be a strictly increasing function with r).

For radii $r \gg 2\sqrt{k}$, all the calculations which have been deduced after Eq. 32 are completely justified. Fortunately, that corresponds to most values of r , since $k \ll 1$ (certainly, the thermal evaporation process takes place at a considerably slow rhythm).

Thus, the steps which we have followed in order to determine $\lambda_s(r)$ must be reviewed in order to obtain a valid expression for small radii. A suitable analytical solution to the problem is far from being straightforward, but we are going to analyse it a bit more of care in the following lines.

Firstly, the complete identity of T_0^0 in Eq. 2 must be used instead of Eq. 32. Therefore, the expression for λ_{in} , instead of the one specified in Eq. 54, according to 52 will be

$$\lambda_{in} = e^{-\phi} \frac{1}{2r} \left(1 - e^{-\lambda} (1 - r\lambda') \right). \tag{62}$$

From this, keeping the same radiation law of Eq. 39 and the expression for λ_{out} of Eq. 51, it is not hard to follow that the stability condition in Eq. 55 entails

$$e^{\lambda_s} = \frac{r^2}{4k} (1 - e^{-\lambda_s} (1 - r\lambda'_s)). \quad (63)$$

When $\lambda_s \gg 1$, Eq. 57 is recovered. As we had already signalled, its resolution in the regions where the mentioned limit ceases to be valid is far from being trivial. Nonetheless, a possibility could consist in the application of an iterative method. Instead of making $e^{\lambda_s} \rightarrow 0$, in the right side of the equation we may use as a first approximation (well, actually as a *second* approximation) the expression for λ_s obtained in Eq. 58 (being its derivative $\lambda'_s = 2/r$):

$$e^{*\lambda_s} \sim \frac{r^2}{4k} \left(1 - \frac{4k}{r^2} \left(1 - r\frac{2}{r} \right) \right) = \frac{r^2}{4k} + 1, \quad (64)$$

where the asterisk (*) stands for “iterated”.

Thus,

$$\lambda_{s*} \sim \ln \left(\frac{r^2}{4k} + 1 \right), \quad (65)$$

which can be assimilated to Eq. 58 for large values, but that has the advantage of accomplishing the necessary condition $\lambda(r, t) \geq 0 \forall r, t$.

In the next subsection, we are not going to have longer into account the corrections for small radii, but we will focus onto temporal variations of $\lambda(r, t)$ when approaching the stability phase described by 58 (only valid for $r > 2\sqrt{k}$).

4.4.3 Small variations of $\lambda(r, t)$ before the stability phase

According to Eqs. 44, 51 and 54 we have

$$\lambda(r, t) = e^{-\phi} \left(\frac{1}{2r} - \frac{2ke^\lambda}{r^3} \right). \quad (66)$$

In the stability phase, defined by Eq. 55, the functional dependence of λ is given by Eq. 57. Now we proceed to study small variations of $\lambda(r, t)$ before it acquires the stability value, that is,

$$\lambda(r, t) = \lambda_s(r) - \lambda_\Delta(r, t). \quad (67)$$

Notice that, by definition, $\dot{\lambda}_s(r) = 0$. This fact implies

$$\dot{\lambda}(r, t) = -\dot{\lambda}_\Delta(r, t). \quad (68)$$

Furthermore, because of the inequality $\lambda_\Delta \ll \lambda$, we will consider $\phi \simeq \phi_s$. Therefore, from Eqs. 57, 66, 67 and 68 we obtain the expression

$$\dot{\lambda}_\Delta = -\frac{e^{-\phi_s}}{2r} (1 - e^{-\lambda_\Delta}). \quad (69)$$

In the limit $\lambda_\Delta \ll 1$ we can approximate $1 - e^{-\lambda_\Delta} \sim \lambda_\Delta$, so that

$$\dot{\lambda}_\Delta = -\frac{e^{-\phi_s}}{2r} \lambda_\Delta + O(\lambda_\Delta^2), \quad (70)$$

whose integration over t leads to the following solution

$$\lambda_\Delta = A(r) \exp \left(-\frac{e^{-\phi_s}}{2r} t \right) = A(r) \exp \left(-e^{\frac{-1}{8k}(R^2-r^2)} \frac{t}{2r} \right), \quad (71)$$

where $A(r)$ is an arbitrary positive defined function depending on the initial conditions of the problem.

Therefore, according to the hypothesis of the model, $\lambda(r, t)$ asymptotically approaches its stability value:

$$\lambda(r, t) = -\ln(4k) + \ln(r^2) - A(r) \exp \left(-e^{\frac{-1}{8k}(R^2-r^2)} \frac{t}{2r} \right). \quad (72)$$

4.5 Some considerations about the mass and the edge of the collapsing body

From Eq. 19 the infalling velocity \dot{r}_{in} of any collapsing shell in the present model is given by

$$\dot{r}_{in} \equiv \frac{dr}{dt} = \frac{dr}{d\tau} \frac{d\tau}{dt} = \frac{u_{in}^1}{u^0} = -e^{-\phi} e^{-\lambda}. \quad (73)$$

According to Eqs. 42 and 73 and with account of the contour condition $\phi(R, t) = 0 \forall t$, the motion of the edge R of a collapsing body of mass M must be given by the expression

$$\dot{R} = -\left(1 - \frac{2M}{R} \right), \quad (74)$$

whose solution for large enough times is

$$R = 2M + \Delta R_0 e^{\frac{-t}{2M}} \quad (75)$$

with ΔR_0 being a constant depending on the initial conditions of the collapse.

An important detail must be pointed out. In the previous equations we have dealt with the total mass M of the collapsing body as if it was a constant. It may be actually considered constant in practice for long periods of time but, in fact, it slowly diminishes due to the emission of thermal radiation, unless the surrounding background presents a greater CMB temperature or news amounts of infalling mass are provided. Thus, having into account that $R_S = 2M$, from Eq. 39,

$$\dot{M} = \frac{-k}{R_S^2} = \frac{-k}{4M^2}. \quad (76)$$

Therefore,

$$M(t) = \left(M_0^3 - \frac{3kt}{4} \right)^{\frac{1}{3}}, \quad (77)$$

from which the evaporation time t_v may be isolated:

$$t_v = \frac{4M_0^3}{3k}. \quad (78)$$

5 Discussion

The model of gravitational collapse presented in this paper contains an important number of simplifications which have allowed us to find analytical solutions of the coefficients of the metric all over the space at any given time (for small radius values, we have seen that some special considerations must be taken into account, but no essential contradiction is risen). The results obtained are self-consistent and do not lead to the formation of an event horizon, what would provide a simpler interpretation of the information loss problem: if no event horizon is formed, thermal radiation should be directly emitted by the collapsing body. Hence, there is no need for postulating a special mechanism of radiation such the one that S. Hawking proposed *ad hoc* for black holes. Let us now analyse more carefully the hypothesis that we have made, their implications and the consequences that would have been derived from making slightly different considerations.

Our starting point has been a time-dependent spherically symmetric metric. It is a well-known fact that spherical symmetry is an almost universal *approximate* characteristic of any celestial body. Two kind of phenomena certainly prevents it from being *perfect*: the first one is rotation (which implies the modification from spherical surfaces to ellipsoidal ones), while the second one consists of the local inhomogeneities of any *real* system.

Concerning rotation, it constitutes *per se* a very interesting but mathematically complex problem. To deal properly with a rotating process of gravitational collapse, a kind of modified time dependent Kerr metric should be formulated (in the same way that in this paper a kind of “time-dependent Schwarzschild metric” has been proposed). From an intuitive point of view, however, one would expect that rotation should lead to a genuinely *slower* collapsing process (due to the “centrifugal” effect of angular momentum). Concerning local inhomogeneities, a detailed study of the effect of small perturbations on the metric could constitute another *per se* attractive problem, but *a priori* it is not unreasonable to assume that the emission of gravitational waves should tend to diminish these effects with time. This is a consequence of the “no hair” theorem for black holes (even when we have found no black hole in the mathematical development of this article).

About the temporal dependence of the metric coefficients, it appears to be a strict logical requirement of the problem. The displacement of the infalling matter along the collapsing process must necessarily imply a temporal change in the metric coefficients. In this sense, Schwarzschild metric -a good solution for the stationary “punctual mass” problem- is not the best choice for the question of collapse itself. In words of J. A. Wheeler, “matter tells spacetime how to curve, and curved spacetime tells matter how to move”. With our choice of time-dependent metric, Kruskal-Szekeres coordinates are not needed because the ordinary polar spherical coordinates cover the entire spacetime manifold and the functions $\lambda(r, t)$

and $\nu(r, t)$ are analytic all over the space.

With respect to the choice of stress-momentum tensor, its dust-like nature has been greatly aimed for the sake of simplicity. As it has been already emphasized in the pertinent section, it seems paradoxical to consider simultaneously the features of “dust-like” and “ultrarelativistic” because the relation between pressure and energy density in an ultrarelativistic *gas* turns out to be $p = \frac{1}{3} \rho$. Nonetheless, two subtle points should be raised here: First of all, the concept of “ultrarelativistic dust” is not as strange as it appears to be, since a privileged direction of motion has been considered (the ultrarelativistic motion is highly “directed” towards purely radial lines). Secondly, even if a relation of proportionality between p and ρ would have been chosen, that would not have changed the fact that all the other stress-momentum tensor components could be expressed as a product of certain factors and T_0^0 . It is straightforward to check that changing the aforementioned factors would not alter drastically the subsequent mathematical development. As a matter of fact, the “linearity” between T_0^1 and T_0^0 has allowed us to set a temporal dependence for λ . In fact, as λ turns out to be proportional to T_0^0 , the function λ would only diverge if T_0^0 became infinite too. Nevertheless, when λ increases T_0^0 does not diverge but tends to $\frac{1}{8\pi r^2}$. In a similar way, it may be proved that ν , or $\phi = -\frac{1}{2}(\nu + \lambda)$, is also a well-behaved function despite [reasonable] modifications in the stress-momentum tensor.

Thus, whether we consider thermal radiation or not, the study of the temporal evolution of a spherically symmetric gravitational collapse in spherical polar coordinates does not lead to incoherences, but constitutes a sensible alternative to the usual black hole model. In addition, when thermal radiation is considered, very high (but finite) values of λ are obtained at any given r . Definitely, the radiation law proposed in this paper has been deduced in a rather “heuristic” way by assuming the extensibility of the calculations detailed in Ref. [12] to a model of *scarcely interacting* collapsing shells. Certainly, in the original paper by Vachaspati *et al.* the emission of radiation was calculated from a spherical Nambu-Goto domain wall using the functional Schrödinger formalism, with vacuum close to the wall. Therefore, our *analytical* extension of their results to “inner shells” may be cautiously considered, but it is a reasonable hypothesis, specially having into account Birkhoff theorem (according to which, in a system with spherical symmetry, the gravity in a surface is basically determined by the mass of the matter contained in the inner, not outer, shells). As a matter of fact, it is a much more consistent assumption than some of those that may be found in the published works, as the use of a *strictu sensu* Hawking radiation in a *process* of gravitational collapse (as, for instance, in Ref. [28]), as Hawking radiation implies (essentially, not just formally) a transition from vacuum, and in truth a collapsing star is not void.

On the other hand, even if the genuine radiation law ap-

peared to be completely different, it would still be true that an asymptotic approach to a “stationary” phase (where the value of λ would stop increasing) should happen. In fact, this phase should be always reached just by assuming the reasonable hypothesis that the outgoing flux of thermal radiation should not diminish with time (the temperature of the collapsing body should be expected to rise with the progression of collapse), while the ingoing flux of collapsing matter should become smaller as the spacetime deformation becomes larger.

In summary, even when several of the assumptions of the model of gravitational collapse proposed in this paper may be considered excessively “idealistic”, it provides an illustrative description of how a time-dependent metric should be the most logical choice for the study of gravitational collapse and that the polar spherical coordinates of an asymptotic observer (a scientific on the Earth, not an astronaut falling into a black hole) are sufficient to cover the whole collapsing process. The supposed completion of the collapsing process in a finite proper time for a co-mobile observer would never be truly accomplished due to the invariance of causal order for any relativistic system (in a finite and lesser proper time, the co-mobile observer would be fully evaporated by the emission of thermal radiation). The astronomic objects already *identified* as “black holes” could equally correspond to “asymptotically collapsing bodies”. Empirically, few differences would be expected. From a theoretical point of view, the latter ones may be obtained in a very natural way from the Einstein field equations and avoid many of the paradoxes and illogical aspects of the former ones. Thus, according to Occam’s razor, asymptotic collapse should be preferred to black holes.

Acknowledgements

The author acknowledges very specially the help and support of I. López-Aylagas, as well as D. Jou and R. Zarzuela for their encouragement, sensible advices and careful review of the whole work.

Submitted on September 8, 2015 / Accepted on September 11, 2015

References

- Schwarzschild K. Über das gravitationsfeld eines massenpunktes nach der einsteinschen theorie. *Sitzungsberichte der Königlich Preußischen Akademie der Wissenschaften (Berlin)*, 1916, v. 1 Seite 189–196.
- Birkhoff G. D., Langer R. E. Relativity and modern physics. Cambridge MA: Harvard University Press, 1924.
- Oppenheimer J. R., Volkoff G. M. On massive neutron cores. *Physical Review*, 1939, v. 55 (4), 374.
- Oppenheimer J. R., Snyder H. On continued gravitational contraction. *Physical Review*, 1939, v. 56 (5), 455.
- Wheeler J. A., Ford K. W. Geons, black holes, and quantum foam: a life in physics. Norton and Company, New York, 1998.
- Hawking S. W., Ellis G. F. R. The large scale structure of space-time (Vol. 1). Cambridge university press, 1973.
- Bekenstein J. D. Black holes and entropy. *Physical Review D*, 1973, v. 7 (8), 2333.
- Hawking S. W. Black hole explosions? *Nature*, 1974, v. 248 (5443), 30–31.
- Hawking S. W. Information preservation and weather forecasting for black holes. arXiv:1401.5761, 2014.
- Penrose R. Gravitational collapse: the role of general relativity. Birkbeck College, London, 1969.
- Vachaspati T., Stojkovic D., Krauss L.M. Observation of incipient black holes and the information loss problem. *Physical Review D*, 2007, v. 76 (2), 024005.
- Vachaspati T., Stojkovic D., Krauss L.M. Quantum radiation from quantum gravitational collapse. *Physics Letters B*, 2008, v. 663 (1), 107–110.
- Piñol M., Aylagas I. L. Transition from Established Stationary Vision of Black Holes to Never-Stationary Gravitational Collapse. arXiv: 1007.2734.
- Mitra A. The Mass of the Oppenheimer-Snyder black hole. arXiv: astro-ph/9904163.
- Mitra A. Non-occurrence of trapped surfaces and black holes in spherical gravitational collapse. *Foundations of Physics Letters*, 2000, v. 13 (6), 543–579.
- Mitra A. Why gravitational contraction must be accompanied by emission of radiation in both Newtonian and Einstein gravity. *Physical Review D*, 2006, v. 74 (2), 024010.
- Mitra A. Radiation pressure supported stars in Einstein gravity: eternally collapsing objects. *Monthly Notices of the Royal Astronomical Society*, 2006, v. 369 (1), 492–496.
- Mitra A. The fallacy of Oppenheimer Snyder collapse: no general relativistic collapse at all, no black hole, no physical singularity. *Astrophysics and Space Science*, 2011, v. 332 (1), 43–48.
- Robertson, S. L., Leiter, D. J. Evidence for intrinsic magnetic moments in black hole candidates. *The Astrophysical Journal*, 2002, v. 565 (1), 447.
- Robertson S. L., Leiter D. J. On intrinsic magnetic moments in black hole candidates. *The Astrophysical Journal Letters*, 2003, v. 596 (2), L203.
- Robertson S. L., Leiter D. J. The magnetospheric eternally collapsing object (MECO) model of galactic black hole candidates and active galactic nuclei. arXiv: astro-ph/0602453.
- Karczmarek J. L., Maldacena J., Strominger A. Black hole non-formation in the matrix model. *Journal of High Energy Physics*, 2006, v. 2006 (01), 039.
- Landau L. D., Lifshitz E. M. The classical theory of fields (Volume 2). University of Minnesota, 1987.
- Lu Y. Black Hole Radiation and Energy-Momentum Tensor. Diploma Thesis for Theoretical Physics in Utrecht University. Netherlands, 2010.
- Hazlehurst J., Sargent W. L. W. Hydrodynamics in a Radiation Field-A Covariant Treatment. *The Astrophysical Journal*, 1959, v. 130 276.
- Borkar M. S., Dhongle P. R. Pre-Hawking Radiating Gravitational Collapse in Stationary Space-Time. *International Journal of Theoretical and Applied Sciences*, 2013, v. 5 (2), 27–31.
- Delsate T., Rocha J. V., Santarelli R. Collapsing thin shells with rotation. *Physical Review D*, 2014, v. 89 (12), 121501.Sc.
- Mersini-Houghton L. Backreaction of Hawking radiation on a gravitationally collapsing star I: Black holes? *Physics Letters B*, 2014, v. 738 61–67.

LETTERS TO PROGRESS IN PHYSICS

The c -global Revival in Physics

Otto E. Rossler

Division of Theoretical Chemistry, University of Tübingen, Auf der Morgenstelle 18, 72076 Tübingen, Germany
E-mail: oeross00@yahoo.com

A return is proposed to the 6-years-long period before Einstein gave up on the global constancy of the speed of light c in the vacuum. c -global remains implicit in Maxwell's equations and in quantum electrodynamics. Reluctantly, Einstein abandoned c -global in 1911 after a $3\frac{1}{2}$ years long silence kept on gravitation during which he had tried in vain to avoid the conclusion that c is only an everywhere locally but not a globally valid constant of nature. It is shown that Einstein just overlooked a *corollary* to his own finding of an optically reduced speed of an horizontal light ray downstairs in his constantly accelerating long rocketship in outer space. The new corollary reads: *slantedness relative to the tip* of the locally horizontal light ray. Hence Einstein's famous gravitational redshift — the increase in wavelength compared to above of a *vertically* emitted light ray — is accompanied by a proportional enlargement of space. The new horizontal size increase is masked from above by the upwards slant valid relative to the tip. Einstein's *gravitational time dilation* thus goes hand in hand with an equal *gravitational space dilation*. Surprisingly, Quantum Mechanics enforces the same conclusion independently: the reduced energy of the locally normal-appearing photons downstairs generates (via Quantum Mechanics' creation and annihilation operators) atoms of a proportionally reduced mass and hence proportionally enlarged size. Two disappointing implications follow: c -global rules out both cosmological space expansion and black hole evaporation. The uplifting third implication is: c -global makes the equivalence principle compatible with Quantum Mechanics for the first time. This new compatibility predictably extends to the implied " c -global-rescaled General Relativity". Hence the "holy grail of physics" is bound to exist. The *cgr-GR* only waits to be written down.

1 Foreword

The following text seems to represent a footnote on the early prehistory of General Relativity, dealing only with long overhauled ways of thinking and of groping in the dark, because since 1915 we have the indubitable final reality of the theory of space and time in the large. The purpose of the present note is to show that this is not so. In the very foundations of the grandiose recipe, there is hidden a tiny minor oversight. It has little influence on most implications, but it nonetheless allows one to improve the theory eventually by at last putting straight an element that belongs into it since 1915: the non-globality of c .

Many specialists will strongly disagree with the view that it could pay to return to the most early stage of this beautiful superhuman theory to find a little oversight in it and repair it. But this is exactly the purpose and aim of the following text. As the reader will see, the consequences — if this friendly detour into a long-gone stage of science is followed for the fun of it for a short stretch since everything is maximally simple on that level — are maximally far-reaching and rewarding.

Admittedly, such "nostalgic physics" à la Yul Brynner in the movie "Westworld" is an unusual approach. It looks like History of Science and has a dusty smell to it. But IF it un-

earths something that was really and actually overlooked, it has an important role to play. So with this Foreword, which owes its existence to a spirited written dialogue with the Editor-in-Chief, the present note belongs into a twilight category of theoretical physics. But it is the fruits that make results recognizable eventually. So if the result derived below, a so far overlooked gravitational-redshift-proportional size increase in gravitation, is correct — as is shown on the limited level of knowledge available in 1907 below, aided only by an independent development in physics that did not exist at the time, quantum electrodynamics —, then a major progress in today's thinking occurs. So the paper which follows after this acutely added preface is perhaps indeed worth the scrutiny of the specialists.

It is rare that such a naive but rigorous spatial thinking is used in theoretical physics. It reminds its author of the early phase in chaos theory when "absurdly simple" geometric ideas, like overlaying two transparencies with an expanding spiral drawn on each and defining straight threshold lines of transitions between them, sufficed to catapult chaos theory into the applied sciences. In that latter case, the specialists arrived at the same trick called "singular perturbation" eventually. In the present case, a similar "canonization" is hoped for.

2 Introduction

Einstein's biggest early discovery was an intuitive understanding of Maxwell's *c-global*: he saw in his mind that a light flash can expand as a sphere with the *same* speed c around each of two observers who are passing by each other at a high speed while the flash goes off at their feet at that moment.

This logical impossibility (one expects *two* light spheres around the two mutually fast receding observers) becomes a logical truth if the *simultaneities* valid for the two runners which coincide at the encounter, are *mutually slanted* as two equal-rights cuts through the same light cone. This fact Einstein was able to picture in his mind after a long nightly discussion with his by a few years older friend Michele Besso. On the next morning, he excitedly returned to Besso's front door to tell him: "*Thanks to you*, I have solved the problem!" This event Einstein reported to a Japanese audience 17 years later when he had just received the news of his Nobel Prize. His rare German phrase "Dank Dir" (thanks to you) got confounded with the conventional German phrase "danke Dir" (thank you) in the ensuing translation — so the co-authorship of Einstein's lifelong friend Besso never became public.

The miracle of the individualized global constancy of c fell in doubt with Einstein himself $2\frac{1}{2}$ years later, in December of 1907 [1], to be abandoned for good in mid-1911 [2]. By serendipity, *c-global* was retrieved a century later in 2007 as an allowed formal implication of the Schwarzschild metric of General Relativity [3, 4]. Subsequently, *c-global* was also discovered in the equivalence principle of Special Relativity [5], the very theory in which it had become questionable in late 1907 and been abandoned in 1911.

3 Motivation

The return of *c-global* into the foundations is important because a "facelift of physics" is implicit. For instance, the long-accepted paradigm of the *Big Bang* ceases to be tenable since it implies that two sufficiently distant objects on the expanding "balloon" recede from each other at a *superluminal* speed. As a second implication, black holes can now no longer "evaporate" since the well-known infinite *temporal distance* of their surface (called horizon) from the outside world is, by virtue of the global c , accompanied by an equally large *spatial distance*. Hence there can be no "tunneling" to the horizon anymore and thence no *Hawking radiation*. Thirdly, metrology acquires a whole new face [5].

What is the best way to convince the reader that *c-global* holds true again after a century? The answer lies in a return to the early Einstein. In 1905, he had described two radically new implications of *c-global*: the *twins paradox* (one twin ageing faster as if in a *Grimm Brothers'* fairy tale) and the *transversal Doppler effect*, which had both been overlooked by his great predecessors in the developing discovery of Special Relativity, Lorentz and Poincaré.

4 Genealogy

The drama with *c-global* began in 1907 with the last step in the discovery of the equivalence principle. The latter principle [1, 6] had just yielded the absolutely incredible but in retrospect true prediction of the *gravitational redshift*: inside a constantly accelerating long rocketship in outer space described by Special Relativity, a light pulse ascending with a finite c from the bottom reaches the tip only when the latter has picked up a fixed relative speed away from the original emission point. The GPS satellites confirm this absurdly daring insight of "gravitational time dilation" downstairs every minute.

Einstein's look at a *vertically* emitted light ray was then followed by his also having a look at a locally *horizontal* light ray that hugs the flat bottom of the ignited rocketship. This led him to his final discovery in the equivalence principle: a horizontal light pulse automatically *looks slowed* by the gravitational redshift factor when watched from above [1] (see the last unnumbered equation on the last-but-second page).

5 Main result

The second revolutionary finding of Einstein regarding gravitation is again absolutely correct notwithstanding its absurdity from a common-sense point of view. However, it happens to admit of a final touch. The latter takes the first Einstein result (the fact that the bottom is in constant recession relative to the tip) into account in the second (the apparent transversal slowdown of c). The synthesis is that the locally *horizontal* light ray hugging the floor is necessarily at the same time *slanted-upwards* relative to the tip at every point due to the continual falling-back of the bottom. Note that when the light from the neighboring spatial cell downstairs reaches the next, the latter is a bit faster already, etc. Owing to this new *relative slant*, the horizontal reduction of c discovered by Einstein becomes a mere *projection effect*: the new upwards slant restores *c-global*.

It is worth pointing out here that *c-global* formally underlies the equivalence principle from the outset since the latter is exclusively based on Special Relativity with its built-in global c . This fact was not sufficient, however, to directly rule out the conclusion that c is locally reduced. The lack of confidence shown has to do with the fact that the rocketship paradigm is so impossibly hard to think-through in every respect [6].

The newly retrieved global speed of light c downstairs in the equivalence principle now has its consequences: all *transversal lengths* downstairs which at first sight look unchanged from above are actually increased by the gravitational redshift factor relative to the tip. They only look optically compressed towards the original length by virtue of the slant. The only readily visible consequence upstairs is the seemingly reduced transversal speed of light c' downstairs, discovered by Einstein [1].

6 Consistency

The new found *transversal size increase downstairs matches* the increase in wavelength of all light emitted downstairs. Moreover, these lower-energy photons emitted downstairs remain, with their locally unchanged-appearing frequencies, *locally interconvertible* with particles of matter (as in positronium creation and annihilation) as a consequence of the much later discovered quantum electrodynamics. Hence *all* local atoms have a mass that is lower by the redshift factor valid relative to above. This *mass reduction*, in turn, entails a proportional size increase of these atoms via the Bohr radius formula of Quantum Mechanics. Therefore, space is enlarged downstairs, *both* by the *c-global* of Special Relativity and by virtue of Quantum Mechanics, in an identical fashion. The two theories confirm each other independently. The optically unchanged-appearing horizontal distances downstairs with their creeping c' seen by Einstein do therefore indeed mask a *size increase* proportional to the gravitational redshift.

Note that the thus doubly confirmed *new Einstein effect* of “gravitational space dilation” exactly matches the *old Einstein effect* of “gravitational time dilation” (implying *c-global*). The equivalence principle thus becomes even more powerful by the fact that the size change derived geometrically in it via the laws of Special Relativity gets independently confirmed by the creation and annihilation operators of quantum electrodynamics.

Thus, the original interpretation of Einstein’s creeping effect (as a reduction in c [1, 2]) can be given up for good to date. However, it is important to realize that in the days *before* the advent of quantum electrodynamics with its creation and annihilation operators, the double-tiered consistency obtained above was *inaccessible*. Hence the above-described fractal-like *relative local slant*, which saves *c-global* on the part of Special Relativity downstairs, was in the absence of Quantum Mechanics’ own rest-mass-dependent size increase impossible to spot. Einstein’s giving *c-global* up for good in 1911 after more than 3 years of trying to preserve it was therefore preprogrammed.

The *new Einstein effect* of “gravitational space dilation,” when added to the *old Einstein effect* of “gravitational time dilation” (so that c remains a global constant of nature), has mind-boggling consequences like the two already mentioned (no Big Bang and no Hawking evaporation). The second implication is especially important in view of the fact that it renders the most hoped-for success of a currently running experiment — generation of miniature black holes down on earth — undetectable by virtue of the absence of their generally expected Hawking signature. Any unrecognized success at CERN will then grow exponentially inside earth [3]. So the return to *c-global* implies “tangible consequences” for an experiment rated innocuous in its last — still *pre-c-global* — safety report LSAG of 2008. Einstein’s results are notorious for entailing existential consequences.

7 Discussion

It is a good idea to “return to the mothers” from time to time, poet Goethe advised. In the present case, a trip back to the *pioneer phase* of relativistic gravitation theory was offered. The retrieved crumb from Einstein’s table — *c-global* — is still big enough to revolutionize cosmology and metrology.

All of this is only possible because in 1907, a young outsider dared think clearly in three dimensions with an almost superhuman exactitude including motion effects and their entailed delays — much as a computer-games freak of today would do with the aid of modern simulation tools, cf. [7]. Composing the computer game “*Einstein Rocket*” and putting it on the web will greatly aid physics. In this way, a modern young Einstein may be enabled to let the only “to some extent accessible” [6] thought experiment of the younger Einstein reveal its most important if presently still unfathomable secret.

To conclude, a *revolution in physics* based on Einstein’s early work was described. A *corollary* to his optically manifest reduced speed of light c' downstairs in gravitation was pointed out — a gravitational-redshift proportional *size increase* downstairs in gravity that is masked from above. The *new space dilation* is proportional to the *old time dilation* and thus restores *c-global* in accordance with the special-relativistic nature of the equivalence principle of Einstein. Consistency of the equivalence principle with Quantum Mechanics arises for the first time (the previous absence of this feature had gone unnoticed). As a bonus, the new size dilation predictably enables the long-missed unification of General Relativity with Quantum Mechanics — “the holy grail of physics” [8].

Acknowledgments

I thank Wolfgang Rindler for decades of correspondence and Christophe Letellier and Valérie Messenger for early discussions. For J.O.R.

Submitted on September 27, 2015 / Accepted on September 28, 2015

References

1. Einstein A. On the relativity principle and the conclusions drawn from it (in German). *Jahrbuch der Radioaktivität*, 1907, Bd. 4, 411–462 (ref. to p. 458).
2. Einstein A. On the influence of gravitation on the propagation of light (in German). *Annalen der Physik*, 1911, Bd. 35, 898–908 (ref. to p. 906).
3. Rossler O.E. Abraham solution to Schwarzschild metric implies that CERN miniblack holes pose a planetary risk. *Vernetzte Wissenschaften — Crosslinks in Natural and Social Sciences* (P. J. Plath and E. C. Hass, eds.), Logos Verlag, Berlin, 2008, pp. 263–270. [Correction: the phrase “infinite proper in-falling time” must read “finite proper in-falling time”].
4. Rossler O.E. Abraham-like return to constant c in general relativity: Gothic- R theorem demonstrated in Schwarzschild metric. *Fractal Spacetime and Noncommutative Geometry in Quantum and High Energy Physics*, 2012, v. 2, 1–14.

5. Rossler O. E. Einstein's equivalence principle has three further implications besides affecting time: T-L-M-Ch theorem ("Telemach"). *African Journal of Mathematics and Computer Science Research*, 2012, v. 5, 44–47.
 6. The essential phrase in Einstein's paper on the equivalence principle [1], p. 454 (p. 302 of the English translation) reads as follows: "[...] in the discussion that follows, we shall therefore assume the complete physical *equivalence* of a gravitational [field] and a corresponding acceleration of the reference system. This assumption extends the principle of relativity to the uniformly accelerated translational motion of the reference system. The heuristic value of this assumption rests on the fact that it permits the replacement of a homogeneous gravitational field by a uniformly accelerated reference system, the latter case being *to some extent accessible* to theoretical treatment." (Emphases added.)
 7. Rossler O. E. Bye-bye Big Bang due to the analogical thinking of the young Einstein. In: *Das Numen* (Julian Charriere, Andreas Greiner, Markus Hoffmann and Felix Kiessling, eds.), pp. 59–75. Distanz Verlag GmbH & Institut für Raumexperimente, Berlin, 2015.
 8. The remaining task is to write down the "*c-global*-rescaled (*cgr*) general relativity". Hereby, the Einstein field equations must be condensed into a "global-*c* skeleton". Before this job has been finished, "experimentation in the dark" is discouraged. Once the "global-*c* space-time theory" is found, the deeper meaning of the retrieved "Maxwell-Einstein miracle of *c-global*" can start to be addressed.
-

Progress in Physics is an American scientific journal on advanced studies in physics, registered with the Library of Congress (DC, USA): ISSN 1555-5534 (print version) and ISSN 1555-5615 (online version). The journal is peer reviewed and listed in the abstracting and indexing coverage of: Mathematical Reviews of the AMS (USA), DOAJ of Lund University (Sweden), Zentralblatt MATH (Germany), Scientific Commons of the University of St.Gallen (Switzerland), Open-J-Gate (India), Referential Journal of VINITI (Russia), etc. **Progress in Physics** is an open-access journal published and distributed in accordance with the Budapest Open Initiative: this means that the electronic copies of both full-size version of the journal and the individual papers published therein will always be accessed for reading, download, and copying for any user free of charge. The journal is issued quarterly (four volumes per year).

Electronic version of this journal: <http://www.ptep-online.com>

Advisory Board of Founders:

Dmitri Rabounski, Editor-in-Chief
Florentin Smarandache, Assoc. Editor
Larissa Borissova, Assoc. Editor

Editorial Board:

Pierre Millette
Andreas Ries
Gunn Quznetsov
Felix Scholkmann
Ebenezer Chifu

Postal address:

Department of Mathematics and Science, University of New Mexico,
705 Gurley Avenue, Gallup, NM 87301, USA
